Exploring cell autonomous homeostatic plasticity at the synapse.

Humphreys, Lawrence

Awarding institution:
King's College London

Exploring cell autonomous homeostatic plasticity at the synapse.

Kings College London
MRC Centre For Developmental Neurobiology

Lawrence Humphreys
Supervisor:Juan Burrone

2012

Funded by the MRC

CONTENTS PAGE

FIGURES PAGE

ABBREVIATIONS

-AC1-adenylyl cyclase 1
-AC8-adenylyl cyclase 8
-AMPA-α-amino-3-hydroxyl-5-methyl-4-isoxazole-propionate acid
-AMPAR-α-amino-3-hydroxy-5-methyl-4-isoxazolepropionic acid receptor
-A.Ps-action potentials
-APV- 2-amino-5-phosphonopentanoic acid
-ARC-activity-regulated cytoskeleton-associated *protein*
-BDNF-brain derived neurotrophic factor
-cAMP-cyclic adenosine monophosphate
-CASK-calcium/calmodulin-dependent serine protein kinase 3
-CaMKII-calcium/calmodulin-dependent protein kinase II
-Cdc42-cell division control protein 42 homolog
-CBR1-cannabinoid receptor type 1
-ChR1-channelrhodopsin 1
-ChR2-channelrhodopsin 2
-CNQX-6-cyano-7-nitroquinoxaline-2,3-dione
-CREB-cAMP response element-binding
-dlg-discs large
-DIV- Days *In Vitro*
-E17.5- embryonic day 17.5
-EPSC-excitatory post synaptic current
-EPSP-excitatory post synaptic potential
-FBS-fetal bovine serum
-FM4-64-[FM4-64,N-(3-triethylammoniumpropyl)-4-(4-diethylaminophenylhexatrienyl)pyridinium dibromide]
-GABA- γ-Aminobutyric acid
-GAD- glutamic acid decarboxylase
-GFP- Green Fluorescent Protein
-GKAP- guanylate kinase-associated protein
-GluR2-glutamate receptor subunit 2
-GLR-1- (*C.Elegans*) glutamate receptor-1
-GRIP-glutamate receptor interacting protein
-gsb-gooseberry
-HBSS-Hank's buffered salt solution
-IPSC-inhibitory postsynaptic current
-LED-light emitting diode.
-LTD-long term depression
-LTP-long term potentiation
-MAGUK-membrane-associated guanylate kinase homolog
-MEAs-Micro Electrode Arrays
-mEPSC- miniature excitatory post synaptic current
-mGluR-metabotrobic glutamate receptors
-mIPSC-miniature inhibitory post synaptic current

-Munc-18- mammalian uncoordinated-18
-NB-neurobasal medium
-NLG-Neuroligin
-NMDA-N-methyl-D-aspartic acid
-NMDAR-N-methyl-D-aspartic acid receptor
-NMJ-neuromuscular junction
-PBS- Phosphate Buffered Saline
-PDL- Poly-D-Lysine
-Pen/Strep-penicillin streptomycin
-PI3- phosphoinositide-3
-PKA-protein kinase A
-PKC-protein kinase C
-PLC-phospholipase C
-Plk-2-polo-like kinase 2
-PPR-pair pulse ratio
-PSD-Post Synaptic Density
-PSD-95-postsynaptic density 95
-ROS-reactive oxygen species
-RRP-readily realeasable pool
-S818-serine 818
-S831-serine 831
-S845- serine 845
-Shank-SH3 and multiple ankyrin repeat domains protein 1
-SPAR-spine-associated Rap guanosine triphosphatase-activating protein
-SNARE-Soluble NSF attachment protein receptor
-STG -stomatogastric ganglion
-sTNFR- soluble form of TNFα receptor
-T840-threonine T840
-TNF-α- tumor-necrosis factor-α
-TTX- tetrodotoxin
-VAMP2-vesicle associated membrane-2
-vGat-vesicular GABA transporter
-vGlut 2- vesicular glutamate transporter 1
-vGlut 1- vesicular glutamate transporter 2
-VGSCs-voltage gated sodium channels
-VIAAT-vesicular inhibitory amino acid transporter
-VGCCs-voltage gated calcium channels

1.INTRODUCTION

1.1. Activity dependent Hebbian and homeostatic plasticity.

1.1.1. Hebbian plasticity.

The mammalian nervous system, made of billions of neurons each forming up to 100,000 synaptic connections, encodes signals reliably and accurately to direct well-organized behavior. However, the brain hardwired through its genetic make-up is really defined by its ability to continuously undergo experience dependent modification, allowing it to store information and adapt to environmental changes. The synapse, a key structure in neurons, is the site of communication between cells and is composed of over 1000 proteins (Collins *et al.,* 2006). These proteins not only establish the structure of the synapse, but also control the release of neurotransmitter from the presynaptic terminal to the postsynaptic compartment. The arrival of an action potential at the presynaptic terminal results in the opening of voltage gated calcium channels (VGCCs). The influx of calcium ions triggers the release of neurotransmitters into the synaptic cleft as vesicles undergo exocytosis and fuse with the plasma membrane at the active zone. This chemical signal is transduced back into an electrical signal through the activation of postsynaptic ionotropic receptors which bind to the neurotransmitters (Fig.1.1.).

63 years ago Donald Hebb postulated that information within neural circuits is stored through long-lasting changes in synaptic strength which to this day still stands true. To quote " When an axon of cell A is near enough to excite a cell B and repeatedly or presistently takes part in firing it, some growth process of metabolic change takes place in one or both cells such that A´s efficiency, as one of the cells firing B, is increased" (1949). In other words, correlated pre- and postsynaptic activities cause synapsestrengthening/stablization while uncorrelated pre- and postsynaptic activities cause synapse weakening/elimination. This theory was eventually observed experimentally by Bliss & Lømo (1973) when they showed that synaptic strength could

indeed be altered at individual synapses in an activity-dependent manner. They showed that when specific synapses in the rabbit hippocampus were activated by brief tetanic high frequency pulses applied in succession the result was an increase in the amplitude of excitatory postsynaptic potentials (EPSPs) which lasted for hours to days.

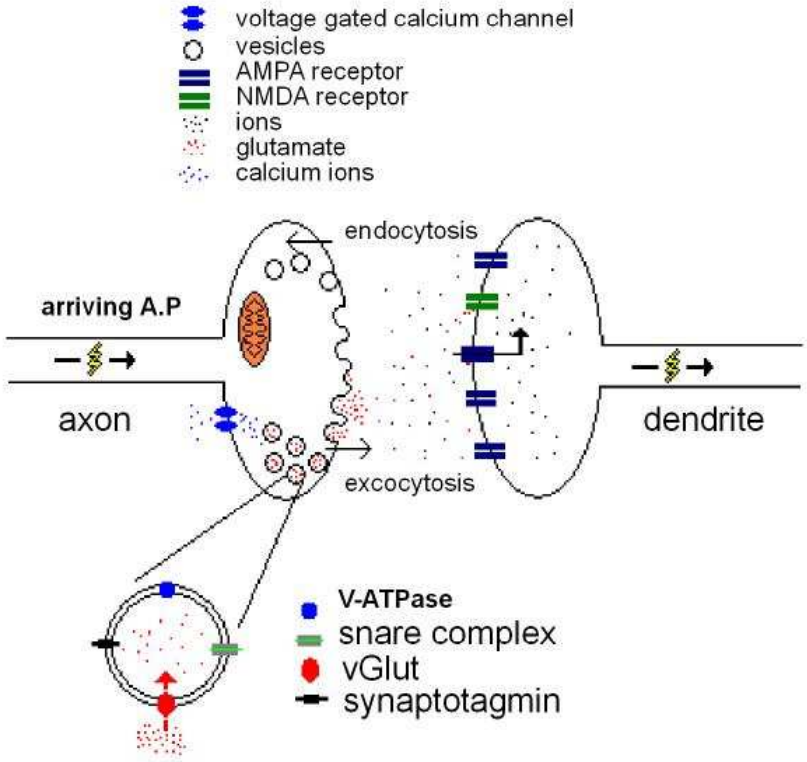

Fig.1.1 Neurotransmission at the synapse.
Neurotransmission takes place at synapses, specialized connections through which information flows from one neuron to another. This information flow is accomplished electrically and chemically at the synapse. The pre- and postsynaptic compartments do not actually touch each other. Rather, they are seperated by a gap, the synaptic cleft, through which neurotransmitters travel across. In brief, the arrival of an action potential at the presynaptic terminal activates voltage gated calcium channels triggering the influx of calcium ions. This in turn initiates neurotransmitter release through vesicles exocytosis. This mechanism is initiated, through the binding of calcium ions to the calcium sensor synaptotagmin located in vesicles. The SNARE complex facilitates the fusion of vesicles to the cell membrane. Vesicles are then retrieved through the process of endocytosis where they are eventually refilled driven by a proton electrochemical gradient generated by the Vacuolar H^+ ATPase. Once neurotransmitters have travelled across the cleft they bind to specific postsynaptic receptors initiating ion influx through the membrane effectively propogated the signal from one neuron to another.

They called this phenomenon “long lasting potentiation” otherwise known as LTP (long term potentiation), which is the result of enduring increases in the efficacy of

neurotransmission between the pre- and postsynaptic cell. Several major excitatory hippocampal synaptic connections have been used to study LTP and demonstrate the synapse specific nature of Hebbian plasticity (Bliss & Lømo, 1973, Douglas, 1977). Soon after the discovery of LTP it became apparent that networks could also exhibit activity-dependent reductions in the synaptic strength also lasting many hours. This phenomenon was termed "Long Term Depression" or LTD (Levy and Steward, 1979, Bear & Abraham, 1996). LTD can either be homosynaptic, typically induced by repetitive low frequency stimulation and is input specific (Christie & Abraham, 1992), or heterosynaptic where it is observed at synapses that are not potentiated (Wickens & Abraham, 1991).

These days we have a much better understanding of the underlying cellular pathways which are involved in the mechanisms LTP and LTD (Bear & Malenka, 1994, Beattie *et al.,* 2000). The induction of LTP ensues once a critical threshold of intracellular calcium has been exceeded in the postsynaptic cell. In most types of LTP, the influx of calcium requires the N-methyl-D-Aspartic acid (NMDA) receptor which is why this form of plasticity is considered to be NMDAR-dependent. Typically, the application of an electrical stimulus in the presynaptic cell will result in the release of neurotransmitter, which in excitatory cells is usually glutamate, onto the postsynaptic cell. Here, glutamate binds to α-amino-3-hydroxyl-5-methyl-4-isoxazole-propionate (AMPA) receptors in the postsynaptic cell membrane. AMPA receptors are the main excitatory receptor in the brain and are responsible for the vast majority of "fast" synaptic transmission. The activation of AMPA receptors results in the influx of sodium ions and subsequent short lived excitatory postsynaptic currents. Repeated high frequency stimulation will sufficiently depolarize the cell and unblock NMDA receptors. Normally NMDA receptors at resting membrane potentials are blocked by the presence of a magnesium ion that prevents the entry of calcium. Sufficient depolarization through the summation of EPSPs (excitatory post synaptic potentials) however, removes the magnesium ion allowing the entry of calcium. Thus NMDA receptors act as biological coincidence detectors through the depolarization-dependent removal of Mg^{2+} and ligand binding which results in the subsequent influx of calcium (Fig.1.2.).

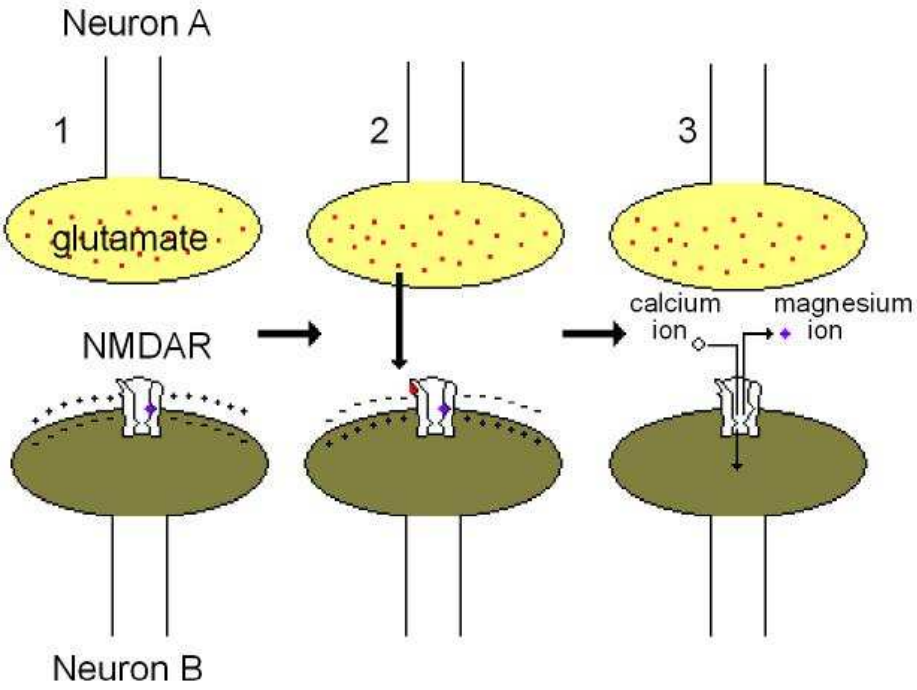

Fig.1.2. NMDA receptors act as coincidence detectors.
1. NMDA receptors located on the postsynaptic membrane are normally blocked by the presence of a magnesium ion.
2. The release of glutamate from the presynaptic compartment binds to the NMDA receptors. At the same time the cell membrane undergoes a reversal of charge and depolarizes.
3. When both events occur at the same time the magnesium ion is released effectively unblocking the NMDA receptor allowing the influx of calcium into the cell, activating secondary signalling necessary for plasticity.

This rise in intracellular calcium activates several enzymes responsible for the induction of LTP, in particular protein kinases such as Ca^{2+}/calmodulin-dependent protein kinsase II (CaMKII) and protein kinase C (PKC). These kinases in turn phosphorylate AMPA receptors that result in regulating its localization, conductance, and open probabilty (Malenka & Bear 2004). For example, GluR1 (glutamate receptor 1), one of the AMPAR subunits has four phosphorylation sites, serine 818 (S818), S831, S845 and threonine 840 (T840). It has been shown that phosphorylation of GluR1 S845 results

in increasing AMPA receptor peak response open probability (Bankel *et al*., 2000). Decreases in GluR1 phosphorylation at T840 have been suggested to play a role in LTD (Delgado *et al.,* 2007) while S831 phosphorylation, by CaMKII and PKC during LTP, results in the delivery of GluR1-containing AMPAR to the synapse (Hayashi *et al.,* 2001). Finally, S818 is phosphorylated by PKC, and is necessary for LTP (Boehm *et al.,* 2006). These kinases also contribute to the process of LTP by initiating the delivery of more AMPA receptors to the postsynaptic membrane. LTP can be sub-categorized into early LTP, a form independent of protein synthesis while more persistent forms of LTP such as late LTP require gene transcription and protein synthesis (Lynch, 2004).

LTD like LTP has since been shown to be input specific, and equally dependent on NMDA receptors activation (Bear & Malenka, 1994, Malenka & Bear, 2004). The magnitude of LTD and LTP is also dependent on the developmental time point and the change in synaptic strength has been hypothesized to depend on the insertion and removal of AMPA receptors and or composition (Malenka & Bear, 2004). It is thought that the type of calcium signal which occurs in the postsynaptic cell determines whether LTD or LTP occurs. High transient levels of postsynaptic Ca^{2+} are thought to result in the activation of protein kinases and LTP while sustained low levels of Ca^{2+} activate phosphatases and LTD (Malenka *et al.,* 1989, Mulkey *et al.,* 1994, Yang *et al.,* 1999). LTP and LTD are also associated with phosphorylation and dephosphorylation of GluR1 AMPARs (Lee *et al.,* 2000).

In hippocampal cell culture and the developing retinotectal system in *Xenopus*, the critical window for the induction of LTP/LTD has been shown by varying the spike time between pre- and postsynaptic neurons. If a postsynaptic spike arrives within 20ms after the presynaptic spike, synapses undergo LTP. However, if it arrives 20ms before the presynaptic spike, then synapses undergo LTD (Bi & Poo, 1998, 2001, Yangling & Poo, 2006). This spike-based plasticity emphasizes the requirement of the precise timing of individual spikes. Furthermore, in the hippocampal culture system, the susceptibility of synapses to potentiate depends strongly on their initial strength. LTP is only observed in synapses with relative low initial strength, whereas the extent to induce LTD does not appear to show any dependence on initial strength. Both were dependent on NMDA

receptor activation and blockade of L-type calcium channels abolishes the induction of LTD and reduced the extent of LTP (Bi & Poo, 1998).

The two forms of plasticity LTP/LTD are now widely considered to be the cellular mechanisms that underlie learning and memory and are referred to as associative or Hebbian plasticity. Since then there has been an abundance of correlation based rules in several biological systems resulting in the trend of "neurons that fire together wire together" (Levy & Steward, 1979, Hawkins *et at.,*1983).

1.1.2. Network instability arises through Hebbian rules.

Through computational modeling of network dynamics however, it was soon recognized that Hebbian positive feedback mechanisms would eventually lead to the destabilization of network properties. It became apparent in models simulating Hebbian rules that for the selective adjustment in synaptic weights to occur, a normalizing mechanism was needed (Bienenstock *et al.,* 1982, Miller & MacKay, 1994).

The reason for this is that hebbian forms of plasticity make the network inherently ustable. Hebbian plasticity is a positive feedback process thus; synapses which have undergone LTP are more excitable with a reduced threshold for undergoing further LTP eventuating in runaway excitation. If synapses were to undergo continuous strengthening through LTP an eventual saturation point would be reached, which could no longer be exceeded.

Likewise, if synapses were to undergo continuous LTD this could lead to quiescence or even pruning of the synapse itself (Miller, 1996). In both cases this would lead to a loss of capacity for information storage which would have detrimental consequences to the computational capacity of neural networks. Therefore, a stabilizing mechanism must exist to counteract the stresses Hebbian plasticity can have on the system if left unchecked.

Neurons appear to maintain a stable pattern of activity in the face of Hebbian and other activity related stresses through regulation of their intrinsic properties. Using activity sensors neurons regulate the number and type of ion channels and receptors keeping their

output constant (Marder & Prinz, 2002). When neurons are forced to perform outside of their optimal operating range with pharmacological activity blockers, they modify a variety of voltage-dependent ion channels which control intrinsic excitability and determine the firing rates. An example of this was observed in cortical neurons where two days of activity deprivation results in an increase in inward sodium currents without any changes in its voltage dependence or kinetics (Desai *et al.,* 1999). This enhancement in current is thought to be due to increases in the sodium channel density in the cell membrane. Similar findings were obtained in hippocampal slices, where the expression of voltage-gated sodium channels (VGSCs) was found to be bidirectionally modulated by neuronal activity, in a homeostatic manner (Aptowicz *et al.,* 2004). Thus, neurons have found a solution to a genetically determined pattern of activity through different combinations of ion channel densities which can be altered homeostatically to maintain a constant output.

These aforementioned experiments reveal the capacity for neurons to alter their intrinsic properties to maintain a constant pre-defined genetic output in terms of activity. However, another form of homeostatic regulation has been proposed, in which synaptic properties influencing neurotransmission are altered in response to chronic perturbations to activity, and we shall be concentrating predominantly on this type of compensatory plasticity for the rest of this thesis.

1.1.3. Synaptic homeostatic plasticity.

The term homeostatic plasticity itself is contradictory in nature. The origins of the word homeostasis are Greek "ὅμοιος, *homoios*, "similar" and ἵστημι, *histēmi*, "standing still"; while plasticity defines the capacity for change. Therefore, homeostatic plasticity is the capacity to remain stable through change. Homeostatic systems were defined by Walter Cannon in 1929 as having the ability to maintain their internal environment constant, which the French physician Claude Bernard described as 'la fixité du milieu intérieur'.

In other words, in a dynamic system, some parameters are tightly regulated and kept constant. There are many physiological variables that are tightly regulated to remain within a set point, such as blood pressure and temperature in warm blooded animals.

When considering neurons in the brain, it is though that the variable that is tightly controlled is some form of electrical activity. The reasons for this are immediately apparent: if the activity of a neuron increases dramatically, it would lead to hyperactivity and may also result in epilepsy. Conversely, if neuronal activity drops significantly, then the neuron or network would lose all processing power. As a result, neurons need to tightly control their activity levels to remain within an optimal operating range.

A new form of synaptic plasticity was described in a seminal paper which was not part of the current understanding of LTP and LTD and provided a normalizing mechanism computational neuroscientists predicted and sought. When activity in cortical cultures was chronically reduced for 48hrs either with the sodium channel blocker tetrodotoxin (TTX) or with the glutamatergic receptor antagonists 6-cyano-7-nitroquinoxaline-2,3-dione (CNQX), it resulted in increased miniature excitatory postsynaptic current (mEPSC) amplitudes when compared to untreated controls. Conversely, when γ-Aminobutyric acid (GABA) mediated inhibition was blocked, the initial increase in the overall firing rates of the network gradually decreased until , 48hrs later, firing rates returned to control levels. Throughout this period there was also a parallel decrease in mEPSC amplitudes, suggesting that the decrease in postsynaptic gain was responsible for the renormalization of firing frequency. This new observed form of synaptic plasticity demonstrated increases or decreases in the strength of all synaptic inputs in a cell wide manner in an effort to maintain the levels of activity within a normal operating range in the face of chronic perturbations in activity (Turrigiano *et al.,* 1998). This also provided a mechanism that could also counteract the destabilizing effects that Hebbian modifications can have on a network.

These changes in mEPSC amplitude after chronic pharmacological treatment were hypothesized to be a result of the removal and insertion of postsynaptic glutamate receptors rather than due to presynaptic mechanism. However, the possibility of some additional presynaptic changes existing was not excluded (see below for a more detailed discussion of presynaptic contributions to homeostatic plasticity). The changes in mEPSC

amplitude were indeed shown to be due to the activity-dependent insertion and removal of glutamate receptors at the synapse (Ibata *et al.,* 2008, Hou *et al.,* 2008). These shifts in mEPSC amplitude were found to be multiplicative in nature, suggesting that all synapses are strengthened or weakened by a set factor. Hence, this form of plasticity is also referred to as 'synaptic scaling' (Turrigiano *et al.,* 1998). If these changes were additive or subtractive one could envisage smaller synapses being affected disproportionately.

Various regions of the mammalian brain exhibit a large repertoire of activity (Buzsaki & Draguhn, 2004) and these variations are even apparent from cell to cell and networks (Wagenaar & Potter, 2006). Consequently, when considering the activity of a neuron or a network we think of it as having a set point, or more likely, operating within an optimal operating range. However, whether homeostatic plasticity in neurons is initiated in response to deviations from a set point or an optimal range still remains to be elucidated. Nevertheless, it is clear in neural networks a homeostatic response is initiated when the activity deviates from within this set point or optimal operating range (Fig.1.3.).

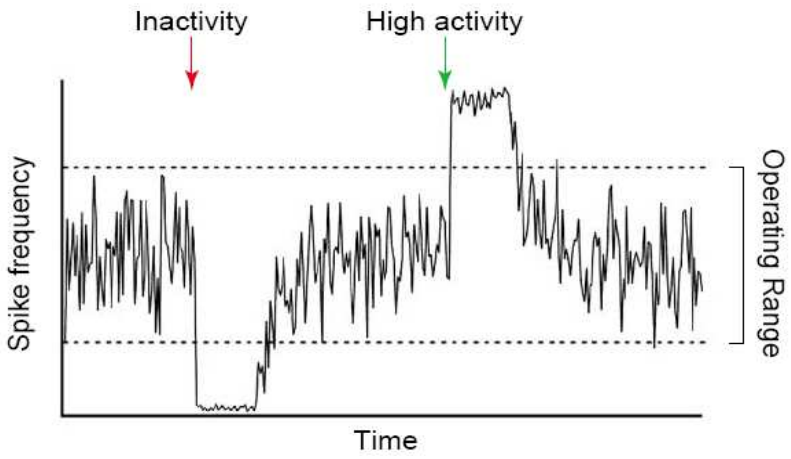

Fig.1.3. Deviations of activity from the optimal operating range initiate a homeostatic response. Theoretical diagram of spiking frequency over time depicting the initiation of homeostatic responses should the activity of a neuron or network deviate from within an optimal range. Red arrow denotes activity falling below a tolerated range and green denotes activity exceeding this range.

A homeostatic system can be defined as having a constant output. There are thus several requirements necessary for a homeostatic signaling system to function. Firstly, a set point in the form of pre-defined output, in the case of neurons, a set activity pattern. Secondly, any disturbances to this controlled variable must be detected by a sensor which will report the difference between the set point and the actual output of the system. Thirdly, any discrepancies must be sent off as error signals through negative feedback to a controller which in turn will rectify this difference by returning the controlled variable to an optimal set point.

The existence of a set point of activity in neural networks has been described *in vitro*. In cortical neurons, when activity is incremented pharmacologically with the addition of bicuculline this is eventually followed by a gradual return to original levels (Turrigiano *et al.,* 1998). Similarly, if activity is reduced genetically in a single neuron through expression of the inward rectifying potassium channel Kir.2.1, the initial firing rates are eventually re-established (Burrone *et al.,* 2002). This set point however, will most likely vary between cell types and regions.

Currently, there are some uncertainties as to what the controlled variable under homeostatic regulation is, although accumulating evidence points towards action potential firing. Furthermore, what disturbances are required for the induction of homeostatic plasticity are unknown, i.e. how much does activity need to be altered by to induce a homeostatic response? Similarly, the synaptic whereabouts and the molecular identity of the sensor in homeostatic plasticity remains elusive, although some readout of intracellular calcium is most likely involved (Marder & Prinz, 2002). Finally, what synaptic effectors are regulated to maintain a stable synaptic output (Fig.1.4.)? Later, we will attempt to address some of these questions by altering the activity through the use of chronic pharmacological manipulations of neural networks and of individual neurons with optogenetic means.

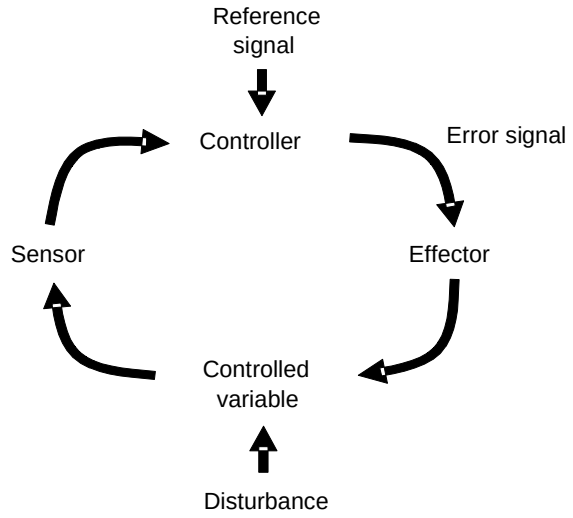

Fig.1.4. A homeostatic setup.
Diagram depicting the homeostatic control of a variable. A disturbance to the controlled variable is detected by a sensor. A controller compares this to a reference signal and, if significantly different, produces and error signal. An effector will then carry out modifications that will bring the controlled variable back to its normal set-point.

1.1.4. Temporal induction profile for Hebbian and homeostatic plasticity.

One major difference between Hebbian and homeostatic plasticity is the temporal framework within which they operate. The effects Hebbian plasticity has on modulating synaptic gain through the insertion of AMPA receptors in the cell membrane can be seen within seconds to minutes (Malenka & Bear, 2004). Homeostatic plasticity however, was originally thought to be a more gradual process with its cumulative effects taking place within hours to days (Turrigiano *et al.,* 1998). This timescale was thought to be important as any faster stabilizing influences might disrupt the role Hebbian plasticity has in storing correlations from the external environment in the form of synaptic alterations.

More recently, descriptions of homeostatic plasticity that occur over much shorter time scales have been reported. In rat neuronal cultures, cells which were expressing GluR2-EYFP exhibited greater fluorescence intensity in dendritic puncta after a four hour treatement with TTX when compared to untreated controls (Ibata *et al.,* 2008). In the extreme, at the *Drosophila* larval neuromuscular junction (NMJ) a 10 min. application of philanthotoxin-43 (a glutamate receptor antagonist) resulted in expected decreased mEPSC amplitudes. However, there was a concurrent presynaptic increase in quantal content that restored EPSC amplitudes back to normal. This demonstrated that presynaptic homeostasis was initiated within minutes following impaired postsynaptic receptor function. In addition, it has been reported that stimulation of afferent fibers in the CA1 region resulted in a rapid and long lasting change in the quantal size of inhibitory mIPSCs (miniature inhibitory postsynaptic currents) in the order of minutes (Hartmann *et al.,* 2002). It is therefore evident that the timescale for homeostatic plasticity has to be revised or even possibly be re-categorized depending on the system under question, how the activity was manipulated and which synaptic property was altered. These more rapid forms of homeostatic plasticity may use different mechanisms, as they are clearly much faster. Homeostatic plasticity in the order of hours and days may require gene expression whereas the more rapid forms may recruit other mechanisms that are expressed locally at the synapse.

1.2. Homeostatic mechanisms: excitatory and inhibitory synaptic scaling.

1.2.1. Evidence of synaptic scaling in excitatory cells through global activity manipulations.

The first experimental evidence in support of the existence of homeostatic regulation within the synapses of excitable cells was originally based on data from the neuromuscular junction and the denervation of skeletal muscle. The resulting denervation supersensitivity manifests as increased excitability and spontaneous muscle contractions due to increases in extrajunctional acetylcholine receptors (Berg & Hall 1975). Soon more evidence began to emerge in various culture systems that used neurons isolated from different regions of the brain.

In rat cortical cultures, activity was compared using exctacellular electrodes, in active controls, or in cultures which had been silenced chronically from DIV (Days *In Vitro*) 5, with TTX, and then returned to control medium. Recordings were taken at various time points from 7 until 42 DIV. In controls, activity emerged from DIV 7 which subsequently increased and plateaued at DIV 21. However, activity from cultures in which TTX was washed out exhibited increased activity at all time points when compared to controls. This increased activity was reminiscent of bursting activity observed after the application of the GABAA antagonist, picrotoxin (Ramakers *et al.,* 1990).

More evidence of homoestatic regulation was also provided in more intact organotypic slice culture preparations. Hippocampal slices which had been treated with bicuculline and/or picrotoxin induced epileptic like activity. However, in a homoestatic fashion they also displayed a decrease in the amplitudes of evoked excitatory postsynaptic currents (Muller *et al.,* 1993). In addition, slices chronically treated with bicuculline resulted in decreased excitability and vice versa when treated with CNQX/APV. This was assessed by measuring EPSPs induced with depolarizing trains. Cells treated with CNQX/APV exhibited increased firing in response to depolarizing trains and decreased firing in bicucculine (Karmakar & Buonomano, 2006).

Here, we will be replicating these global manipulations of activity in our model system and attempt through pharmacological means to block ion channels and receptors critical

to neurotransmission and neuronal activity in general. We aim to bidirectionally alter network activity and assess the requirements of the induction of homeostatic plasticity, as well as for any synaptic structural and functional changes which might ensue at the synapse.

1.2.2. NMDAR blockade and homeostatic plasticity.

Initially, it was believed that blocking NMDA receptor activation did not lead to an increase in quantal amplitude and that the induction of homeostatic plasticity was mainly through the blockade of sodium channels, AMPAR and GABA receptors (Turrigiano *et al.,* 1998, Leslie *et al.,* 2001, Thiagarajan *et al.,* 2005). However, it has since been suggested that NMDA receptors are required in homeostatic plasticity. A reduction in surface GluR1, which occurs after increasing network activity with GABAA receptor antagonists, was prevented when APV was concurrently applied (Lissin *et al.,* 1998). Simultaneous blockade of action potentials and NMDA receptors scales mEPSC amplitudes an order of magnitude faster than that observed when only action potentials are abolished (Sutton *et al.,* 2006). In some experiments blockade of the NMDA receptor by itself also appears to have some homeostatic consequences. In rat hippocampal cultures chronic blockade of NMDA receptors with APV results in a 380% increase in synaptic NMDAR clustering (Rao & Craig 1997). It has also been reported that chronic exposure to NMDA receptor blockers during synaptogenesis did not increase mEPSC amplitudes but did increase the frequency through enhancement of vesicle recycling (Bacci *et al.,* 2001). In addition, synaptic scaling has also been shown to be impaired in hippocampal slices which had mutations in the NMDA receptor calcium permeability (Pawlak *et al.,* 2005).

Interestingly, other compounds which are known to partially block NMDA currents like ethanol have recently been shown to have similar homeostatic effects as glutamatergic blockade. Ethanol exposure increases mEPSC amplitudes but not frequency (Carpenter-Hyland 2004). Ethanol has also been shown to reduce the levels of BDNF (Climent *et al.,* 2002) which has been previously implicated in homeostatic regulation (Rutherford *et al.,* 1998).

However, there are other reports in which NMDARs have not been implicated in homeostatic responses. In one set of experiments dissociated cultures were treated with increased extracellular potassium, CNQX and bicuculline with or without APV. They reasoned that if NMDAR activation is important for synaptic scaling under these conditions, an additional decrease in mEPSC amplitude with intact NMDAR signaling would be observed. However, this decrease was not seen. These results suggest that NMDA receptor activation does not contribute significantly to the reduction in mEPSC amplitudes produced by depolarization with increased extracellular potassium. Moreover, any effect of APV seen by others (Lissin *et al.,* 1998) can be explained by reduced depolarization in bicuculline plus APV conditions (Leslie *et al.,* 2001). Additionally, it has been reported that unlike CNQX, APV treatment in cultures does not increase mEPSC amplitudes or frequency nor does it increase GluR1, 2 or 3 levels (Gong *et al.,* 2007). Also, in the Nucleus accumbens, APV treatment did not affect GluR1 or 2 levels, unlike TTX or CNQX treatment (Sun & Wolf, 2009).

These contradictions in the literature as whether NMDAR plays a role in homeostatic responses may ultimately lie in the differences in experimental procedure used to assess it.

1.2.3. Kainate receptors and mGluRs.

Three identified ionotropic glutamate receptors exist in the central nervous system. The third not mentioned so far are kainate receptors which can be identified by their selective activation by the agonist kainate. Kainate receptors are believed to be important in synaptic plasticity and have been found to exist on both pre- and postsynaptic compartments of the synapse (Lerma, 2003). Postsynaptic kainate receptors contribute to synaptic transmission while presynaptic receptors modulate presynaptic release in excitatory and inhibitory cells (Lerma, 2003).

Kainate receptors are composed of GLUR5,6,7, KA1 and KA2 and are generally not thought to be involved in homeostatic plasticity. Cultures from double knockout mice for GluR5&6 treated with CNQX/APV underwent similar homeostatic changes as wild type (Gong *et al.,* 2007). CNQX is a nonselective antagonist of both AMPA and kainate

receptors thus it is possible that the induction of homeostatic plasticity after chronic treatment with CNQX could be attributed to the blockade of kainate receptors instead of AMPA receptors. In one set of experiments it was shown that when cortical cultures were chronically treated with GYKI 53655, a selective AMPA receptor antagonist, or with CNQX which blocks AMPA and kainate receptors, similar increases mEPSC frequency and amplitude were observed. On these findings they concluded that kainate receptors are not involved in homeostatic plasticity (Gong *et al.,* 2007).

Metabotropic glutamate receptors (mGluRs) on the other hand belong to subfamily C of G protein-coupled receptors and are divided into three groups (Takanori *et al.,* 2007). So far not much effort has been made to establish if these receptors are involved in homeostatic plasticity. However, in dissociated cultures blockade of mGluR with LY341495 was unable to prevent the high potassium induced decrease in quantal amplitude (Leslie *et al.,* 2001) suggesting at least initially, that these receptors are not involved in homeostatic induction or modulation.

1.2.4. Synaptic homeostatic plasticity on inhibitory outputs through global manipulations.

As evidence has begun to accumulate more efforts have focused over the past years on inhibitory cells and whether they too are subject to the same homeostatic influence. For neural networks to function optimally the fine adjustment of excitatory neurons is not sufficient. 20% of the cortex is made of inhibitory neurons which exhibit extensive feedback and feedforward connections onto excitatory cells (Markram *et al.,* 2004). This delicate balance is fundamental to the operation of local cortical circuits (Haider *et al.,* 2006) and ensures the prevention of the network generating epileptiform activity. It is therefore important to establish if these two distinct cell types are both regulated by homeostatic plasticity.

Already there exists a large body of work implicating that inhibitory cells are indeed also under homeostatic control. Chronic bicuculline treatment in rat neocortical circuits resulted in the reduction of presynaptic vesicular inhibitory amino acid transporter (VIIAT) levels while TTX application reversely, lead to an increase (De Gois *et al.,*

2005). Activity blockade with TTX results in a reduction of mIPSC amplitudes as well as postsynaptic levels of GABAA receptors in neocortical neuronal cultures. Additionally, there was a 50% reduction in the number of functional inhibitory synapses (Kilman *et al.,* 2002). Similarly, in neocortical organotypic slices TTX treatment lead to decreases in both mIPSC and unitary IPSC amplitudes (Kim & Alger, 2010). Evoked IPSP in slices appear to block more action potential induced with a 250ms depolarization stimulus in bicuculline treated cells than controls and vice versa with CNQX/APV (Karmarker & Buonomano, 2006).

However, there are also some reports which do not see any homeostatic regulation in inhibitory cells. 3 days of picrotoxin treatment in hippocampal slices cultures showed no difference in GABA-immunoreactivity compared to untreated cultures. Similarly the amplitudes of IPSPS did not differ (Muller *et al.,* 1992).

If inhibitory cells are indeed under homeostatic control, another point of interest will be to establish if different classes of inhibitory neurons which exist in various region of the CNS are regulated differently during homeostatic plasticity.

1.2.5. Different subtypes of inhibitory neurons are differentially regulated during homeostatic plasticity.

Efforts towards distinguishing if there are differences in homeostatic regulation in different classes of inhibitory neurons have been made in neocortical neurons. Two types of inhibitory neurons were assessed: parvalbumin (a calcium binding albumin protein) and somatostatin (an inhibiting hormone) +ive neurons. This was done using trains of action potentials evoked in the presynaptic cell (5 action potentials at 20Hz) and then monitoring the resulting unitary EPSCs. Blocking activity with TTX for 5 days resulted in an increased excitatory drive and intrinsic excitability onto both inhibitory cell types from excitatory cells. However, there was a differential regulation for each cell type when measuring the postsynaptic inhibitory drive onto excitatory cells with that of parvalbumin cells decreasing while that of somatostatic remained unchanged. This appeared to be a result of increased release probability and decreased synapse number. Although unitary IPSCs from somatostatin cells was unchanged their duration was

increased by 22% suggesting paradoxically that after chronic inactivity the net inhibitory charge is actually enhanced (Bartely *et al.,* 2008). Somatostatin inhibitory cells preferentially target the dendrites of excitatory cells while parvalbumin cells target the soma and proximal dendrites (Somogyi *et al.,* 1998). This suggests that somatostatin cells may try to maintain some inhibitory drive to excitatory cells during homeostatic plasticity while parvalbumin cells are subject to homeostatic regulation.

Additional, differences between inhibitory subtypes have also been reported. TTX treatment in hippocampal organotypic cultures lead to a reduction in mIPSC and unitary IPSC size following the stereotypic homeostatic behavior. However, a specific set of cannabinoid receptor type 1 (CB1R) positive synapses were selectively strengthened through increased release probability (Kim & Alger 2010). CB1R is expressed in inhibitory synapses which contain cholecystokinin but not parvalbumin (Marsicano & Lutz 1999). This inactivity induced strengthening of GABAergic synapses at CB1R positive synapses demonstrated how inhibitory synapses are differentially regulated depending on cell type.

Thus, the literature suggests that inhibitory cells are under homeostatic influence depending on the cell type under question, with several synaptic mechanisms which determine output being differentially regulated. This may explain why some labs have not observed homeostatic responses in inhibitory cells. Later on, we will also examine if inhibitory neurons are under similar homeostatic control in the face of chronic perturbation, or whether they obey different rules to that of excitatory neurons.

1.3. Postsynaptic homeostatic mechanisms.

At first, with the discovery of homeostatic plasticity most emphasis was given toward the postsynaptic side and how receptor adjustments can compensate for chronic alterations to activity in excitatory cells. Initially, the first and most commonly studied measure of synaptic scaling has been the spontaneous postsynaptic currents elicited by the release of a single vesicle of transmitter known as miniature excitatory postsynaptic currents or mEPSC's. Recently though, homeostatic change in synaptic gain has been

monitored by visualizing the turnover of synaptic surface GluR (Ibata *et al.,* 2008, Gainey *et al.,* 2009). Both AMPA and NMDA receptor activation can trigger AMPA receptor endocytosis by means of calcium influx and activation of the phosphatase calcineurin which is entirely distinct from the insulin mediated internalization of AMPA receptors (Beattie *et al.,* 2000). Whether AMPA receptors after internalization are sorted in endosomes and later reinserted into the postsynaptic membrane or sent for degradation to lysosomes appears to depend on the relative activation of NMDARs and AMPARs. NMDA activation results in an influx of calcium which activates protein phosphatases. This in turn dephosphorylates AMPAR and causes their endocytosis and trafficking through a PKA sensitive recycling pathway. However, AMPAR activation without NMDAR results in the internalization of AMPAR and degradation in lysosozomes independent of calcium, phosphatase and PKA activation (Ehlers 2000). These glutamatergic receptors are held in place and stabilized through various tethering and scaffolding proteins such as PSD-95, GKAP and Shank (Gerrow *et al.,* 2006).

As synaptic homeostatic plasticity compensates for chronic perturbations to activity through bidirectional insertion and removal of glutamatergic receptors it must therefore impose its influence on a large array of proteins involved in receptor turnover. It is likely that the recycling and transport pathways employed by homeostatic plasticity will converge with some of those recruited during Hebbian LTP/LTD.

Hebbian and homeostatic plasticity are functionally opposed with the former progressively modifying network properties and the latter promoting its stability. However, as both mechanisms influence the machinery involved in receptor insertion it is possible that there may be some convergence between the two. Still, differences may be discovered in the signaling cascades, which determine the speed in which receptor numbers are deployed and also for any subunit preference unique to each mechanism.

AMPAergic receptors consist of 4 subunits GluR1-4 which combine to make tetramers and are considered to mediate fast synaptic neurotransmission. Immature AMPAR-dependent synapses on neocortical pyramidal neurons in general are characterized by inward rectification in contrast to mature synapses. As inward rectification is an attribute of AMPARs lacking the GluR2 subunit, this subunit is largely absent in immature synapses. This developmental increase in GluR2 was concurrently confirmed using

assessment of GluR2 immunoreactivity (Kumar *et al.,* 2002). AMPA receptors containing GluR1/2 subunits during development, are eventually replaced by those composed of GluR 2/3 (Malinow & Malenka, 2002). In the adult hippocampus AMPA receptors made of GluR1/2 and GluR2/3 predominate (Wenthold *et al.,* 1996). Thus, it is important when assessing homoestatic plasticity to take into account the developmental stage and which AMPAR subunit to monitor.

During homeostatic plasticity there is evidence towards the selective up regulation of GluR1 but not GluR2 (Ju *et al.,* 2004, Sutton *et al.,* 2006, Thiagarajan *et al.,* 2005, and Gong *et al.,* 2007). Synaptic scaling due to CNQX/APV application results in the insertion of homomeric GluR1 AMPA receptors (Thiagarajan *et al.,* 2005, Gong *et al.,* 2007). However, things become more complicated with other contradictory results reporting that the GluR2 (Ibata *et al.,* 2008) subunit is required for synaptic scaling but not GluR1 (Gainey *et al.,* 2009). GluR3 is essentially found extrasynaptically but there is some evidence that synaptic scaling can alter the intensity and co-localization with GluR1 (Gainey *et al.,* 2009). However, in contradiction there are other reports that bidirectional regulation of GluR3 during CNQX or bicuculline treatment is not observed (Sun and Wolf, 2009).

Although it is still unclear what subunit is ultimately inserted/removed at the postsynaptic spine, it is clear that receptor insertion/removal is a fundamental mechanism behind homeostatic plasticity. It is possible that different systems and perhaps different approaches to modulating neuron activity can explain some of the uncertainties described above.

1.4. Presynaptic homeostatic mechanisms..

1.4.1. Homeostatic influence on vesicles.

Recently more weight has been given to presynaptic alterations occurring after chronic activity manipulations in the order of hours or days. As glutamate receptors are generally far from saturation during quantal transmission (Liu *et al.,* 1999) it is plausible that the compensatory changes in mEPSC amplitudes observed (Turrigiano *et al.,* 1998) can also

be explained by presynaptic changes in quantal content. The size of a quantal current varies among synapses and in principle their magnitude may be determined by postsynaptic receptor density, or the amount of transmitter released per vesicle.

Although different loading parameters, such as the external concentration of neurotransmitter outside vesicles and pH, can influence neurotransmitter filling there may be a "set point" that is determined by some other parameter such as the vesicular size and capacity. Varying the external glutamate concentration affects the loading rate (Wilson *et al.,* 2005). More provocatively, recent findings have proposed that altering the number of vGlut molecules per vesicle can affect the amount of vesicle filling and size. This was confirmed experimentally in several ways. Increasing the number of vesicular glutamate transporter (vGlut) expression in hippocampal cultures results in enhanced evoked and miniature amplitudes due to the release of more transmitters per vesicle (Wilson *et al.,* 2005). Conversely, vGlut 1 deficient mice exhibit reduced mEPSC release frequency and amplitude (Wojcik *et al.,* 2004).

This is puzzling, considering that there have been reports that single vGlut molecule is sufficient in vesicle refilling. In *Drosophila* it has been shown that a single transporter is sufficient to fill a vesicle and mutants lacking DVGLUT (the drosophila homologue of vGlut) have vesicles with a smaller diameter (Daniels *et al.,* 2006). If a single transporter is sufficient to load a vesicle, is altering the number of vGlut molecules per vesicles a possible mechanism for homeostatic plasticity? Under normal conditions vesicular filling is a slow process in the order of minutes (Wilson *et al.,* 2005). Therefore, homeostatic increase of transporters may increase the rate of reloading and affect quantal size during a sustained activity, where re-loading times are crucial. Similarly, if we assume that vesicle size is directly influenced by the number of transporters on a vesicle, then increases in vGlut number could lead to larger vesicles with a higher quantal content and vice-versa.

1.4.2. Homeostatic changes to presynaptic properties.

Confirmation of homeostatic regulation of presynaptic strength has come from several labs through genetic and pharmacological manipulations. In mature neocortical cultures, vGlut 1 and VIAAT mRNA and protein expression exhibit bidirectional and opposite

regulation after a 48hr treatment with TTX or bicuculline (De Gois *et al.,* 2005). Decreasing activity genetically with Kir2.1 in *Drosophila* muscle, results in increased evoked presynaptic neurotransmitter release amplitude and increased frequency in spontaneous events (Paradis *et al.,* 2001). Dlg (a tumor suppressor gene) mutant *Drosophila* motor neurons exhibit postsynaptic structural abnormalities. Here, vesicle size presynaptically appears to be larger in diameter suggesting some sort of compensation for the postsynaptic shortcomings (Karanunithi *et al.,* 2002).

Hippocampal cultures silenced with TTX for 5 days exhibit increases in the synaptic size as well as total number of vesicles per synapse and exhibited more FM-143 uptake in response to electrical stimulation. The average vesicle number released was almost double in comparison to controls. The number of docked vesicles which are part of the readily releasable pool (RRP) was also increased but when this was correlated to the size of the active zone it remained unchanged (Murthy *et al.,* 2001). In addition, some have reported that chronic mild depolarization by increasing extracellular K^+ alters vesicle priming (Moulder *et al.,* 2006). More evidence for synaptic vesicle recycling adapting to changes in activity was demonstrated with a combination of electrophysiology and uptake and release of styryl dyes in dissociated hippocampal and neocortical cultures. Hippocampal cells have high while neocortical cells have low intrinsic activity. Each brain region appeared to recruit different pathways to sustain release under repetitive stimulation with hippocampal neurons relying on vesicle mobilization while neocortical cells altered the rate of vesicle re-use (Virmani *et al.,* 2006). These results are interesting as they not only show activity-dependent regulation of presynaptic function but they also demonstrate that different excitatory cells may also utilize different ways to modulate their presynaptic gain during homeostatic plasticity. Thus, homeostatic mechanisms can also alter presynaptic output in response to chronic alterations to activity by regulating synaptic structure, vesicle number and release mechanisms.

Initially with the discovery of synaptic homeostatic plasticity the compensatory mechanisms were thought to be predominantly postsynaptic. This was concluded as a result of the observations in mEPSC amplitudes changes in response to chronic perturbations to activity (Turrigiano *et al.,* 1998, Ju *et al.,* 2004). However, changes only to the frequency of mEPSCs, thought to arise from changes in presynaptic function have

also been reported (Bacci *et al.,* 2001) while in other experiments concurrent increases in both amplitudes and frequencies *in vitro* (Thiagarajan *et al.,* 2002, 2005, Gong *et al.,* 2007) and *in vivo* have been observed (Echegoyen *et al.,* 2007).

An increase in frequency can be explained by more docked vesicles in the readily releasable pool, an increase in the kinetics of recycling or an increase in the number of functional synapses. Generally, most labs have observed that global activity manipulations do not result in a change in excitatory synapse number.

1.5. Synaptic retrograde and anterograde homeostatic plasticity.

Interestingly, the regulation of presynaptic gain appears to be controlled in part by the postsynaptic compartment probably through some retrograde signal. Hyperpolarizing the postsynaptic side through means of Kir2.1 expression on DIV2-5 in hippocampal cultures led to decreases in mEPSC frequency when recorded on DIV14 (Burrone *et al.,* 2002). Similarly in hippocampal cultures, chronic exposure to glutamate receptor blockers during synaptogenesis led to increased mEPSC frequencies (Bacci *et al.,* 2001). In an invertebrate model, postsynaptic blockade of GluRIIA (a glutamatergic receptor subunit) in *Drosophila* NMJ with philanthotoxin results in compensatory increases in presynaptic quantal content (Frank *et al.,* 2006). As alterations to the postsynaptic compartment appear to result in compensatory mechanisms presynaptically these results strongly suggest the existence of a retrograde signal from the postsynaptic compartment (Tao & Poo, 2001).

Interestingly, in *C.Elegans* eat-4 mutants, who have severely reduced function of vGlut, appear to exhibit compensatory increases in postsynaptic GLR-1 (Grunwald *et al.,* 2004). This implies either glutamate or some other presynaptic signal regulates the abundance of GLR-1 in an anterograde fashion and that both sides of the synaptic compartment can communicate to each other their needs in term of synaptic output. Although there are several candidates, who will be discussed in more detail later on, the transynaptic signals which control pre- and postsynaptic gain have not yet been identified.

In summary, it is now generally acknowledged that the presynaptic compartment plays just as vital a role as the postsynaptic compartment in the effort to compensate for

chronic alterations to activity during homeostatic regulation. This can be achieved through alterations to changes in synaptic structures involved in neurotransmission, vesicle number as well as the kinetics of release.

1.6. Developmental and spatial regulation of homeostatic plasticity.

With various experiments reporting either pre-/post-synaptic changes in response to chronic perturbations to activity, it is unclear whether presynaptic or postsynaptic mechanisms play a greater role or are equally important during homeostatic regulation. Some of the contradictions within the literature however, have been resolved by showing that the source of variation in the locus of homeostatic plasticity is dependent on the developmental time point the perturbations were made. It has been proposed that in neocortical cultures younger than ≤DIV14 chronic inactivity has a postsynaptic homeostatic locus as determined by an increase in mEPSC amplitudes. However, in more mature cultures (DIV18 or older) similar treatments result in an increase in mEPSC frequency and amplitude (Wierenga *et al.,* 2006). Critically this is dependent on the time the cells have spent *in vitro* rather than their post natal age as neurons cultured from older animals still behaved in a similar fashion. What determines this switch still remains unclear? However, these observations do reconcile some of the contradictions within the literature.

Complementary findings were reported when activity was manipulated in hippocampal cultures either at DIV 7 when synaptogenesis is in full swing or at DIV 14 when synaptogenesis has reached a plateau (Han & Stevens 2009). Here, it was reported that young neurons treated with TTX for 1 day use exclusively postsynaptic mechanisms to alter synaptic gain, whereas older cells increase synaptic strength through presynaptic mechanisms. However, if the duration of TTX is increased to 2 days both pre- and postsynaptic mechanisms are adjusted homeostatically in both young and mature cells.

In other experiments when functional inhibition was assessed after CNQX/APV or bicucculine treatment, a bi-directional homeostatic response was observed in terms of intrinsic excitability. This homeostatic response was determined to be sequential as

hippocampal slices treated with CNQX/APV on DIV 10 for 2 days exhibited altered excitatory but not inhibitory excitability. However, a 4 day treatment altered both. Moreover, when the same manipulation was carried out in older slices at DIV 18 a similar homeostatic change in functional inhibition was not observed (Karmarker & Buonomano, 2006).

As mentioned briefly before, individual cells which have had there activity reduced through the expression of Kir2.1 before the onset of synapse formation exhibit less functional inputs. On the other hand, suppression of activity after synaptogenesis results in a homeostatic increase in synaptic input (Burrone *et al.,* 2002). These results together demonstrate that the time point at which activity is altered and for how long clearly plays an important role in the locus and type of homeostatic response neurons deploy to compensate the perturbation.

1.7. Calcium and homeostatic plasticity.

Calcium has been considered a critical mediator in homeostatic plasticity. It was previously reported that calcium influx triggers receptor immobilization and accumulation at the cell surface while preventing lateral movement from synaptic to extrasynaptic sites (Borgdorff & Choquet, 2002). It has also been shown that homeostatic regulation can preferentially increase the levels of calcium permeable AMPA receptors lacking GluR2 (Gong *et al.,* 2007, Hou *et al.,* 2008). Therefore, it is possible that homeostatic insertion of calcium permeable AMPA receptors acts to increase and stabilize receptor numbers in the face of chronic inactivity.

Modeling studies have shown that an effective way of designing a homeostatic feedback loop is to use an integrator of calcium levels and to maintain this calcium signal at a "set point" (Marder & Prinz, 2002). However, what is the source of calcium involved in signaling homeostatic plasticity?

One possible source is NMDA receptors which have been implicated in playing an important role in both Hebbian and compensatory mechanisms. Concurrent blockade of NMDA receptors and sodium channels with TTX rapidly scaled synaptic strength faster

than that observed with TTX alone (Sutton *et al.,* 2006). Another possible source is L-type calcium channels. Chronic blockade of L-type calcium channels in forebrain cortical neurons results in enhanced mEPSC amplitudes (Gong *et al.,* 2007).

However, there are reports that L-type calcium channels do not contribute towards homeostatic changes. Chronic depolarization in dissociated cultures by means of increased extracellular potassium chloride results in increased mEPSC amplitudes. Application of nifedipine, an L-type calcium channel blocker though, did not prevent the reduction on quantal amplitude induced by high levels of potassium (Leslie *et al.,* 2001). Similarly, neurons from the Nucleus accumbens, a critical region in addiction, co-cultured with prefrontal cortical neurons to restore excitatory input, also did not exhibit synaptic scaling after treatments with nifedipine (Sun & Wolf, 2009).

In the mouse NMJ treatment with TTX increases the probability of release particularly in synapses with low probability of release. This was dependent on calcium influx into the presynaptic terminals entry through P/Q calcium channels (Wang *et al.,* 2004). Analogous results were observed in another model system. In the Drosophila NMJ the rapid and sustained expression of homeostatic plasticity was similarly dependent on $Ca_V2.1$, which is a P/Q voltage-gated calcium channel (Frank *et al.,* 2006). In addition, nematodes (*C.Elegans*) with mutations in *unc*-2, a gene which is responsible for encoding the α-subunit of a voltage-dependent calcium channel, exhibit greatly increases synaptic GLR-1 (a *C.Elegans* glutamate receptor) expression (Grunwald *et al.,* 2004).

Calcium thus appears to play an important role in the induction of homeostatic mechanisms. But what are some of the molecular effectors downstream which are activated by calcium influx?

Adenylyl cyclase 1 (AC1) and AC8 are the only ACs found in the central nervous system. After chronic blockade of L-type calcium channels AC1 but not AC8, was activated resulting in the insertion of homomeric GluR1 AMPA receptors. Genetic deletion of AC1 however, did not hinder inactivity induced GluR1 insertion when compared to wild-type (Gong *et al.,* 2007).

Other calcium activated proteins such as CAMKIV, which has a predominantly somatic/nuclear localization (Nakamura *et al.,* 1995), has also emerged as a possible protagonist in homeostatic plasticity. A 4hr treatment with TTX results in the

deactivation of somatic CaMKIV by a reduction in normally high phosphorylation levels exhibited during basal activity. The phosphorylation of CaMKIV requires CaM kinase kinase. Addition of the CaMKK inhibitor Sto-609 results in increased mEPSC amplitudes and synaptic accumulation of AMPAR (Ibata *et al.,* 2008). These results strongly suggest that a drop in postsynaptic activity results in a reduction of somatic calcium which subsequently reduces CaMKIV signaling.

More evidence in support of this enzyme´s involvement in homeostatic responses comes from studies showing that an inhibitor of CAMKII, KN93, prevents activity blockade-induced changes to mEPSC amplitudes (Thiagarajan *et al.,* 2002). In addition, findings show that the expression levels of the two isoforms of CaMKII, α & β, are inversely regulated by activity within hippocampal cultures. During increased activity there are higher expression levels of α than βCAMKII and vice versa during decreased activity. NMDA receptors appear to direct the activity dependent regulation of αCAMKII while AMPA receptors seem to control the levels of βCAMKII (Thiagarajan *et al.*, 2002). It will be important to discover possible proteins further downstream, which translate the actions of CAMKII into pre- and postsynaptic alterations during synaptic scaling such as the likes of hippocalcin, calbindin, calretinin and parvalbumin.

Raising intracellular calcium from IP_3 stores with adenophostin-A enhances EPSCs as well as IPSCs however, this effect was more pronounced in excitatory cells (Chen *et al.,* 2008). Therefore, another possible outlet of homeostatic plasticity could be the retrieval of intracellular calcium stores.

All these experiments imply that a palette of calcium related mechanisms can be brought into play during homeostatic plasticity which is not purely confined to postsynaptic alterations.

1.8. Evidence towards and against cell autonomous and synapse specific homeostatic regulation.

1.8.1. Cell autonomous homeostatic plasticity.

One pressing question in the field of homeostatic plasticity which is still actively pursued is whether it is a cell autonomous phenomenon. Evidence is beginning to accumulate suggesting that single cells are able to respond homeostatically to chronic perturbations to activity. Single cells which normally exhibit rhythmic busting behavior had been removed from the lobster STG (stomatogastric ganglion) and cultured individually. With the absence of any synaptic inputs and neuromodulators these cells initially fell silent. However, 3 days later the cells recovered the ability to generate bursting behavior by adjusting the densities of several voltage-gated gated channels (Turrigiano *et al.,* 1993). These results suggested cells could autonomously recognize they were not exhibiting appropriate levels of activity and were able of self regulation. In other experiments individual excitatory cells had their activity manipulated genetic means. When the inward rectifying potassium channel Kir2.1 was expressed in hippocampal cultures the activity was initially decreased. This is due to the hyperpolarizing current which is generated by the channel. Suppressing activity before synapse formation led to less functional synaptic inputs onto these cells. However, expressing the channel after synapse formation resulted in the activity within these cells returning to normal levels (Burrone *et al.,* 2002).

Interestingly, the homeostatic rules which govern inhibitory neurons do not seem to be cell autonomous as with excitatory cells. Rather, GABAergic synapses appear to alter their neurotransmitter content in response to the activity of the surrounding cells. Blocking activity globally with TTX on DIV 5 reduced GABAergic terminals as well as mIPSC frequency and amplitude. Suppressing activity later in development at DIV10 did not alter GABAergic synapse density. It did however, lower mIPSC amplitude. When single cells expressed Kir.2.1 at DIV5 & 10 reducing their activity, there was no change to GABAergic inputs. Reducing activity in cells using a siRNA towards sodium channels also did result in the change in GABAergic synapses (Hartman *et al.,* 2006). Thus, different rules may be in place governing synaptic strength during homeostatic plasticity in excitatory and inhibitory cells with the former being cell autonomous and the latter influenced from network wide activity.

1.8.2. Non cell autonomous influences.

Other studies however, have suggested that the network as a whole might be influencing compensatory changes. Excitatory synapses onto GABAergic cells appear to be homeostatically regulated through the release of BDNF (brain derived neurotrophic factor) from pyramidal neurons. It was demonstrated that exogenous BDNF prevented, while TrkB-IgG (tyrosine kinase receptor) mimicked the effects of activity blockade in terms of mEPSC amplitudes. These effects appear to also be opposite in excitatory and inhibitory rat visual cortical neurons (Desai *et al.,* 1998).

Additionally, it has been shown that pro-inflammatory cytokine tumor-necrosis factor-a (TNFα) induces synaptic scaling in response to prolonged activity blockade. TNFα was first described in inflammatory responses to injury and has been shown to play a critical role in cell proliferation, differentiation and apoptosis (Liu *et al.,* 2005). Surprisingly, the source of TNFα is glial cells rather than neurons and cause rapid exocytosis AMPA receptors lacking GluR2 through activation of PI3K. Reversely, TNFα causes $GABA_A$ receptors to endocytose. When conditioned medium was placed on untreated cultures from sister cultures which had their activity blocked with TTX for 48hrs this induced synaptic scaling. If the conditioned medium had been treated however, with a soluble form of TNFα receptor (sTNFR), this prevented synaptic strengthening. This confirmed that a soluble factor was indeed involved (Stellwagen *et al.,* 2006). TNFα until recently was not thought to be involved in modulating LTP suggesting that Hebbian and homeostatic regulatory pathways are distinct. This however, may not be the case as TNFα has been shown to inhibit LTP (Pickering *et al.,* 2005). This data argues an equal partnership between glial and neurons in homeostatic regulation.

Interestingly though, synaptic scaling tends to materialize within 24hrs or even earlier as mentioned in previous experiments, TNFα though, increased synaptic strength after 48hrs. This suggests that homeostatic scaling induced before 24 hours is not mediated by TNFα. Maybe TNFα is recruited after sustained activity deprivation as an additional measure. Therefore, classical homeostatic regulation may be activated initially within under 24hrs after activity perturbations. However, if the aberrant activity continues glial influences are recruited to strengthen even more the homeostatic drive. Glial release of

TNFα and its effect on neuronal homeostatic plasticity can be thought of as a network influence as its release has sway on the surrounding neurons and its extent depends on how far it can reach from its source before it is taken up or degraded. However, synapses are now considered to be tripartite and glial cells have been shown to interact at the level of individual synapses (Araque *et al.,* 1999). Thus glial induced homeostatic plasticity could theoretically still operate locally.

1.8.3. Synapse specific homeostatic plasticity.

Recently, a fundamental concept of homeostatic plasticity is beginning to be questioned. That is, does it act by scaling up or down the strength of all synapses in a cell wide manner or can homeostatic plasticity act at the level of individual synapse? When homeostatic responses are induced by global pharmacological manipulations it is difficult to determine if individual synapses can be homeostatically regulated as all neural components are affected indiscriminately. Under such experimental conditions similar results would be observed if homeostatic plasticity is synapse specific or cell wide. Similarly, it is difficult to ascertain if altered pre- or postsynaptic neuronal excitability is what initiates these responses.

However, several experiments have been carried out demonstrating that homeostatic regulation can occur at the level of the individual neuronal segments or synapses. Individual synapses which had presynaptic axonal activity selectively reduced through overexpression of Kir2.1 had increased GluR1 and Glur2/3 accumulation at the corresponding postsynaptic partner (Hou *et al.,* 2008).

However, other experiments which expressed tetanus toxin in single cells reducing presynaptic activity by blocking all vesicles mediated membrane fusion, found no change in postsynaptic GluR2/3 or PSD-95 and showed a decrease in synaptic GluR1 levels. Surprisingly, silenced neurons formed as many presynaptic terminals as their active neighbors suggesting neurotransmitter release is not necessary for axons to compete for synaptic terminal (Harms *et al.,* 2005). The discrepancies between these experiments that selectively inhibit activity presynaptically in individual synapses may be due to

differences in experimental procedure. With overexpression of Kir2.1, only the action potential-mediated synaptic activity is suppressed leaving the machinery involved in vesicle fusion intact. The tetanus toxin approach however, completely ablates vesicle fusion.

The Kir2.1 experiments were interesting because they showed that inhibition of the presynaptic side induced homeostatic responses postsynaptically. However, when they looked at the postsynaptic side of cells expressing Kir2.1 no changes in AMPAR accumulation was observed. Similar manipulations with Kir2.1 at the postsynaptic side however, resulted in enhanced presynaptic neurotransmitter release in rodent (Burrone *et al.,* 2002) and Drosophila models (Paradis *et al.,* 2001). The implication of individual synapses being able to respond homeostatically suggests that a sensor must exist within each synapse, possibly on both pre- and post synaptic compartments (Rich & Wenner, 2006).

Moreover, more evidence has emerged in support that synapses can be individually regulated locally by homeostatic mechanisms. Using ReScH-EDT(2) and FlAsH-EDT(2) staining, to monitor AMPA receptor subunits synthesis and trafficking, it was shown that activity blockade increases dendritic GluR1 but had much smaller effects on GluR2 in transected dendrites, i.e. dendrites which have physically been severed from the rest of the cell. However, when they used an acute manipulation and applied a high concentration of extracellular K^+, a protocol thought to induce LTP, this increased both GluR1 and 2 in isolated dendrites. This visualization method of AMPA receptors is accomplished by inserting a tetracysteine motif into the intracellular C terminal of GluR1 and 2 which when bound to biarsenical dyes become fluorescent (Ju *et al.,* 2004). These results suggest that local translation can drive GluR expression during homeostatic plasticity further strengthening the possibility of synapse specific homeostatic. In addition it implies that the machinery involved in sensing chronic perturbations to activity is located locally within the vicinity of synapses rather than at the cell soma.

1.8.4. Contradictions, caveats in synapse specific homeostatic plasticity and how they can be reconciled.

Evidence against synapse specific homeostatic plasticity has come from experiments in which individual cortical pyramidal neurons had their activity blocked through local perfusion of TTX at the cell soma. This induced synaptic scaling as a result of a drop in somatic calcium influx and reduced activation of CAMKII. However, when activity was blocked locally at individual synapses, this was not sufficient to induce a homeostatic response locally as assessed by synaptic AMPAR accumulation (Ibata *et al.,* 2008).

There is a caveat with synapse specific homeostatic plasticity. This phenomenon implies that any modifications made by Hebbian mechanisms could be erased. This would inevitably counteract any associative strengthening or weakening bringing all synapses to their set points. However, this paradox can be explained if you envisage that synapses are not isolated from their adjacent neighbors. Rather they are interconnected through calcium fluctuations and electrical interactions. A potentiated synapse will not only alter activity locally but also to surrounding synapses. Thus, homeostatic influences will not only influence a potentiated synapse but the adjacent ones as well. In doing so, individual synapses can maintain a significant fraction of their potentiation during homeostatic mechanisms as surrounding non potentiated synapses will also be affected (Rabinowitch & Segev 2006/8). This theoretical study suggests that homeostatic plasticity can scale the neighboring synapses in the opposite direction to the one that has undergone Hebbian plasticity allowing the two mechanisms to co-exist.

1.9. Genetic mechanisms of homeostatic plasticity.

The field of homeostatic plasticity and synaptic-scaling is relatively young and the molecular signaling pathways involved are still poorly understood. How are extremes in activity sensed and translated to modifications in synaptic gain? Although the effects of homeostatic plasticity are evident in the various structural and functional changes that

occur at the level of the synapse it is still not clear which genes control and regulate this process.

One gene which has been implicated is ARC/ARG3.1. This early immediate gene during high levels of activity is turned on resulting in removal of AMPA receptors by activating an endocytic pathway that internalizes GluRs (Shepherd *et al.,* 2006). Over expression of this gene blocks synaptic scaling observed after chronic inactivity while loss of the gene results in increased AMPAR insertion.

CREB, a stimulus-induced transcription factor was shown to be phosphorlylated at Ser133, a prerequisite for CREB induced gene transcription, after CNQX treatment. This was thought to be calcium dependent as nifedipine replicated these results (Gong *et al.,* 2007). Therefore, genes implicated in LTP, i.e. CREB, are also able to regulate homeostatic pathways. Undoubtedly, more genes will be discovered which are involved in homeostatic plasticity revealing how the various biochemical pathways are controlled.

Many additional questions remain. How is the set point of neural activity achieved? What are the mechanisms involved in monitoring activity (Turrigiano *et al.,* 2007) or receptor blockade (Wilhelm & Wenner, 2008)? Three cell types may be involved in sensing changes in activity: the presynaptic neurons, postsynaptic neurons and glial cells. This, to some extent, is dependent on when activity is altered. Blocking activity before, throughout or after synapse formation produces different results (Burrone *et al.,* 2002, Wierenga *et al.,* 2006). Also which proteins coordinate the insertion and removal postsynaptic receptors is still not clear? Are the same proteins recruited during homeostatic and Hebbian plasticity to chaperone these receptors to the cell membrane?

Homeostatic regulation has been demonstrated in various brain regions such as the Nucleus accumbens (Sun & Wolf, 2009), visual cortex (Desai *et al.,* 2002), hippocampus (Burrone *et al.,* 2002), spinal cord (Borodinsky *et al.,* 2004) as well as *in vivo* (Echegoyen *et al.,* 2007) and *in vitro* (Turrigiano *et al.,* 1998) systems. There is a large body of literature on homeostatic plasticity; however, with a lot of labs reporting contradictory results, as yet, there is still no clear mechanism on the induction of homeostatic plasticity and the ensuing compensatory changes which occur.

In light of all the information at hand and the confusion at times of trying to reconcile them, we set out to explore how homeostatic plasticity manifests itself structurally and

functionally at the level of the synapse in response to chronic perturbations to activity. Here, in hippocampal cultures, we demonstrate that homeostatic plasticity results in activity-dependent bidirectional changes in synaptic proteins in such a manner that opposes the disturbance. We also demonstrate that these structural changes directly result in corresponding functional changes. In addition, we probed for any differential homeostatic regulation between excitatory and inhibitory cells. Homeostatic synaptic alterations were defined structurally with immunohistochemistry and high resolution electron microscopy and functionally with whole cell patch electrophysiology.

Our final goal was to further explore if perturbations in single cells can result in homeostatic plasticity, in other words, whether this phenomenon is a cell autonomous feature. This was achieved with optogenetic tools. We provide compelling evidence with immunohistochemistry and whole cell patch electrophysiology that genetically modified single cells, were able to exhibit cell autonomous homeostatic regulation when their activity was precisely controlled. In addition, we show how optogenetics can be used to further explore more facets of cell autonomous homeostatic plasticity.

2.METHODS

Animals

E17.5 pregnant rats (Sprague Dawley) were purchased from Charles River Laboratories.

Cell Culture.

Dissociated cultures of hippocampal CA1-CA3 neurons were prepared from E17.5 sibling embryos. During the extraction of the hippocampus a small amount of cortical tissue will have inevitably also been included. Tissue was kept in 2ml of HBSS. 10mg/ml of trypsin was added to the medium and placed in a 37° C water bath for 13 min for subsequent dissociaton. The tissue was then transferred to a 15 ml falcon containing 4ml of NB/FBS and triturated using combination of fine pore fire polished Pasteur pipettes (Volac). Once the tissue was dissociated the cell density was determined using a haemocytometer. Cells were then transferred onto 12 well plates (Corning Incorporated) containing glass coverslips (Thermo Scientific). The coverslips were pre-treated overnight with PDL (50mg/ml), a synthetic molecule used as a coating to enhance cell attachment. The PDL was then aspirated away and the coverslips washed twice with PBS. This was then followed by a final coating of laminin (50µg/ml), a protein found in the extracellular matrix, to further help anchor the dissociated hippocampal cells. The cells were maintained in a mixture of 500ml NB/B27 (promotes neural growth) and 500ml NB/FBS (promotes glial growth), each supplemented with Glutamax and Pen/Strep (dilution 1/100). Glutamax improves cells viability and growth while preventing build up of ammonia and Pen/Strep helps to prevent any infections. Cell density for each coverslip lied between 75000-9000 cells. Cells were kept in an incubator at 37˚ C in 6% CO2.

Media.

-Hanks Balanced Salt Solution (HBSS) - Invitrogen
-Trypsin derived from bovine pancreas - Worthingtons

-Neurobasal Media (NB) - Invitrogen.
-B27 supplement - Gibco-Invitrogen
-Fetal Bovine Serum (FBS) - Invitrogen
-Glutamax - Sigma
-Penicillin Streptomycin (Pen/Strep) - Sigma
-Poly-D-Lysine - Sigma
-Laminin - Invitrogen
-Phosphate Buffered Saline (PBS) - Invitrogen

Plasmids and vectors

We used under normal transfection procedures the lentiviral vector pLenti which expressed ChR2 under a synapsin promoter. pLenti-Synapsin-hChR2(H134R)-EYFP-WPRE. Information on the pLenti ChR2 construct with synapsin promoter is available at this resource, http://www.everyvector.com/sequences/show_public/2506
In addition we also used a vector with the alpha-CAMKII promoter expressing an EGFP.

Drug treatment and Pharmacology

Drugs were added directly to culture medium or extracellular HBS at the concentrations given below; from a 1000 X concentrated stock solution.

Drug	**Provider**	**Concentration**	**Target**
Gabazine SR-95531	Sigma	1μM	$GABA_A$ blocker
TTX Tetrodotoxin	Cal-tag Systems Ltd	1μM	Sodium channel blocker
CNQX 6-cyano-7-nitroquinoxaline-2,3-dione	Sigma	1μM	AMPAergic receptors
APV	Sigma	1μM	NMDA

((2*R*)-amino-5-phosphonovaleric acid; (2*R*)-amino-5-phosphonopentanoate)			receptors
Nifedipine	Sigma	1μM	L-Type calcium channels

Electrophysiology & mEPSCs:

Patch clamp recordings from cultured hippcampal neurons were performed using a HEKA EPC10 amplifier. Electrode tips (World Precision Instruments) had a resistance of 2-5 MΩ. The intracellular solution contained 130mM K^+-gluconate, 10mM NaCl, 1mM EGTA, 0.133mM $CaCl_2$, 2mM $MgCl_2$, 10mM HEPES, 3.5mM MgATP and 1mM NaGTP. During an experiment, cells were maintained in an external solution of 136mM NaCl, 2.5mM KCl, 10mM HEPES, 10mM Glucose, 2mM $CaCl_2$ and 1.3mM MgCl at a pH of 7.3 and an osmolality of 290Osm/L. Currents were recorded in voltage-clamp mode at a holding potential of -70 mV. Recordings were filtered at 10kHz and acquired at 20kHz. When recording mEPSCs, the extracellular medium was supplemented with 1nM TTX and 10nM Gabazine to block action potentials and $GABA_A$ receptors, respectively. Patch resistances were monitored throughout the recording and recordings were discarded if the resistance changed by 10% or more. Data was acquired using Pulse software and analyzed using the Mini Analysis program (Synaptosoft). The software automatically detects the amplitude from baseline and relative parameters once a mini is chosen by eye. mEPSCs were analyzed blindly. We used responses to a 10-mV hyperpolarization step to estimate the series resistance (RS) of the recording (<20 MOhms for all cells; from the current peak), and the neuron's membrane resistance (Rm; from the steady holding current at the new voltage) and membrane capacitance (Cm; from the area under the exponential decaying current from peak to holding).

Primary neuronal culture for MEA electrophysiology

Hippocampi were dissected from E17.5 C57BL/6 c/c mouse embryos and transferred to papain (10 units/ml) for 22 min at 37°C. Cells were manually dispersed in PBS and centrifuged twice at 400 x *g* for 3.5 min. The final pellet was resuspended in NB/B27 0.5 mM Gln, and dissociated cells were plated onto poly D lysine and laminin-coated substrates at a density of 500 cells/mm2.

MEA Electrophysiology.

Cells were plated directly onto coated MEA that consisted of 8 x 8 grids of titanium nitride electrodes of 30μm diameter and inter electrode spacing of 200 μm (Multi Channel Systems, Reutlingen, Germany). Spontaneous action potentials were recorded (30-min epochs at 2- to 3-day intervals) in Mg2_-free Locke solution (140 mM NaCl, 3 mM KCl, 15 mM Hepes, 10 mM glucose, 1 mM CaCl2). Cultures were maintained in $Mg2^{+}$ containing medium (Neurobasal), but recordings were made in the absence of this ion to allow full activation of NMDA receptors. Spikes were detected and analyzed by using MC Rack (Multi Channel Systems) and Neuroexplorer (Nex Technologies, Littleton, MA). To construct the sigmoidal curve, normalized total spike count was fitted to the equation $y = 1 - 1/(1 + \exp((X - X_0)/dX))$, in which X is time of recording, $X0$ is the time for half of the maximum number of spikes, and dX is a time constant. In parallel, the number of active electrodes, i.e., the electrodes able to detect at least one action potential per min, was also plotted against time in culture. The percentage of total mean frequency is the average of the normalized spike count expressed as a percentage of the maximum value.

Transfections

All constructs were transfected using Lipofectamine 2000. On the day of transfections, half the conditioned medium (NB/B27/FBS/Glutamax/pen-strep) from each well was removed (i.e. 500ml) and mixed in with an additional 500ml of fresh medium. This was then filtered to remove any cell debris and kept at 37˚ C in a water bath. Each well was

then replenished with 500ml of fresh medium. For each coverslip a mixture of Lipoefectamine and DNA in 50µl of Optimem was prepared at a ratio of 1µg:1 µl and was placed in each well for approximately 10-20min while kept in the incubator. The entire medium from each well was then aspirated and replaced with the medium that was kept in the water bath.

Fixation and Immunohistochemistry

Cells where fixed in one of two ways:
4% PFA- Cells were fixed with PFA for 20 min
Methanol- Cells were fixed in methanol for 5 min at -20˚C

Cells were then permeabalized using 0.25% Triton X-100 for 5 min. Cells were then placed in 10% Bovine Serum Albumin (BSA) for 1hr at room temperature to block any non-specific protein interactions. All antibodies were prepared in 3% BSA. Cells were incubated in primary antibodies overnight at 4˚C and then washed three times PBS. Secondary antibodies were then applied and kept at room temperature for 1hr followed by another 3 washes with PBS. Coverslips were then mounted with Mowiol onto glass coverslides.

Mowiol 4-88 Reagent-Calbiochem

2.4 g of Mowiol was added to every 6 g of glycerol and stirred at room temperature for several hours. 12 ml of 0.2 M Tris (pH 8.5) was added and heated to 50˚C for 10min with occasional mixing. Once the Mowiol has dissolved the solution was clarified by centrifugation at 5000 x g for 15 min. Before use DABCO (Sigma) was added.

Primary Antibodies

Antibody	Supplier (Product Code)	Dilution	Developed in / conjugate
PSD95 Clone 7E3-1B8	Millipore (Chemicon) MAB1598	1:200	mouse
vGlut1	Synaptic Systems 135 303	1:2000	rabbit
Synaptotagmin 1	Synaptic Systems 105221 lumen domain	1:500	mouse
Gephyrin	Synaptic Systems 147011	1:1000	mouse
vGAT	Synaptic Systems 131003	1:1000	rabbit
Synaptobrevin, Vamp2	Synaptic Systems 104211	1:500	mouse
GluR2	Millipore MABN71	1:300	mouse
Synapsin 1	Synaptic Systems 106001	1:500	mouse
Anti chicken	Molecular Probes A11039	1:1000	Alexa Fluor 488
Anti-mouse	Molecular Probes A31621	1:1000	Alexa Fluor 555
Anti-rabbit	Molecular Probes A21071	1:1000	Alexa Fluor 633

Imaging

All live cell imaging was done with a FV1000 Olympus confocal microscope using a water immersion 40x objective with a N.A. of 0.80. Images were taken using a combination of lasers and filters depending on the fluorophores used. The following lasers were regularly used: 488 nm, 543 nm and 633 nm. Lasers scans on samples with multiple fluorophores were performed sequentially to avoid any cross talk between channels and the corresponding excitation/emission filters were used in each case. Bleed-through between different channels was assessed whenever a new setting was implemented and found to be negligible for all experiments described here. Images were taken at 1024 x 1024 resolution, at a zoom of 2 X. This provided a good resolution to properly resolve synapses, whilst also acquiring a large field of view. In each case, care was taken to work within an optimal fluorescence range, avoiding saturation of any of the fluorephores. The pin-hole size was adjusted automatically by the software to achieve maximal confocality and minimal interference form out-of-focus light. Z-stacks were taken at 0.5 μm intervals to image the entire field of view.

Image analysis

Image stacks (0.5 μm *z*-axis steps) were exported as raw 16-bit TIFF files, and imported into Matlab (Mathworks) for analysis using custom-written routines. Regions of interest (12 by 12 pixels large) were selected, encompassing the entire synapse with both pre and postsynaptic compartments. A measurement of back ground levels of fluorescence was taken from a non-labelled area to establish the amount of noise in the signal. The fluorescence intensity for each channel was measured for all z-planes and subsequently background subtracted. The largest fluorescence intensity value for each synapse within the stack was taken to indicate the best focal plane. In general , 30 regions of interest were selected for each image and for each condition and averaged. Data sets compiled from different experiments were normalized to controls and analysed blindly.

Measurement of synapse density

Within a field of view, all dendritic sections of neurons, excluding any axons, expressing EGFP or ChR2-EYFP were traced using the Neuron J plugin image J. Using a known scale for each image we converted length in pixels into actual dendritic lengths in image J (65μm=1024 pixels). The sum of all dendritic branches was then calculated. Using a custom written routine in Matlab, ROIs were chosen for all synapses that were in direct contact with the dendrite which had been traced in neuron J. An index of dendritic synapse density per cell was then calculated by dividing the number of synapses by the sum dendritic length. Values from various cells where then averaged per each condition.

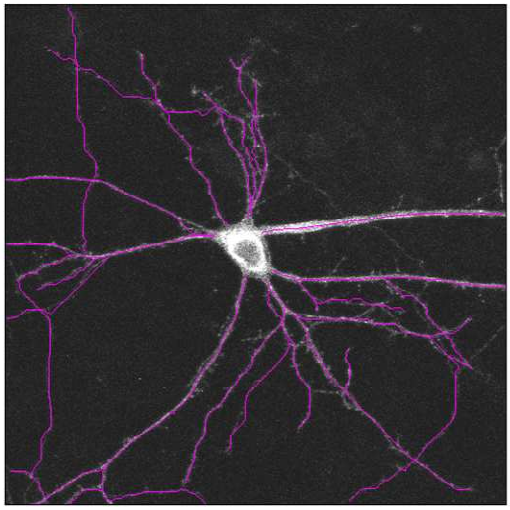

Fig.2.1. Example of image processed in Neuron J plug in, for image J software. Example of a cell expressing GFP processed with Neuron J in which dendritic arborizations were traced providing a measurement of total dendritic length within the field of view.

Electron Microscopy

All fixations, embedding and cutting were carried out by Ken Bradey and Alice Warley from the Centre for Ultrastructural Imaging, Kings College as follows.

-Tissue was fixed in 2.5% Glutaraldehyde Fixative (pH7.3) and left in the fridge (4˚C) for 4 hours and then transferred to glutaraldhehyde solution (phospahate buffer at pH 7.3) for storage in a fridge until ready to process.
-Tissue was then post-fix in osmium tetroxide fixative (Millonigs Buffer pH 7.3) for 90 minutes in the fridge at 4˚C.
-TAAB premix medium resin kit was then mixed. Resin was added to the hardener and placed in a bottle on a Luckham Multimix Major (Roller).
- Embedding labels were prepared, cut and then placed into the embedding moulds. Embedding boxes where labeled ready for the resin blocks.
-Samples were dehydrated in 10% ethanol for 10 minutes and placed on the roller at room temperature.
-Samples were then dehydrated in 70% ethanol for 30 minutes and placed back onto the roller.
-Samples were then dehydrated in 100% ethanol for 20 minutes and placed back onto the roller.
-Samples were then dehydrated in 100% ethanol for 20 minutes. The accelerator was then added to the resin and the samples and the resin were once more placed on the roller.
-Samples were dehydrate in 100% ethanol for 20 minutes one final time and placed back on the roller.
-The samples were then put into propylene oxide for 10minutes which is a link reagent for the resin and placed back onto the roller.
-Samples were placed into a resin/propylene oxide mixture of about 50% of each, for 90minutes and placed back on the roller.

-Samples were put into 100% resin to roll for about 6 hour and stored in the fridge overnight and the resin was kept in the freezer.
- TAAB Embedding oven was warmed up and the prepared embedding moulds were placed inside. Samples were removed from the fridge and resin from the freezer and placed on the roller for 30 minutes.
-Embedding was setup: tissue paper, glass slide, razor blade, small pipette, fine pipette, flat stick and cocktail stick.
-We pipetted 3 drops of resin to each coffin mould and placed the tissue in the coffin mould and orientated it to the desired cutting surface. Coffin mould was topped up with resin and any visible air bubbles were removed.
-The complete embedding mould was placed into the embedding oven and left to polymerize for 24hours.
- Polymerized resin blocks were removed and put into the prepared embedding boxes.
-Ultra thin sections of the selected viewing area (60nm thickness) were cut on Leica Ultra-cut machines and picked up on to 150 mesh Guilder grids with a support film of Pioloform.
-The grids were then stained with Uranyl Acetate and lead Citrate.
-The grids were viewed in the Hitachi H&600 Transmission Electron Microscope at X 70000 magnification.

Electron microscopy Analysis.

Electron microscope images were analysed using the free software *reconstruct* provided by www.synapses.bu.edu. Structures such as vesicles and post synaptic densities were traced manually using the function available in the software. Reconstruct works in arbitrary system of units. The user defines the units of measurement. Calibrations for values and conversions into actual lengths and sizes of structures were done using the scale provided in each image and the according magnification. To calculate the number of docked vesicles, i.e. the Ready Releasable Pool, we counted all vesicles within a distance of 2 vesicles from the cell membrane at the active zone.

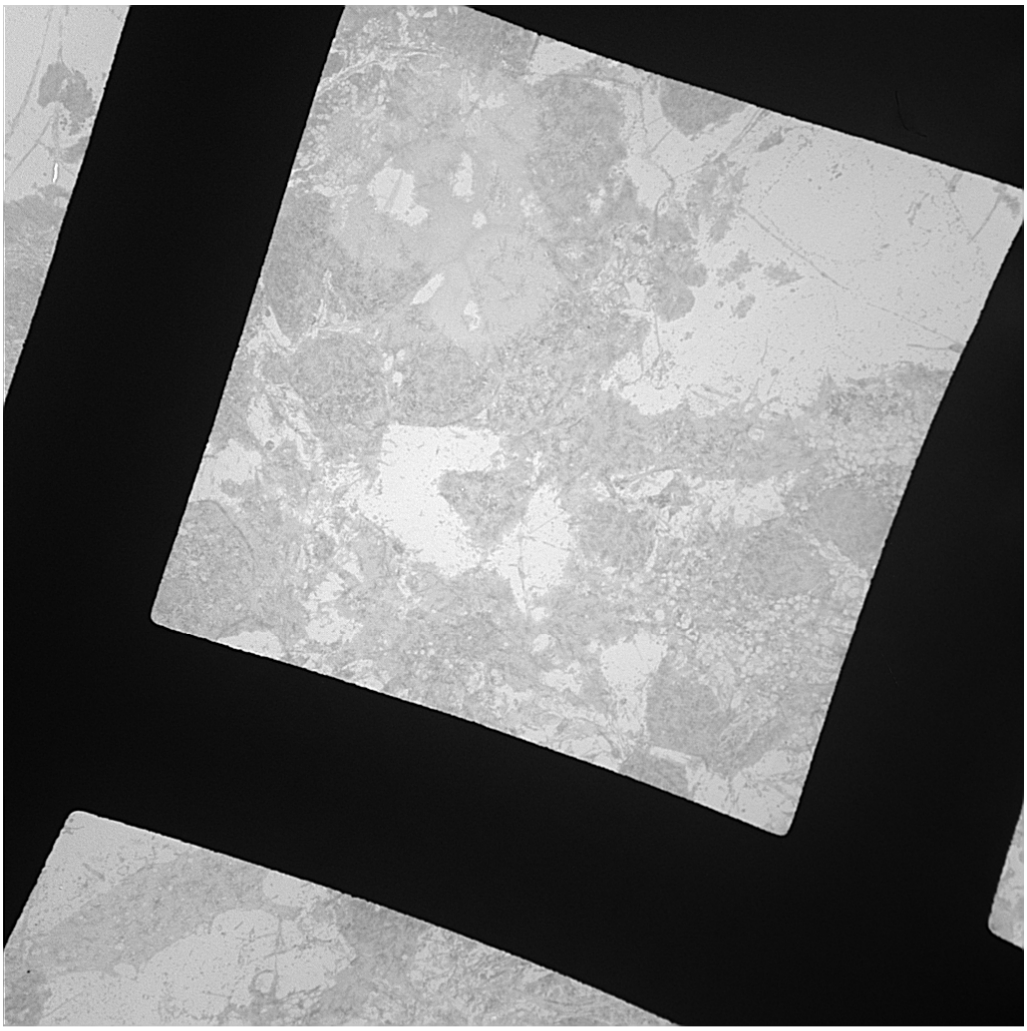

Fig.2.2. Example of an *In Vitro* Hippocampal culture embedded in a Guilder's grid.

Example image of an DIV 13 hippocampal culture embedded in a Guilder's grid. Image was taken at a low magnification (700 X) encompassing an entire grid block.

Photostimulations

Acute photostimulation of ChR2+ive neurons was carried out with a Xenon-arc lamp - (Lambda-LS, Sutter Instruments) using the appropriate excitation filter (470 +/- 15 nm; Chroma Tech. Corp.), and an Olympus 40× oil immersion objective, that had a power at the output of the lense of 170 mW.mm^{2}**.** For long-term photostimulation within the incubator, we placed 12-well culture plates directly onto a bed of collimator-topped blue LEDs (Royal Blue Luxeon K2, Philips LumiLEDs; 455 ± 10 nm; ~1 mW mm^{-2} at the coverslip surface), powered by a custom-made driver (a gift from N. Grossman and P. Degenaar) and controlled by a Master-8 stimulator (AMPI) that fed into a custom-made interface driver (a gift from Dr. Grossman) and powered by a high current power source (Thurlby Thandor Instruments, PL320) that could reach the 1Amp currents that optimally drive the LEDs. The flash duration used for all experiments was 30 ms. Pulses were delivered in bursts of **7** flashes at 20Hz very 75 seconds, ensuring at least one spike per stimulus (an average of 2 in all cells tested) in all ChR2-positive neurons. All coverslips in a given plate received the same pattern of photostimulation. Control (unstimulated) plates were kept in the same incubator and covered in tin foil to avoid any photostimulation from stray LED light.

Fig.2.3. Royal Blue Luxeon K2, Philips LumiLEDs.

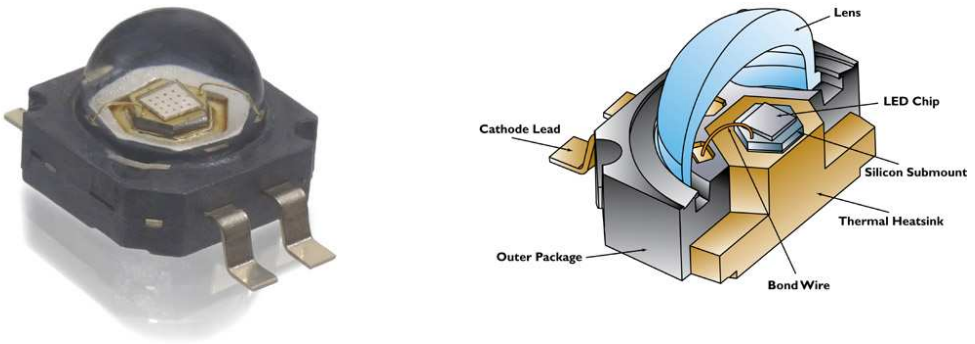

Statistical Analysis

All means were compared using a student's t-test or One-way ANOVA where suitable and normality was determined by a Kalmogorov-Smirnov test and D'Agostino & Pearson omnibus normality test. When not normally distributed, means were compared using a Kruskal-Wallis test unless otherwise stated. All experiments were analyzed blind to the experimenter. Error bars in figures represents s.e.m.

Power calculation.

Post hoc power analysis does not provide any more information than that provided by the appropriate statistical test. If a test is significant, then by definition it will have a high power (and a low one if not significant). The only situation in which the power calculation can be useful is to calculate the measurements needed to establish with confidence a difference that may be scientifically important. However, we have performed power calculations in a few key experiments, to show the power of the experiment in detecting a difference between conditions. These are shown in the annex. Ultimately, what is important is to perform the experiments using the right controls. This is especially the case in situations where the variable being measured can be changed from one set of cultures to the next. This is one of the main reasons why the data is always normalized to its corresponding controls. This was done for both imaging and electrophysiology data. Power calculations were done using GraphPad Statemate software to determine the power of completed experiments between 2 groups using standard deviations. Values provided are for 70% power.

FM4-64 imaging

To identify functional presynaptic terminals, we labeled recycling synaptic vesicles using 10 mM FM4-64 (Molecular Probes). Neurons were depolarized for 60 s using a hyperkalaemic solution (in mM): 78.5 NaCl, 60 KCl, 10 HEPES, 10 D-glucose, 2 CaCl2, 1.3 MgCl2, 0.05 AP5 (D(-)-2-amino-5-phosphonovaleric acid), 0.005 CNQX (6-cyano-7-

nitroquinoxaline-2,3-dione), and 0.001 TTX. Coverslips were then washed in regular extracellular medium without FM4-64 for 10 min before imaging to reduce the background fluorescence caused by non-internalized dye binding to the cell membrane. Image stacks (Z steps of 1 μm, 7–10 steps) were obtained using a confocal microscope (Olympus Fluoview attached to a BX50WI, X 40, 0.8NA water lens). EGFP and FM4-64 signals were acquired simultaneously using 488-nm excitation, and 510–550-nm band pass and 585 long-pass emission filters, respectively. Transmitted light images were taken separately to identify cell bodies and processes of non-transfected neurons. We chose to measure the density of presynaptic terminals in the proximal regions of the dendrites (about 100 μm from the soma) as these could be identified unequivocally by the EGFP fluorescence

3. Results Chapter.1- Synaptic homeostatic plasticity in response to global activity manipulations.

3.1. Synaptic maturation.

Neurons are required to detect correlations in the external environment and store them in the form of synaptic modifications. This is accomplished through mechanisms such as long term potentiating and long term depression which are widely considered to be the cellular models of learning and memory. These forms of plasticity otherwise known as associative or Hebbian plasticity adjust specific synaptic weights according to how correlated the activity between the pre- and postsynaptic compartment is. Through computational modelling studies though, it has been appreciated that their implementation in neural networks carries an inherent stability problem (Miller & Mackay, 1994). In the absence of any normalising features, neural circuits undergoing Hebbian forms of plasticity could result in one of two outcomes: runaway excitation, resulting in saturation of synaptic gain, causing synapses to become unresponsive due to ceiling effects or quiescence, resulting in a loss of information transfer (Turrigiano & Nelson, 2004). This, therefore, raises the question as to how neurons are able to maintain a stable network against a backdrop of ongoing perturbations from Hebbian plasticity. In response to this problem it recently emerged that neural circuits are subject to homeostatic regulation which serves to stabilize neural function (Turrigiano, 2007). One way in which this is achieved is through the detection of changes to the average firing rate and the subsequent 'scaling' of synaptic strengths (Turrigiano *et al.,* 1998). If this negative feedback mechanism was not in place it could lead to neuronal activity reaching detrimental extremes.

Two important distinctions between Hebbian and homeostatic forms of plasticity are the temporal and spatial scales in which they functionally and structurally shape networks. LTP can induce the insertion of AMPA receptors into the postsynaptic membrane in a synapse specific manner within a timescale of minutes (Hayashi *et al,* 2000, Malinow & Malenka, 2002, Malinow *et al.,* 2004), while synaptic scaling works

more gradually over a period of hours and days, inserting AMPA receptors at synapses throughout the dendritic arbours in a cell wide manner (Ibata *et al.,* 2008). Homeostatic plasticity is still in its infancy and there is still much that remains unclear. We know that extreme chronic changes in activity trigger a homeostatic response which results in presynaptic structural changes as well as receptor numbers being adjusted in the postsynaptic membrane. However, the underlying mechanisms behind homeostatic plasticity and how it manifests itself structurally and functionally at the level of the synapse is far less understood than the classical forms of Hebbian plasticity and are only recently beginning to be unravelled.

To try to shed some light on these issues we first sought to elicit a homeostatic response in rat hippocampal cultures. Although findings in culture may represent an exaggerated phenomenon in comparison to that *in vivo*, the simplicity of this system allows investigation of neuronal processes and network dynamics that may be present to some degree in more complex *in vivo* systems. Homeostatic responses were induced by chronically altering the activity of neurons and assessed by exploring for any structural changes at the level of the synapse that may have occurred in response to this perturbation. Chronic changes in activity were achieved by adding pharmacological blockers to the culture medium at a developmental time point in which the bulk of synaptogenesis had occurred and was considered to be synaptically mature (Renger *et al.,* 2001). Characterising a mature synapse in the central nervous system has been challenging due to the diversity of both their functional and molecular properties including release and ion channel/receptor complements. Efforts, however, have been made to determine this time-point structurally as well as functionally using rodent models. In rodent hippocampal cultures the developmental timeline of synaptogenesis has been well described using imaging and electrophysiology techniques (Valour *et al.,* 2007, Renger *et al*., 2001).

A synapse is defined fundamentally as the locus of synaptic transmission. While this criterion is of unique importance it has limited usefulness in developmental studies. To determine when synapses become mature within rodent systems we chose to use electrophysiological and imaging techniques. Electrophysiological characterization of synapse development can be complicated by the existence of electrically silent synapses

as stable synaptic connections can exist in the absence of transmission. Intracellular recordings are sensitive enough to measure the function of a single synapse but quickly lead to cell death and are therefore unsuited for long term studies. Thus, we chose to measure electrophysiological development of activity using an array of extracellular electrodes allowing us to monitor activity in a long term non-invasive manner while sampling several interconnected neurons simultaneously. More specifically using multi-channel microelectrode arrays to measure action potentials; we observed that the first signs of activity were detected around 4DIV. This was followed by a sharp rise soon after 10-12 DIV reaching a plateau around 20DIV (Valour *et al.,* 2007) (Fig.3.1. c&d). Additionally, imaging of functional synapses during development using FM4-64, showed that they first emerge around 5DIV and their numbers increased until reaching a plateau after 14DIV (Burrone *et al.,* 2002) (Fig.3.1 a&b). FM dyes are lipophilic styryl compounds that are trapped inside retrieved vesicles during endocytosis.

Together these results show that synapses start to "cement" 3-4 days after plating at which point synaptic transmission between the pre- and postsynaptic compartments initiates. By 10-14DIV, once most of synaptogenesis has been completed, the network appears to proliferate as the synapses begin to strengthen functionally becoming synaptically mature.

Our results are in close agreement with other experiments which have plotted synaptogenesis development in hippocampal cultures as defined by puncta co-localization of the presynaptic marker synaptophysin and the postsynaptic, cell surface GluR1, normalized by dendritic length. Here too, synapse density was seen to increase rapidly between 7 to 12 DIV before levelling off (Han & Stevens, 2008).
Previous published work using synapsin and AM1-43 visualization, showed that the density of synapsin puncta reached saturation levels at DIV12 and that most puncta co-localized with AM1-43 validating our findings (Renger & Liu, 2001). However, FM staining is not an absolute indication of a functional synapse as staining of synaptotagmin and FM puncta have been observed in isolated axons in the absence of a postsynaptic partner (Kraszewski *et al.,* 1995).

It is also possible that other factors may influence the time-course of synapse development. Perhaps the most prominent of these are differences in cell density between

experiments. Increasing the density of neurons in the network may result in an increased rate of synaptogenesis. For this reason we were careful to always plate neurons at similar densities, to avoid, as much as possible, any changes to the process of synaptogenesis. Finally, our results are in close agreement with previous published work (Renger & Liu, 2001, Han & Stevens, 2008).

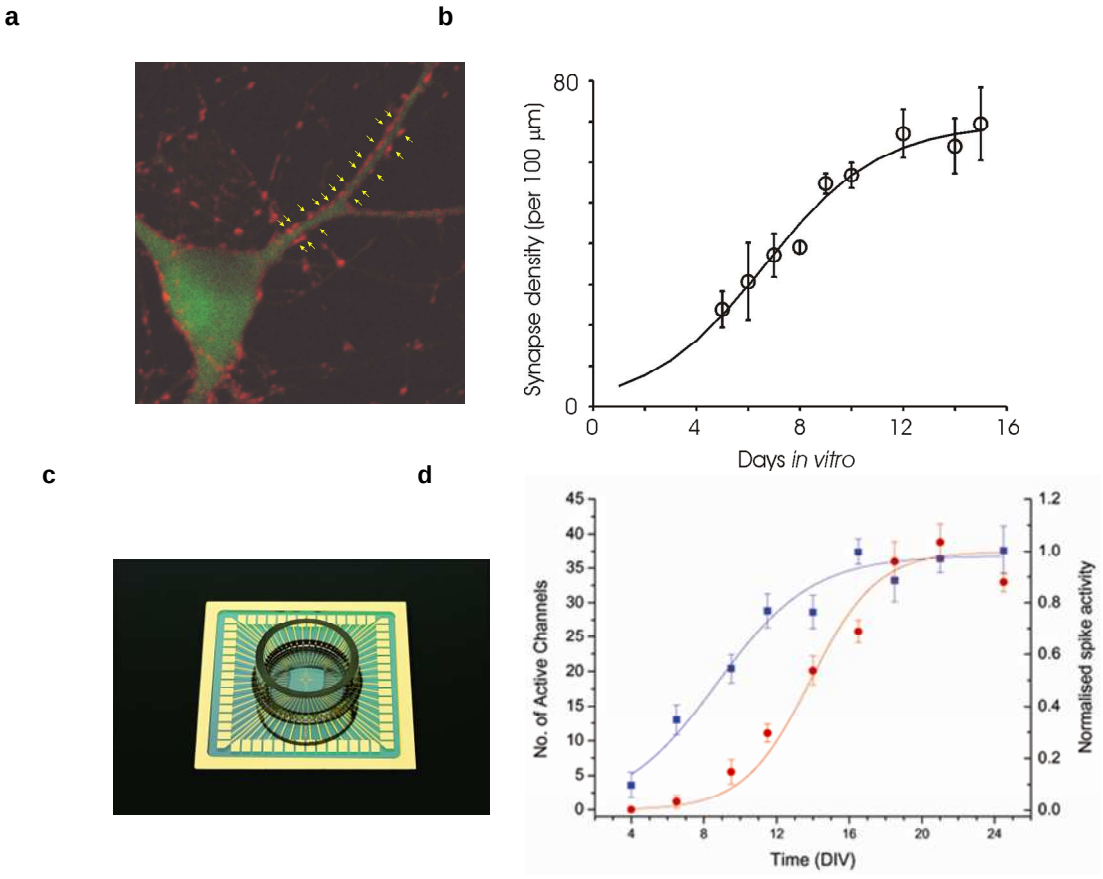

Fig.3.1. Development of synaptic maturity & synapse formation within hippocampal cultures.

a. Confocal image of a hippocampal pyramidal neuron**.** Yellow arrows denote functional synapses identified by the uptake of FM4-64. Synapses from the apical dendrite were measured from cells transfected with GFP.

b. Time course of synapse formation in cultures. The number of active presynaptic terminals was measured using the vesicle dye FM4-64, and each point is an average of at least three cells. The continuous line is a sigmoidal function with half-maximum at about 6.5 days. Data are expressed as mean ± SEM. Modified from Burrone et al. 2002.

c. Network activity profile recorded with MEAs. Example of a MicroElectrode array from MultiChannel Systems, planar electrode size 30µm, electrode interspacing 200 µm.

d..Mean values of the number of active channels (squares) and the array-wide spike activity (circles) from five independent recordings. Data are expressed as mean ± SEM and were fitted to sigmoidal curves (lines) (Valour *et al,* 2007).

3.2. Experimental outline.

Having established that hippocampal synapses at around DIV10-14 had reached a developmental time-point in which they are considered "mature", we proceeded to induce homeostatic plasticity by decreasing or increasing the activity of the entire culture. Decrease in activity was accomplished in one of two ways: 1-blocking action potentials in the entire network by adding tetrodotoxin (TTX) to the growth medium; 2- blocking synaptic transmission by adding the AMPA and NMDA glutamate receptor antagonists, 6-cyano-7-nitroquinoxaline-2,3-dione (CNQX), and D-2-amino-5-phosphonopentanoate (APV), respectively. The TTX manipulation results in the complete abolishment of Na-dependent action potentials, but does not interfere with any spontaneous neurotransmitter release that occurs at the synapse. In essence, neurons will be electrically silent, but some synaptic activity will remain. This is in contrast to CNQX/APV, where fast synaptic transmission is abolished, but some spontaneous intrinsic levels of activity may still be present. Conversely, to increase activity within the network we applied gabazine, a $GABA_A$ receptor blocker, which silences inhibitory synapses and therefore significantly increases network activity (Yu & Ho, 1990). We chose to incubate our cultures for 3 to 5 days with these pharmacological agents, a period of time previously shown to induce homeostatic plasticity (Turrigiano *et al.,* 1998, Gong *et al.,* 2007, Han *et al.,* 2008) (Fig.3.2.).

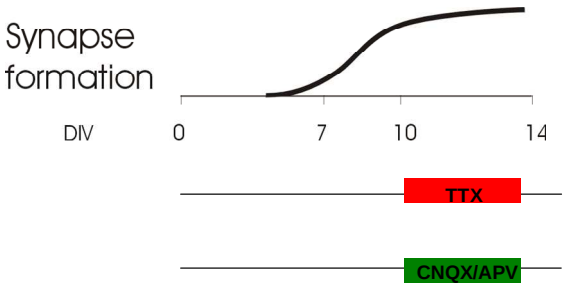

Fig.3.2. Schematic depiction of synapse formation and time course of pharmacological treatment.
Hippocampal culture were bathed in either the sodium channel blocker TTX or ionotropic glutamate receptor blockers CNQX, APV from DIV10 for several days in order to elicit homeostatic responses.

One of our assays for probing how homeostatic plasticity manifested itself at the level of the synapse was to measure 'structural' changes by performing immunocytochemistry of specific synaptic proteins. Other studies have used FM dyes to label synapses, which has its advantages, but also its problems. One of the main issues with FM dye labeling, is that it is not restricted to one type of synapse (excitatory or inhibitory) and does not give a simultaneous read-out of the postsynaptic compartment. Antibody staining is a useful tool for visualizing synapse assembly but, despite its advantages, it also shares pitfalls. Specifically, antibody labeling is highly heterogeneous from one preparation to another, resulting in a large variability of fluorescence intensities that could make it hard to detect any changes in fluorescence, unless they are very large. To try to minimize heterogeneity and allow us to use immunofluorescence in a semi-quantitative manner (i.e.: allowing comparisons of amount of labeling across different conditions) we rigorously observed the following procedures: 1- all antibody incubations (primary and secondary) were performed using the same stock for all conditions tested; 2- all experiments were

performed and analyzed blind to the experimenter; 3- all settings on the imaging set-up were kept constant; 4- all data was normalized to its corresponding control; 5- we made sure to acquire a large data set, using different coverslips from at least two to three different animals in each case. By keeping to these procedures we made sure to minimize any background noise and therefore provided the best chances of observing significant phenotypes. One other problem we encountered when performing the analysis on our acquired images, was the presence of postsynaptic labeling without any corresponding presynaptic markers (Kannenburg *et al.,* 1999) and vice versa (Kraszewski *et al.,* 1995). Thus, we only measured puncta where both pre- and postsynaptic markers co-localized.

Finally, it is also known that presynaptic puncta labeled with antibodies against specific synaptic proteins did not all show evidence of vesicle cycling, even in mature cultures. In fact, a study by Moulder *et al*. (2008) showed that around 20 % of puncta labeled with antibodies against vGlut did not show any FM4-64 labeling and that the number of inactive boutons was tightly controlled by network activity. Our labeling procedure does not distinguish between actively cycling and inactive presynaptic terminals.

One of the great advantages of using immunofluorescence, is that it provides a measure of endogenous levels of proteins, without the need to over-express any reporter that could alter normal cellular function. It also allows for specific labeling of proteins or compartments. For example, we chose to stain for the presynaptic marker vGlut1 (Fig.3.3.a-d), a vesicular protein involved in transporting glutamate into vesicles, which only labels excitatory glutamatergic presynaptic boutons. This specificity not only provides a more in-depth description of synapse function, but also reduces any heterogeneity that may arise when using more generic synaptic labels, that cannot distinguish between excitatory and inhibitory synapses. For our postsynaptic marker we chose PSD-95 (Fig.3.3.a-d) a member of the closely related membrane-associated guanylate kinase homolog (MAGUKS) which is a scaffolding protein for AMPA receptors and is thought to be crucial for the trafficking and stability of receptors at the membrane. Indeed, the development of PSD-95 in hippocampal neurons parallels the appearance of GluR1 (Martin *et al.,* 1998, Sans *et al.,* 2000, Aoki *et al.,* 2003) and over-expression of PSD-95 in hippocampal neurons can drive maturation of pre- and postsynaptic components in glutamatergic synapses, as well as increases in synaptic size

and evoked postsynaptic responses (El- Husseini *et al.,* 2000, Shnell *et al.,* 2002, Ingrid & Malinow, 2004). In our hands, staining for vGlut1 and PSD-95 in mature (DIV14) hippocampal cultures resulted in clearly identifiable puncta, which co-localized, as expected for pre- and postsynaptic structures (Fig.3.3.d).

3.3. Structural correlations.

Initially, we picked individual regions of interest (ROIs) from hippocampal DIV14 neurons and for each synapse we correlated the fluorescence intensity of PSD-95, with that of its corresponding vGlut1 puncta. An example from one cell is shown in Fig.3.3.e were we found a strong correlation between the two (R=0.86). The correlation persisted when data was pooled from many different cells (Fig.3.4.a). To further investigate if this structural correlations was altered in response to changes in network activity, we treated neurons with TTX or CNQX/APV for 2 days. Fig.3.4.a-c shows the fluorescence intensities for each marker in control and treated neurons. A clear correlation is seen when plotting fluorescence intensities per synapse (gray dots in Fig.3.4.a-c). For greater visual ease, the data was also plotted in bins of 10 (black dots). The line of best fit is indicated by the dashed line. These values were then superimposed on top of each other for comparison (Fig.3.4.d) with the mean shown by the large circles. These comparisons revealed that decreasing activity by blocking either sodium channels or ionotropic glutamate receptors does not appear to have changed the correlation between the two markers suggesting that once this correlation has been established, chronic alterations in neuronal or synaptic activity do not disrupt it. However, there was a strong increase in the overall fluorescence intensities for both proteins in response to prolonged decreases in activity. Thus, neurons within the network appear to be sensing their own inactivity, and in an attempt to rectify this have homeostatically increased the amount of vGlut present presynaptically as well as the amount of PSD-95 potsynaptically.

Interestingly, others have shown that presynaptic release probability (p_r), assessed using FM1-43, didn't correlate with synaptic surface GluR2 under basal conditions or after chronic disuse. A pre- and postsynaptic correlation was however, observed when they

elevated activity (Tokuoka & Goda, 2008). A more recent study showed that although synapses are structurally correlated early in synapse formation, they only gradually became functionally matched with time and that this was dependent on ongoing activity (Kay *et al.,* 2011).

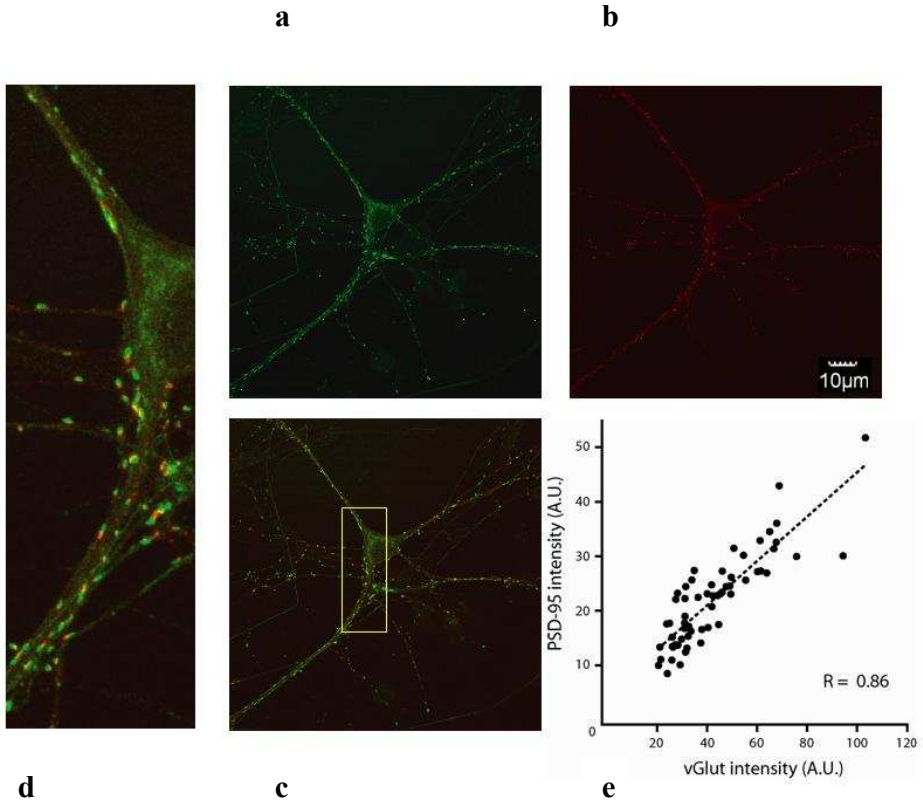

Fig.3.3. Pre- and postsynaptic structural correlation.
(a&b) Hippocampal neurons on DIV 14 were fixed/stained with antibodies against vGlut1 in green and PSD-95 in red. Scale=20µm **(c)** Merged image of both Fig.a+b.**(d)** Magnified segment denoted by the yellow box in fig c clearly showing distinct puncta of vGlut and PSD-95 co-localising indicative of a synaptic region. Scale=10µm **(e)** Correlation plots of vGlut vs. PSD-95. Black dots represent fluorescence intensity values for both proteins for 50 individual randomly selected synapses. Dashed line represents best linear fit through values yielding a correlation of 0.86.

All of the structural synaptic characterizations in this chapter were done by using immunocytochemistry. Only in some experiments, where we also had a postsynaptic neuron and its dendrites labeled, did we also measure synapse density. Our findings (see

Fig.3.6.) suggest that the density of excitatory inputs onto a neuron is not altered by chronic changes in neuronal activity. We therefore continued to assess the changes in protein composition observed by immuno-labeling under different activity paradigms.

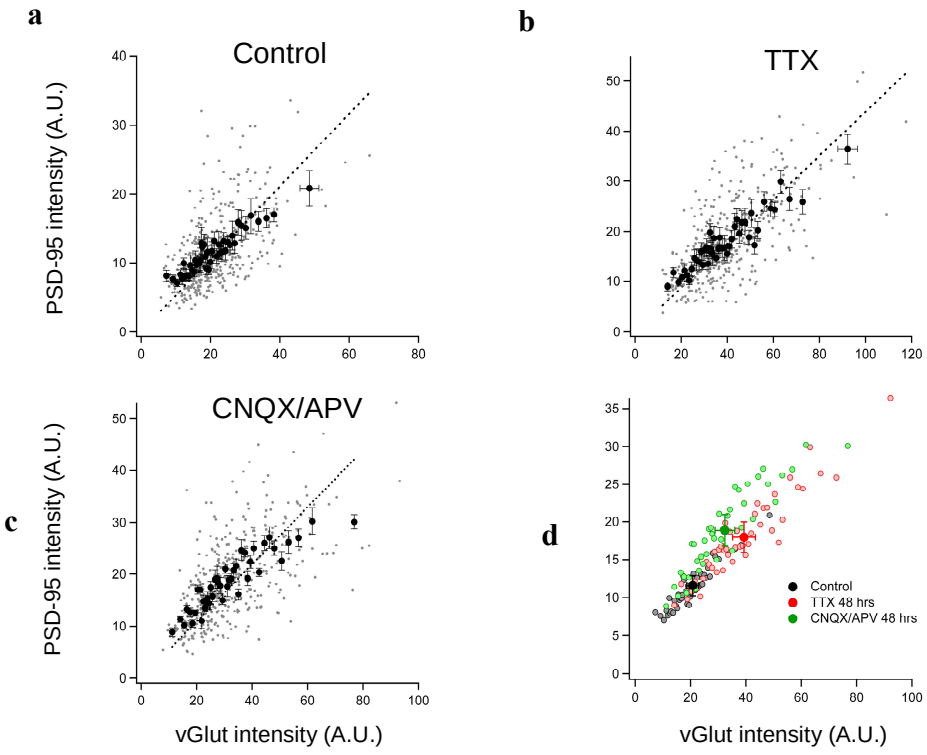

Fig.3.4. Parallel increases in pre- and postsynaptic markers.

- **a.** Fluorescence intensities in arbitrary units for vGlut1 vs. PSD-95 plotted for individual hippocampal DIV13 control synapses (grey dots). Data binned in values of 10 for greater visual ease (black dots). Line of best fit indicated by dashed line.
- **b.** Fluorescence intensities in arbitrary units for vGlut1 vs. PSD-95 plotted for individual hippocampal DIV13 synapses after 48hr treatment with TTX (grey dots). Data binned in values of 10 for greater visual ease (black dots). Line of best fit indicated by dashed line.
- **c.** Fluorescence intensities in arbitrary units for vGlut1 vs. PSD-95 plotted for individual hippocampal DIV13 synapses after 48hr treatment with CNQX/APV (grey dots). Data binned in values of 10 for greater visual ease (black dots). Line of best fit indicated by dashed line.
- **d.** Binned values of vGlut1 vs. PSD-95 fluorescence from all three treatments (black = cntrl, red = TTX, green = CNQX/APV) superimposed for visual comparison. Larger crossed circles indicate the overall average value for each treatment. Fluorescence intensities are in arbitrary units. Data are expressed as mean ± SEM. Data was taken from 3 different experiments.

We next set out to study the structure of individual synapses and establish whether any correlation exists between pre- and postsynaptic compartments at various developmental time-points. In addition, if any correlation does exist early on we wanted to determine if chronic inactivity could perturb it. As expected from the previous figure, immunostaining of synaptic proteins in mature neurons (14 DIV) showed a strong correlation between the fluorescence intensity of the vesicular glutamate transporter (vGlut-1) puncta and their corresponding postsynaptic density-95 (PSD-95) or glutamate receptor subunit, GluR2, puncta (Fig.3.5.a-d). More interestingly, this correlation was already apparent at earlier time points, as early as 7 DIV, a time when synapses are just beginning to form in our hippocampal cultures. In addition, blocking action potentials in the entire network, from 10 to 14DIV, by incubating neurons with TTX, had no effect on this correlation (Fig.3.5.a-d) (Kay *et al*., 2011). This data suggests that a strong pre- and postsynaptic structural correlation is established at very early stages of synaptogenesis and is maintained throughout development but is not sensitive to blockers of neuronal/synaptic activity.

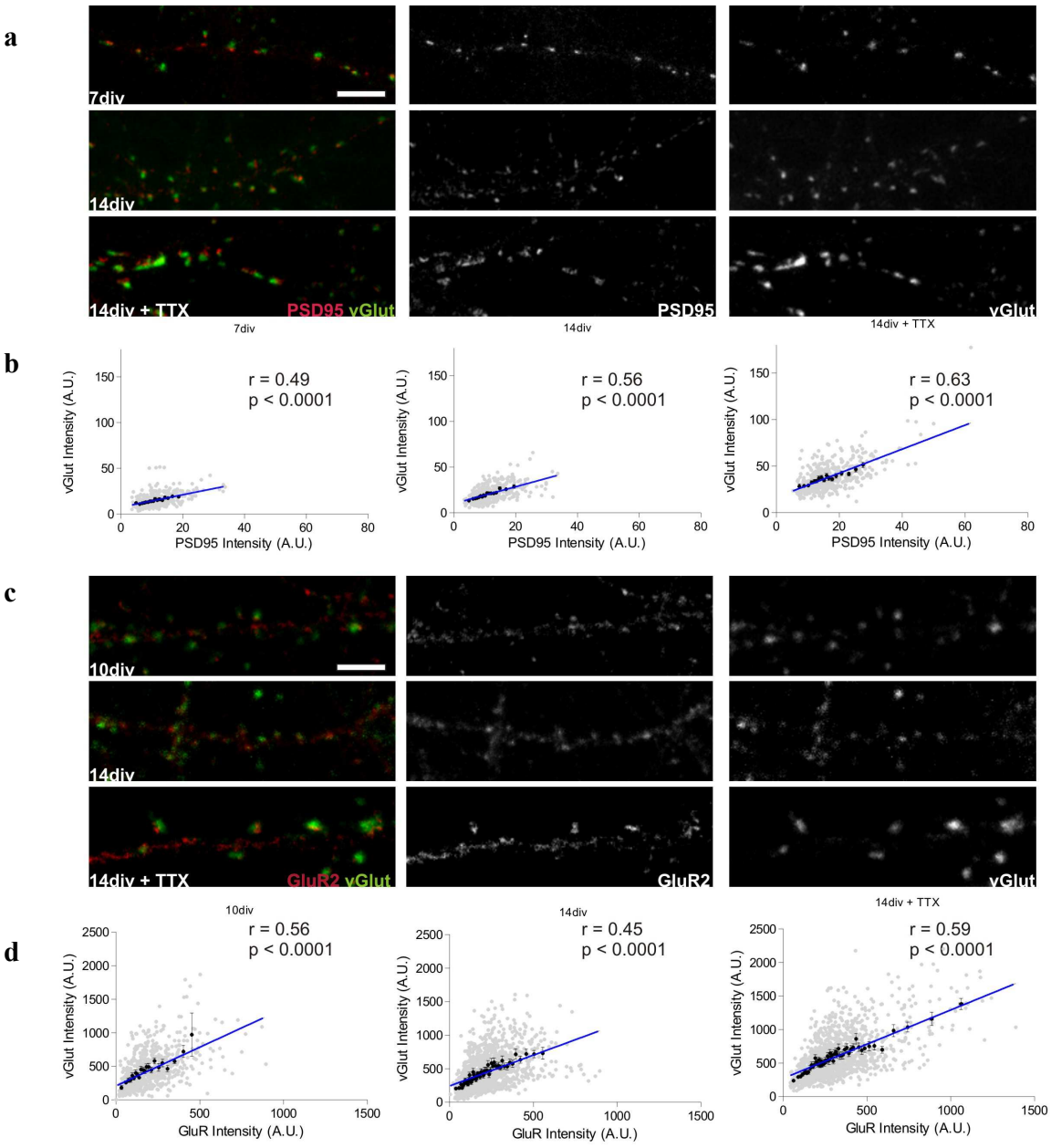

Fig.3.5. Matching of synaptic structure in young and mature neurons. (**a**) Example images of hippocampal neurons stained with vGlut (green) and PSD-95 (red) at two different developmental stages (7 and 14 div) for control neurons and neurons treated with TTX from 7 div. Scale bar represents 5 µm. (**b**) Plot of fluorescence intensity for vGlut staining as a function of PSD-95 staining per synapse (gray points) and grouped in bins of 25 (black circles) for 10 cells and 450 synapses (mean fluorescence intensity at 7 div: vGlut, 15.44 ± 0.32; PSD-95, 11.64 ± 0.23; at 14 div: vGlut, 20.80 ± 0.39; PSD-95, 11.57 ± 0.24; at 14 div after TTX treatment: vGlut, 38.72 ± 0.71; PSD95, 17.13 ± 0.35). Error bars represent s.e.m. (**c**) Example images of neurons stained with vGlut (green) and GluR2 (red) at two different developmental stages (10 and 14 div), for control neurons and neurons treated with TTX from 10 div. Scale bar represents 5 µm. (**d**) Mean fluorescence intensity at 10 div: vGlut, 422.1 ± 9.49; GluR2, 184.6 ± 4.60; at 14 div: vGlut, 442.0 ± 7.38; GluR2, 218.0 ± 3.58; at 14 div after TTX treatment: vGlut, 597.2 ± 8.91; GluR2, 319.4 ± 5.18. Plot of fluorescence intensity for vGlut staining as a function of GluR2 staining per synapse (gray points) and grouped in bins of 25 (black circles) for 9 cells and ≥780 synapses. A.u = arbitrary units. Error bars represent SEM. Graph taken from Kay *et al., 2011.*

3.4. Homeostatic control of receptor insertion.

From a postsynaptic perspective we have shown homeostatic increases in PSD-95 in response to chronic inactivity. There have been numerous reports showing that more AMPA receptors are actively inserted in the postsynaptic membrane in response to chronic inactivity (Hou *et al.,* 2007, Ibata *et al.,* 2008). As PSD-95 has been implicated in trafficking AMPA receptors into the postsynaptic membrane (Schnell *et al.,* 2002) we wanted to establish if our observed increase in PSD-95 also coincided with an increase in AMPA receptors within our cultures. Additionally, we wanted to determine if our pharmacological treatments were also altering synapse density within our cultures. For this purpose, we chose to stain with antibodies against GluR2, rather than GluR1, (Fig.3.6.c) as it has been implicated specifically in synaptic scaling (Gainey *et al.,* 2009) and vGlut1.

We thus checked synapse development in individual neurons at different time points and explored if reduction of activity altered these synaptic protein levels as well as the average dendritic synapse density formation. We sparsely transfected a subset of neurons with GFP on DIV7 and then fixed them either at DIV10 (Fig.3.6.c top row) or at DIV14 (Fig.3.6.c middle row). Additionally, we also treated some cells with TTX on DIV10 and fixed them on DIV14 (Fig.3.6.c bottom row). All neurons were stained for antibodies against vGlut and GluR2. The presence of GFP clearly resolves the dendrites of individual neurons and therefore allowed us to measure all the synapses on all the dendrites of a single cell within the field of view. We then compared GluR2 and vGlut levels between cells from DIV10 and 14, with or without TTX, and established their density along a dendrite.

Developmentally, both the levels and density of synaptic vGlut and GluR2 did not change significantly from DIV10 to DIV14 (Fig.3.6.a), which further strengthens our assertion that synapse formation is over soon after DIV10 (Density, 0.43 ± 0.05, synapses/µm, 9 cells to DIV14: 0.50 ± 0.07, synapses/µm, 10 cells). Nevertheless, we cannot exclude the possibility that there are some additional processes of maturity still occurring during these time points. For example, glutamate uncaging experiments have

shown important increases in postsynaptic AMPA receptor currents, during these four days (Kay *et al.,* 2011). It is important to note that our GluR2 labelling did not measure surface receptor levels, but rather overall synaptic levels. Treatment with TTX resulted in a significant increase in both synaptic markers when compared to untreated cells (Fig.3.6.a&b), but no change in synapse density (Control = 0.50 ± 0.07, synapses/µm, 10 cells); TTX: 0.48± 0.07 synapses/um, 9 cells; P=0.93, Kruskal-Wallis test). Together, these results point to a coordinated presynaptic and postsynaptic readjustment in the structure existing synapses.

Finally, we also looked at the degree of correlation between the fluorescence intensity of vGlut1 and GluR2 at DIV10 (r = 0.31 ± 0.05) and DIV14 with (r = 0.35 ± 0.06) or without TTX (r = 0.32 ± 0.03) and found no significant differences (P=0.86 Kruskal-Wallis test). As expected from our previous data, these results further strengthen the notion that in response to chronic inactivity pre- and postsynaptic proteins are up regulated while maintaining their structural correlations.

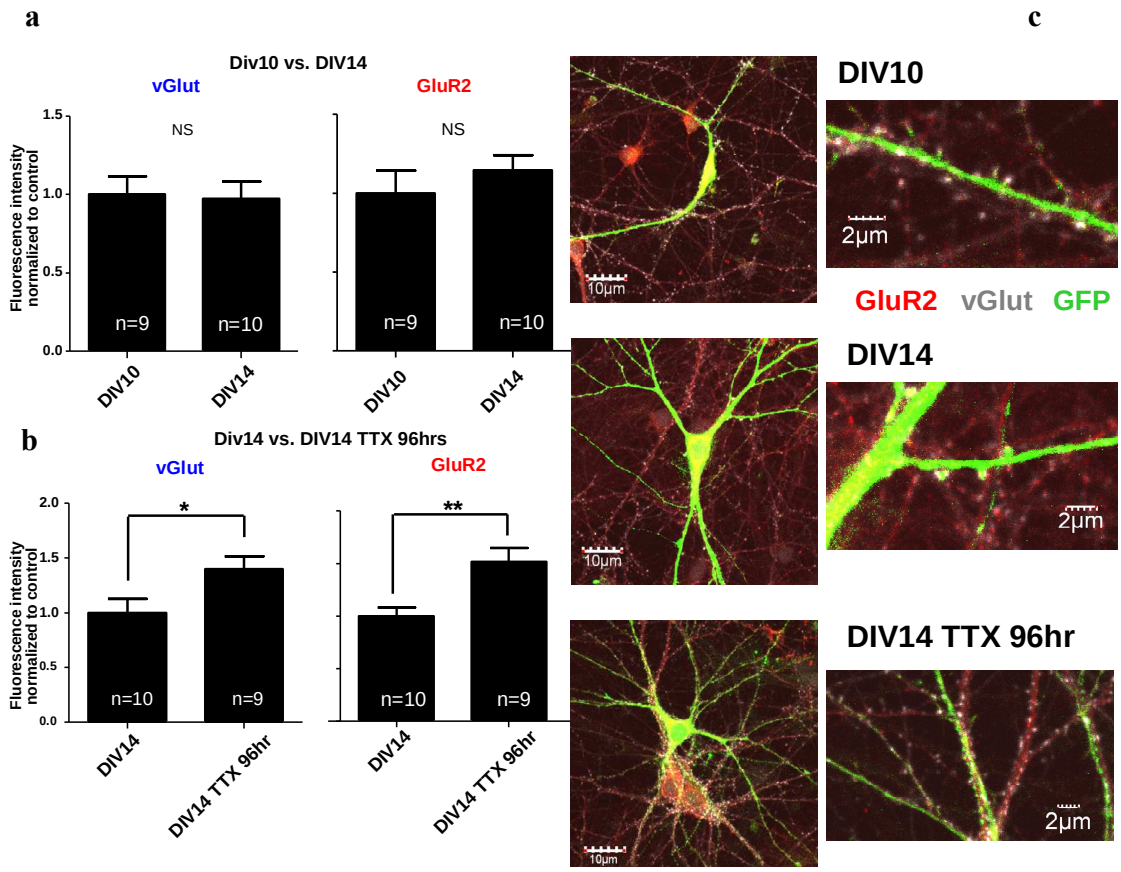

Fig.3.6. Levels of GluR2 and vGlut1 in individual cells increased from DIV10-14 only in response chronic inactivity rather than developmentally.

- **a.** Fluorescent intensities of vGlut1 and GluR2 did not increase developmentally from DIV10 (vGlut1 =1.00 ± 0.11, n=9, 270 synapses, GluR2=1.00 ± 0.15, n=9 cells, 270 synapses) to DIV14 (vGlut1= 0.97 ± 0.11, n=10, 300 synapses, P=0.88, GluR2 = 1.147 ± 0.10, n=10, 300 synapses, P= 0.40 unpaired t-test) in hippocampal GFP expressing cells. Fluorescence intensities were normalized to controls and are expressed as mean ± SEM. Data from 2 separate experiments.
- **b.** Fluorescent intensities of vGlut1 and GluR2 at DIV14, in hippocampal GFP expressing cells, exhibited significant increases after 96hrs of TTX (vGlut1 = 1.40 ± 0.13, n=10, 300 synapses, GluR2 = 1.52 ± 0.13, n= 9 cells, 270 synapses) when compared to untreated cells (vGlut1 = 1.00 ± 0.13, P=0.04, GluR2 = 1.00 ± 0.08, n=10, unpaired t-test, P=0.003). Data from 2 separate experiments and are expressed as mean ± SEM.
- **c.** Representative images from cells at DIV10 (top row) and DIV14 which haven't (middle row) or have (bottom row) been treated with TTX for 96hrs. Images on the right column are magnified areas of dendrite from images on the left column. (Green=GFP, Red=PSD-95, Gray=vGlut). Scale on left images = 10μm, right images = 2 μm.

3.5. Developmental influences on homeostatic locus.

It has been suggested that the expression locus of homeostatic plasticity, i.e. whether it lies pre-or postsynaptically, depends on the developmental time point the network has reached *in vitro*. It was first suggested that in visual cortical pyramidal and hippocampal cultures a 48hr treatment with TTX at ≤ DIV14 led to an increase in mEPSC amplitude without affecting frequency. However, a similar treatment ≥ DIV18 resulted in an increase in frequency whereas the amplitude only increased moderately (Turrigiano *et al.,* 2006). This implies there is a shift in the expression locus from a predominantly postsynaptic effect, early in development, to a coordinated pre- and postsynaptic effect after DIV18. The increase in frequency was attributed to an increase in synapse density and presynaptic vesicle release/ and or recycling. Critically, though, it was shown that this shift in homeostatic expression locus was dependent on the time the cultures had spent *in vitro* rather the post-natal age. Similar experiments testing the influence the developmental time point has on homeostatic plasticity *in vivo*, reported that 48hr action potential blockade, led to an increase in mEPSC amplitudes in juveniles (P15) but not in adults (P30). However, increases in mEPSC frequencies in both cases were also reported (Echegoyen *et al.,* 2007). It therefore appears that the synapses respond differently depending on the developmental point in which activity is altered. The reason for this phenomenon is still unclear.

We set out to repeat these experiments in our model system by ablating activity early in development with TTX, for different durations of time: from DIV3 to 7, a time when synapses are only beginning to form and from DIV3-13, to span the entire period of synaptogenesis and maturation. As expected, we found that silencing neurons with TTX form DIV3 to 13 resulted in a significant increase in both vGlut and PSD-95 when compared to controls (Fig.3.7.a&b). These results show that in terms of structural changes, the homeostatic locus is both pre-and postsynaptic when activity is manipulated early in development on the onset of synaptogenesis as well as later when the system is more mature.

We then explored if the homeostatic synaptic locus changed for the younger synapses (from DIV 3 to 7). Here, again, we also observed increases in the levels of both vGlut1 and PSD-95 when compared to controls (Fig.3.7.c&d).

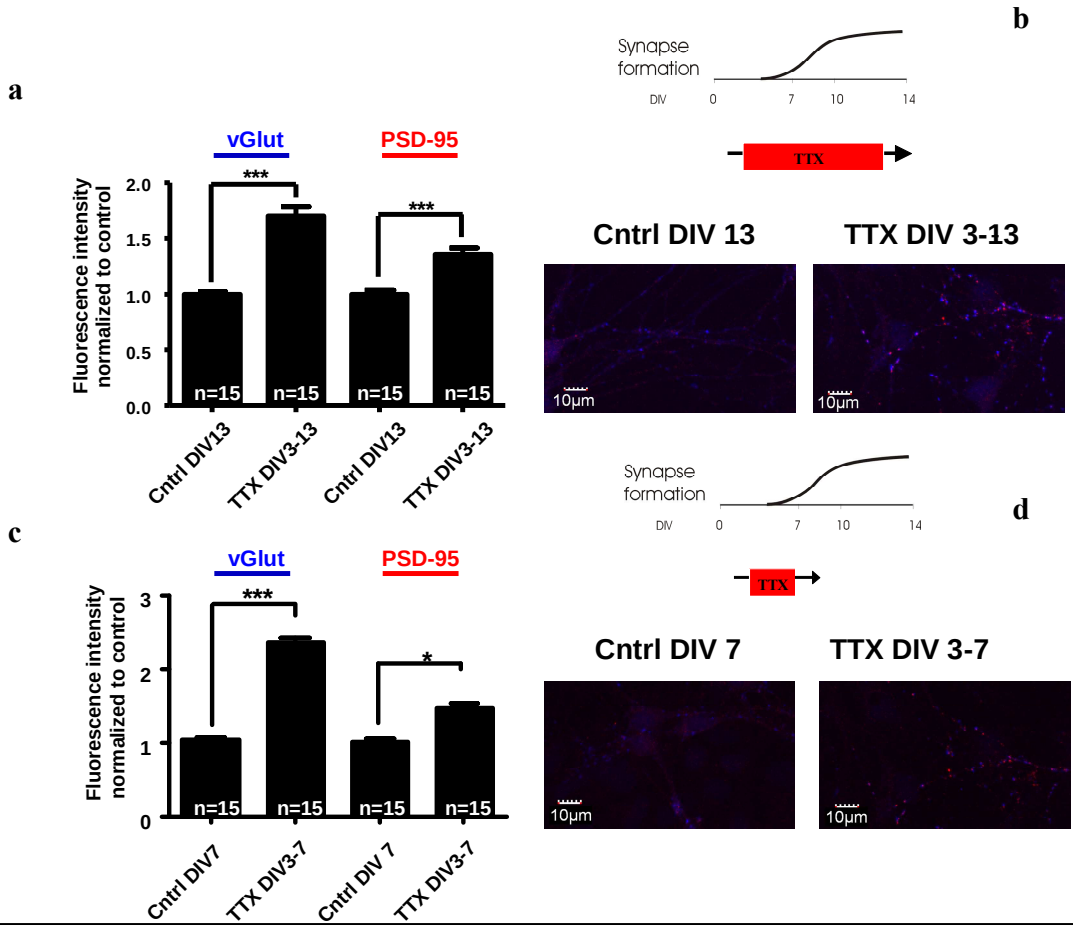

Fig.3.7. Synaptic homeostatic plasticity after long-term exposure to TTX, during and after synaptogenesis.
a. Hippocampal neurons were treated with TTX from DIV3 to 13 and then fixed/stained with antibodies against vGlut1 and PSD-95. Cells treated with TTX showed a significant increase in vGlut1 when compared to untreated controls (control: mean = 1.00 ± 0.03 n=15, 450 synapses; TTX: mean = 1.70 ± 0.08, n=15, 450 synapses) and in PSD-95 (control: mean=1.00 ± 0.04 n=15, 450 synapses, TTX mean=1.35 ± 0.06 n=15, 450 synapses, Unpaired t-test. P<0.0001 Fluorescence intensities were normalized to controls. Data from 2 separate experiments. Data are expressed as mean ± SEM
b. Images of cells with punctate co-localization of PSD-95 (red) and vGlut1 (blue). Left image is from an untreated culture on DIV13 and image on right is from a culture treated with TTX from DIV3 to 13. Diagram above shows the synapse development within our cultures and the time at which TTX was applied. Scale bar = 10µm.
c. Hippocampal cultures were treated early in development with TTX from DIV3-7 and fixed/stained with antibodies against vGlut1 and PSD-95. In both cases drug treatment led to a significant increase in the levels of both proteins (vGlut1 mean=2.37 ± 0.05, n=15 450 synapses, PSD-95 mean=1.47 ± 0.06, n=15 450 synapses) when compared to untreated controls (vGlut1 mean= 1.00 ± 0.05, P<0.0001 unpaired t-test, n=15 450 synapses, PSD-95 mean=1.00 ± 0.05, P<0.0001, Mann Whitney. Fluorescence intensities were normalized to controls from 2 separate experiments. Data are expressed as mean ± SEM.
d. Images of cells with punctate co-localization of PSD-95 (red) and vGlut1 (blue). Left image is from an untreated culture on DIV7 and image on right is from a culture treated with TTX from DIV3 to 7. Diagram above shows the synapse development within our cultures and the time at which TTX was applied. Scale bar = 10µm.

These results suggest that reducing activity even before the onset of synaptogenesis and neurotransmission is sufficient to induce a homeostatic response, which is expressed in both pre- and postsynaptic compartments.

3.6. Bidirectional homeostatic plasticity.

We next investigated if this homeostatic response was bidirectional in nature by exploring the effects of elevating the activity of the network. This was accomplished by using gabazine (1μM), a $GABA_A$ receptor antagonist that acts as an allosteric inhibitor of channel opening (Yu & Ho, 1990). The net effect is the reduction of inhibitory drive, increasing the overall activity within the network. We treated cultures at DIV10 for 72, 96 or 120hrs and looked at the effects on our excitatory pre- and postsynaptic markers.

After increasing the overall activity of the network for 72hrs with gabazine there was no change in the fluorescence intensities for either vGlut or PSD-95 when compared to controls. However, by 96hrs we began to see significant decreases in the levels of both markers when compared to controls, which persisted up to 120 hrs (Fig.3.8.a&b). These results further support the notion that homeostatic plasticity is bidirectional in nature and that these synaptic proteins can be up- or down-regulated to meet the demands of the network in the face of chronic perturbations in activity. Notably, the effects of gabazine on homeostatic induction within excitatory cells took longer to appear when compared to TTX or CNQX/APV (Fig.3.4.)

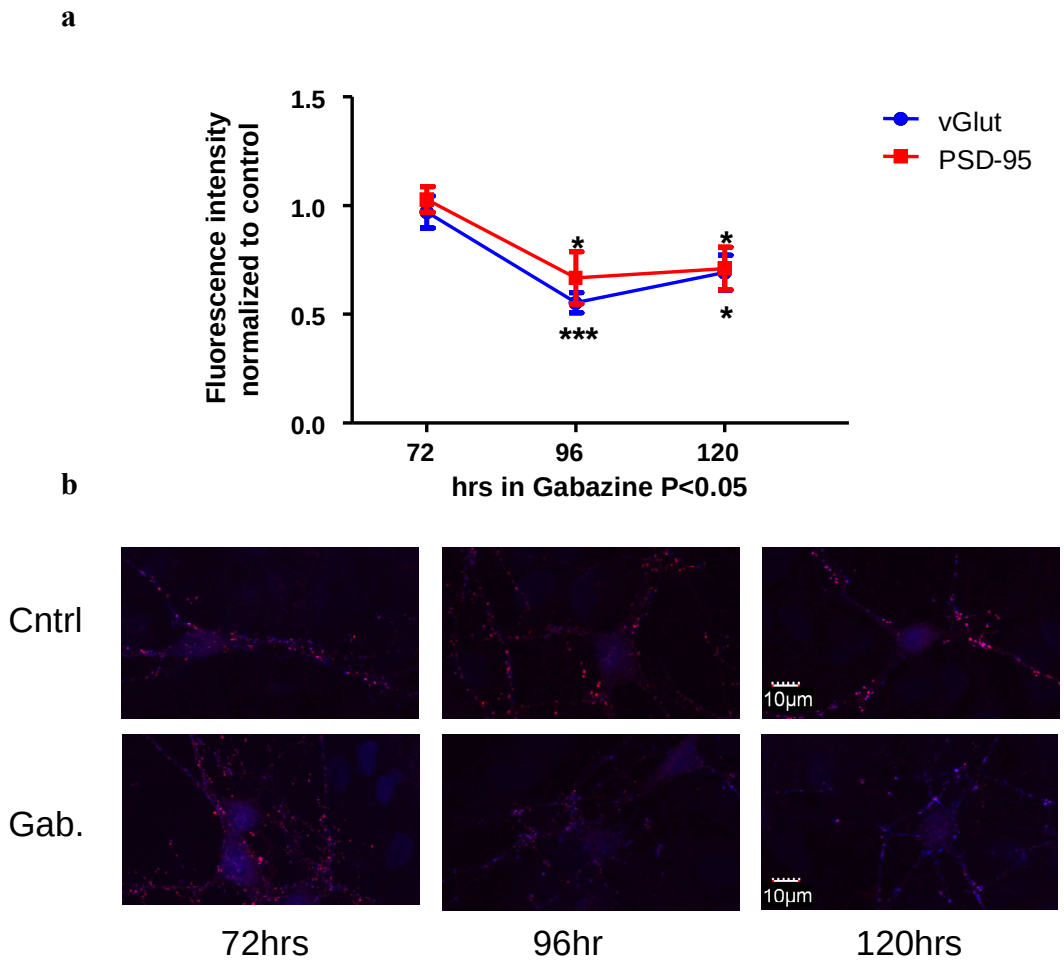

Fig.3.8. Homeostatic plasticity achieved by increasing network activity with gabazine. **a**. Cells were treated on DIV 10 with gabazine for 72 up to 120hrs and then fixed and stained for vGlut1 and PSD-95. After 72 hrs there was no significant decrease in the amount of vGlut1 (mean = 0.97 ± 0.07 n=19, 570 synapses) when compared to controls (mean = 1.00 ± = 0.07 n=23, 690 synapses, P=0.7). However, after 96hr we began to see significant decreases (96hr:mean = 0.55 ± 0.05 n=19, 570 synapses, Control:mean = 1.00 ± 0.08 n=20, 600 synapses, P=0.0004). This decrease persisted up until 120hrs (mean = 0.70 ± 0.08 n=10, 300 synapses, Control:mean = 1.00 ± 0.10 n=10, 300 synapses P=0.02). Similarly, after 72 hrs there was no significant decrease in the amount of PSD-95 (mean = 1.03, ± 0.06 n=19, 570 synapses) when compared to controls (mean = 1.00 ± 0.06 n=23, 690 synapses, P=0.45). However, after 96hr we began to see a significant decreases (mean = 0.67, ± 0.12 n=19, 570 synapses, Control:mean = 1.00 ± 0.22 n=20, 600 synapses, P=0.047) which persisted up until 120hrs (mean = 0.71 ± 0.01 n=10, Controls:mean = 1.00 ± 0.08 n=10, 300 synapses P=0.035) All statistical test used Mann Whitney test. Fluorescence intensities were normalized to controls. For each time point two separate experiments were averaged except for in the case of 120hrs in which a single experiment was evaluated. Data are expressed as mean ± S.E.M. **b**. Representative images of control and gabazine treated hippocampal cultures stained for vGlut (blue) and PSD-95 (red) for 3 to 5 days from DIV10. Scale=10µm.

3.7. Homeostatic influences on inhibitory cells.

We next turned our attention to inhibitory synapses. We wanted to probe if they behave in a similar fashion when they are subject to chronic activity manipulations. Previous studies have revealed that inhibitory synapses are under the influence of homeostatic plasticity (Hartmann *et al.,* 2006). To visualise inhibitory synapses, we chose two specific synaptic protein markers: gephyrin (Fig.3.9. top row), a postsynaptic protein responsible for displacing GABA receptors from the GABARAP/P130 complex and bringing them to the synapse, and vGat (vesicular GABA transporter), a presynaptic vesicular protein which transports GABA into vesicles (Fig.3.9 middle row). Having previously established the effect that increasing network activity with gabazine had on excitatory synapses, we then set out to establish the effects on inhibitory synapses. Elevating activity on DIV10 for 72hrs or 120hrs appeared to have no effect on the levels of vGat or gephyrin when compared to controls (Fig.3.9 a&b).

Our results suggest that although perturbing network activity causes a compensatory structural change at the synapses of excitatory synapses, inhibitory synapses do not follow the same homeostatic rules.

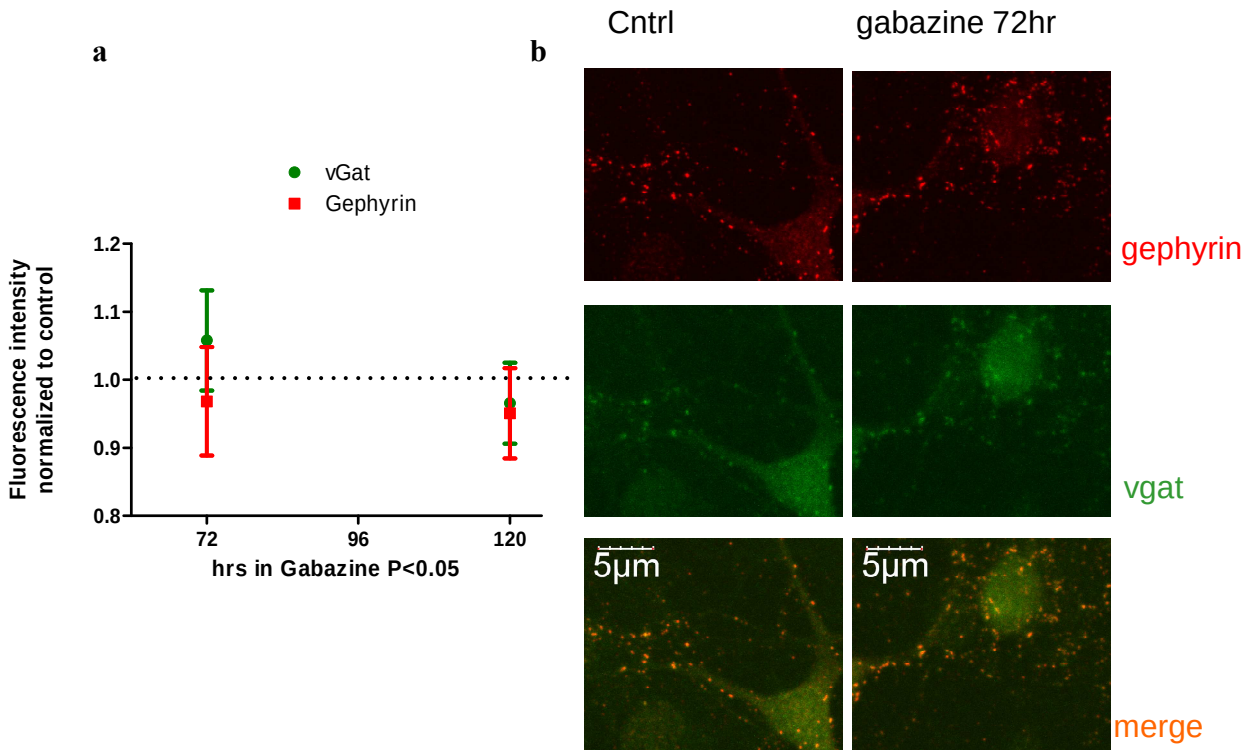

Fig.3.9. Inhibitory synapses do not undergo homeostatic plasticity in response to increases in network activity.

a. Cultures where treated on DIV 10 for 72 and 120hrs with gabazine and fixed/stained with antibodies against the postsynaptic inhibitory marker vGat. We did not observe any significant changes in the levels of vGat (72hrs mean = 1.06 ± 0.07, n=10, 300 synapses, 120hrs mean = 0.97 ± 0.06, n=9, 270 synapses) when compared to controls (72hrs mean = 1.00 ± 0.07, n=10, 300 synapses, P=0.57, 120hrs mean = 1.00 ± 0.07, n=10, 300 synapses, P=0.72, unpaired t test). Cultures were also stained with antibodies against the presynaptic inhibitory marker gephyrin. We did not observe any significant changes in the levels of gephyrin (72hrs mean = 0.97 ± 0.08 n=10, 300 synapses, 120hrs mean = 0.95 ± 0.07, n=9, 270 synapses) when compared to controls (72hrs mean 1.00 ± 0.06, n=10, 300 synapses, P=0.76, 120 hrs mean =1.00 ± 0.07 n=10, 300 synapses, P=0.63, unpaired t-test). Fluorescence intensities were normalized to controls. Data are expressed as mean ± SEM from 2 separate experiments for each time point.

b. Images of hippocampal cells treated with gabazine for 72hrs (right column) or left untreated (left column) and fixed and stained with antibodies against gephyrin (top row red) and vGat (middle row green). The bottom row of images is merged demonstrating co-localisation of both inhibitory synaptic proteins. Scale = 5µm.

3.8. Functional homeostatic plasticity.

Having observed the structural changes that occur during homeostatic plasticity in excitatory cells, we wanted to examine whether these changes were correlated with changes in the physiology of synaptic inputs. This was tested by using electrophysiology. We performed whole-cell voltage-clamp recordings to measure miniature Excitatory Postsynaptic Currents (mEPSCs) otherwise known as minis. It is generally agreed that minis are considered to be the postsynaptic response to the release of a single presynaptic vesicle (Katz & Miledi, 1959). We thus set out to record mEPSCs from neurons in which we had pharmacologically perturbed activity for chronic periods of time and assessed whether the synaptic structural changes that occur during homeostatic plasticity manifest into direct functional changes in synaptic strength.

Recordings were taken from cells after they were treated with CNQX/APV for 48hrs on DIV10 which was then washed out (recordings for this condition were carried out by Dr. Matthew Grubb). After activity had been chronically reduced for 2 days, significant increases in the average amplitudes of treated cells were observed when compared to untreated controls (Fig.3.10.a bottom graph). mEPSC frequency however, remained unchanged (Fig.3.10.b bottom graph). A similar increase in mEPSC amplitude was observed after a 72 hrs treatment with TTX (Fig.3.10.a middle graph). However, once again, we did not observe any change in frequency (Fig.3.10.b middle graph). Finally, increasing network activity with gabazine for 72 hours resulted in a significant decrease in mEPSC amplitude when compared to untreated controls (Fig.3.10.a top graph) without any significant change in mEPSC frequency (Fig.3.10.b top graph). These results suggest that in mature cultures, synaptic strength can be modulated homeostatically in a bi-directional manner.

These results further show, that in an attempt to retain stability, neurons are able to increase or decrease the strength of their synapses through both structural and functional changes. This fine-tuning seems to occur through adjustments to the machinery involved in determining quantal amplitude rather than in alterations in synaptic connectivity or presynaptic strength, as we did not observe any changes in mEPSC frequency. In

combination with our previous findings (Fig.3.4.& 3.6.) these results suggest that when activity is reduced for several days, the system responds by increasing the level of proteins involved in quantal amplitude. Conversely, if activity is elevated, these proteins become down regulated and the functional output decreases.

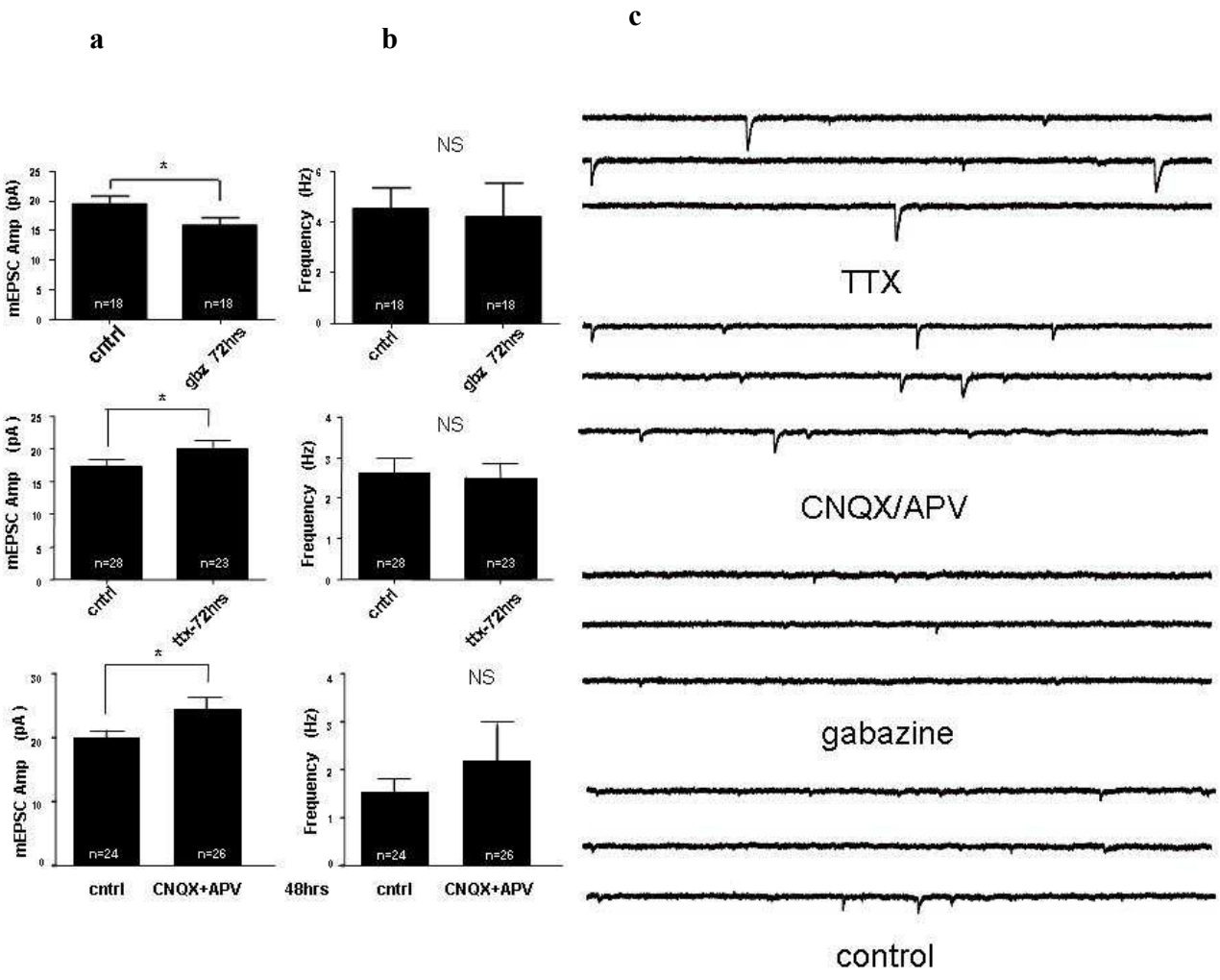

Fig.3.10. Homeostatic plasticity results in bidirectional functional changes in mEPSC amplitude.

- **a.** Hippocampal cells treated with TTX exhibited increased mEPSC amplitudes (19.96 pA ± 1.30 n=23 cells) when compared to untreated controls (17.28 pA ± 1.01 n=28 cells, P=0.03, 3 separate experiments). Cells treated with gabazine showed a significant decrease in amplitudes (15.91 pA ± 1.24, n=18 cells) when compared to controls (19.48 pA ± 1.31, n=18 cells, P=0.04, 4 separate experiments), while cells treated with CNQX/APV had increased amplitudes (24.48 pA ± 1.50, n=26 cells) when compared to controls (20.08 pA ± 0.92, n=24 cells, P=0.03, 3 separate experiments). Mann Whitney test was used for all conditions. Data expressed as mean and SEM.
- **b.** Hippocampal cells treated with TTX exhibited no significant change in frequency (2.495 Hz ± 0.37, n=23) when compared to untreated controls (2.62 Hz ± 0.37, n=28, P=0.86, 3 separate experiments). Cells treated with gabazine showed no significant change in frequency (4.22 ± 1.32, n=18 cells) when compared to untreated controls (4.5 Hz ± 0.82, n=18 cells, P=0.22, 4 separate experiments). Cells treated with CNQX/APV also showed no change in frequency (1.55 Hz ± 0.28 n=26 cells) when compared to untreated controls (2.17 Hz ± 0.82 n=24 cells P=0.82, 3 separate experiments) Mann Whitney test was used for all conditions. Data expressed as mean and SEM.
- **c.** Representative traces from whole cell recordings of mEPSC from DIV13 cells treated with TTX (top trace), CNQX/APV (2nd to bottom), gabazine (3rd to bottom) for 2-3 days or left untreated as controls (bottom trace). Scale=51.2 pA, 106.5 ms, each trace is a recording from a different cell.

In addition, when we compared the rise, decay, membrane capacitance and membrane resistance between each condition and their controls we did not observe any significant differences, with the exception for when we compared the area ,which is not surprising (data not shown). It must be noted that the frequencies of controls between the three conditions differed. Overall the frequencies and amplitudes can vary dramatically from cell to cell. As such we made sure to acquire a large data set, using different coverslips from at least three different animals in each case. In addition, all experiments were performed and analyzed blind to the experimenter and all data was normalized to its corresponding control to ensure the effects we observed were real.

3.9. Blocking L-type calcium channels not required for the induction of homeostatic plasticity.

A recent paper suggested that L-type calcium channels were implicated in having a role in homeostatic plasticity (Gong *et al.,* 2007). It was demonstrated that adenylyl cyclase 1 contributes to synaptic scaling by coupling L-type calcium channels to downstream signalling pathways which may converge with CREB-dependent transcription. It has been suggested that decreasing neuronal activity by blocking AMPA receptors, results in a reduction in the influx of calcium through L-type calcium channels.

To replicate these experiments, we proceeded to block L-type calcium channels with nifedipine (1mM) at DIV10 and recorded mEPSCs at DIV13. In contrast to Gong's findings we did not observe any significant increase in mEPSC amplitude after treatment with nifedipine when compared to untreated controls (Fig.3.11.a). Similarly, we did not observe any significant changes in mean mEPSC frequency (Fig.3.11.b). Our data suggest that blocking L-type calcium channels does not induce homeostatic synaptic plasticity induced by chronic inactivity.

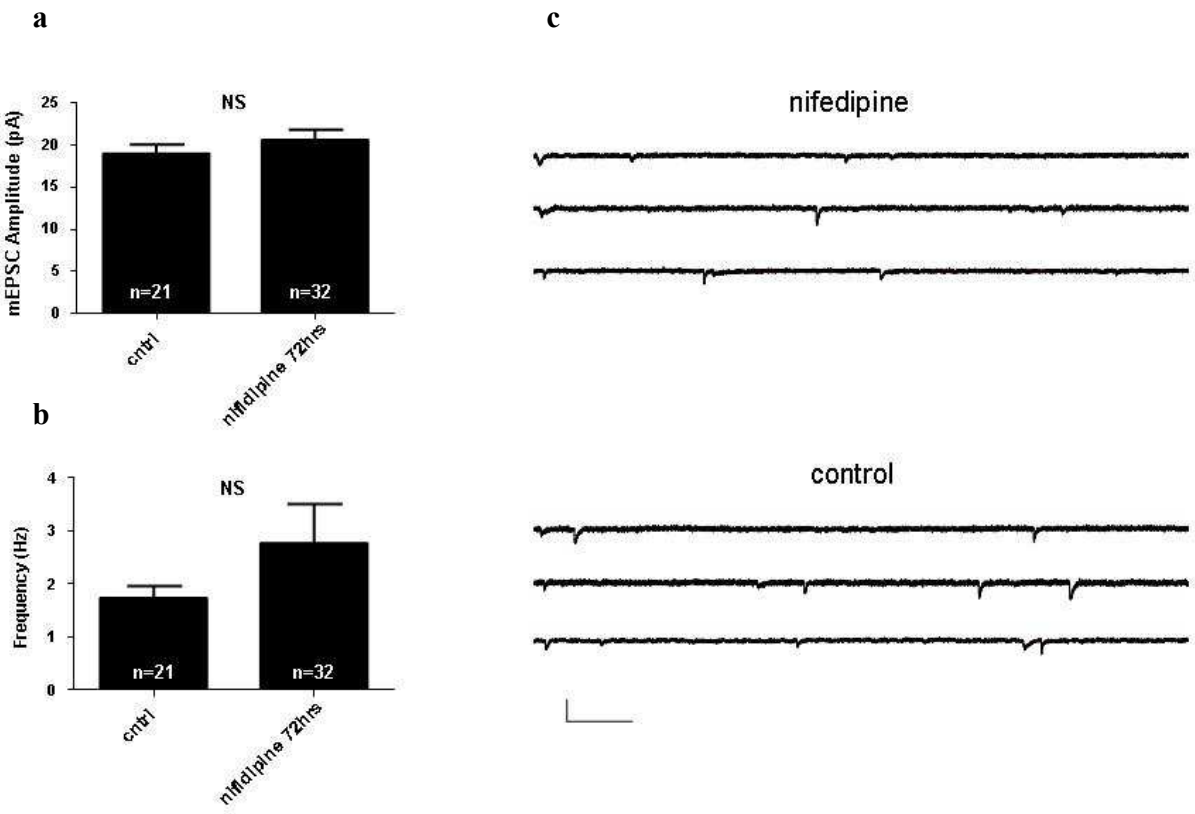

Fig.3.11. Blocking L-type calcium channels does not induce synaptic homeostatic plasticity.
a. Hippocampal cultures were treated on DIV10 with nifedipine until DIV13 at which point whole cell recordings of mEPSCs were taken. Mean mEPSC amplitudes were calculated and plotted. After 72hrs of nifedipine treatment we did not observe any significant changes in mean mEPSC amplitudes (20.60pA ± 1.2, n=32 cells) when compared to untreated controls (18.96pA ± 1.10, n=21 cells, P= 0.345) unpaired t-test. Data expressed as mean and S.E.M from 3 separate experiments.
b. Similarly, after 72hrs of nifedipine treatment we did not observe any significant changes in mean mEPSC frequency (2.76 Hz ± 0.74, n=32 cells) when compared to untreated controls (1.73 Hz ± 0.23, n=21 cells, P=0.60) Mann Whitney Test. Data expressed as mean and S.E.M from 3 separate experiments.
c. Representative mEPSC traces taken from cells treated with nifedipine (to traces) or from untreated controls (top trace) scale = 51.2 pA, 106.5 ms. Each trace represents a recording from a different cell.

3.10. Presynaptic homeostatic regulation.

Over the recent years several labs within the field of homeostatic plasticity have demonstrated the effects of this stabilising mechanism in different regions of the nervous system, such as the visual cortex (Turrigiano *et al.,* 1998), hippocampus (Corette *et al.,* 2006), nucleus accumbens (Sun & Wolf, 2009), and in a different range of model organisms, such as *C. Elegans* (Burbea *et al.,* 2003), *Drosophila* (Frank *et al.,* 2006), Gallus (Borodinsky *et al.,* 2004), as well as *in vivo* (Echegoyen *et al.,* 2007, Mrsic-Flogel *et al.,* 2007) and *in vitro* systems (Hou *et al.,* 2008). Initially, most efforts focused on the effects on the postsynaptic compartment, while less emphasis has been assigned to the presynaptic compartment. While it was soon realised homeostatic mechanisms maintain activity within an optimal operating range through the insertion and removal of AMPA receptors (Gainey *et al.,* 2009) less was known about the participation the presynaptic side plays during this compensatory mechanism. Eventually, scientific momentum picked up with the realisation that the presynaptic compartment plays an equally important role and exhibits flexibility in tuning its output in the face of chronic perturbations

Wanting to concentrate our efforts on any possible presynaptic effects that homeostatic plasticity may have within our system, we looked at the levels of another vesicular presynaptic protein following chronic inactivity, synaptotagmin-1, a putative calcium sensor for neurotransmitter release (Koh and Bellen, 2004, Martens *et al.,* 2007), and a non vesicular protein, synapsin. Synapsins are believed to regulate the number of synaptic vesicles available for release during exocytosis (Evergren *et al.,* 2007, Ferreira, 2000, Ferreira & Rapoport 2002). When hippocampal cultures were treated on DIV10 with TTX or CNQX/APV for 96hrs, the levels of synaptotagmin and synapsin increased significantly in comparison to controls (Fig.3.12.a-d). In addition, we observed significant increases at shorter durations of drug treatment and an opposite effect when we treated our cultures with gabazine in both presynaptic proteins (data not shown).

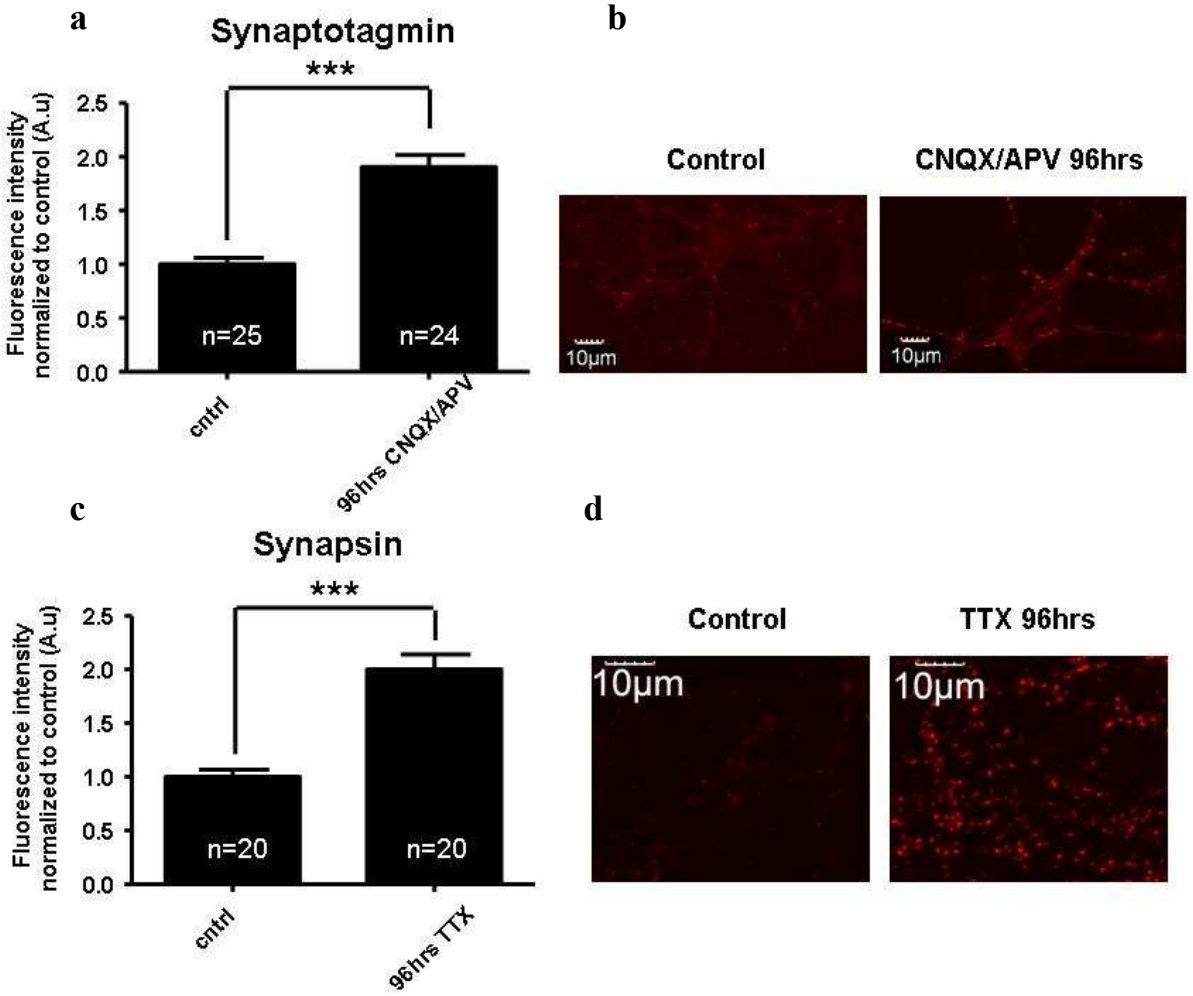

Fig.3.12. Homeostatic up-regulation of vesicular and non vesicular proteins.
a. Hippocampal cultures were treated on DIV10 with CNQX/APV for 96hrs and then fixed/stained with antibodies against synaptotagmin. CNQX/APV treated cells showed a significant increases in fluorescence intensity when compared to controls (CNQX/APV =1.91 ± 0.11 n=24, 720 synapses, Controls: =1.00 ± 0.06 n=25, 750 synapses $P<0.0001$, unpaired t-test. Fluorescence intensity is plotted as arbitrary units and normalized to controls. Data is expressed as mean and S.E.M from 2 separate experiments.
b. Images of hippocampal cells treated with CNQX/APV for 96hrs (right) or left untreated (left) and fixed/stained with antibodies against Synaptotagmin. Scale = 10µm.
c. Hippocampal cultures were treated on DIV10 with TTX for 96hrs and then fixed/stained with antibodies against synapsin. TTX treated cells showed a significant increase in fluorescence intensity when compared to controls (TTX: 2.006 ± 0.14, n=20, 600 synapses, Controls: =1.000 ± 0.07 n=20, 600 synapses, $P<0.0001$, unpaired t-test). Fluorescence intensity is plotted as arbitrary units and normalized to controls. Data is expressed as mean and S.E.M from 2 separate experiments.
d. Images of hippocampal cells treated with TTX for 96hrs (right) or left untreated (left) and fixed/stained with antibodies against Synapsin. Scale = 10µm.

We next turned our attention to the vesicle-associated membrane protein 2 (synaptobrevin 2), also known as VAMP-2. Synaptobrevin is an intrinsic membrane protein of synaptic vesicles which is involved in the molecular events underlying neurotransmitter release (Baumert *et al.,* 1989). We treated our cultures with CNQX/APV for 48, 72 and up to120hrs and stained for VAMP2 and vGlut1 on DIV 15 (Fig.3.13.b). As VAMP2 is found in vesicles in both inhibitory and excitatory neurons co-staining with vGlut was necessary to identify the VAMP2 found in excitatory rather than inhibitory neurons. 48hrs of drug treatment resulted in increases in VAMP2 in excitatory neurons which persisted at 72hrs and 120hs. When we looked at vGlut1 levels after 48hrs of drug treatment we observed a slight increase but this did not reach significant levels, however at 72 hrs we began to see significant increases which persisted until 120hrs when compared to controls (Fig.3.13.a).

We were able to extract more information from our cultures treated with CNQX/APV which had been stained for VAMP2 and vGlut1. As VAMP2 is found in both inhibitory and excitatory cells, any VAMP2 which did not co-localize with vGlut1 must belong to inhibitory neurons. Wanting to assess whether this protein would behave in a similar manner in inhibitory neurons after chronic disuse; we analyzed any VAMP2 puncta which did not co-localize with vGlut1. We did not observe any significant changes in the levels of VAMP2 after 48hrs or at 120hrs of drug treatment when compared to controls (Fig.3.13.a). These results are in compliance with out previous findings with vGat and gephyrin (Fig.3.9.), suggesting that inhibitory neurons are not under the same homeostatic influence as excitatory cells are.

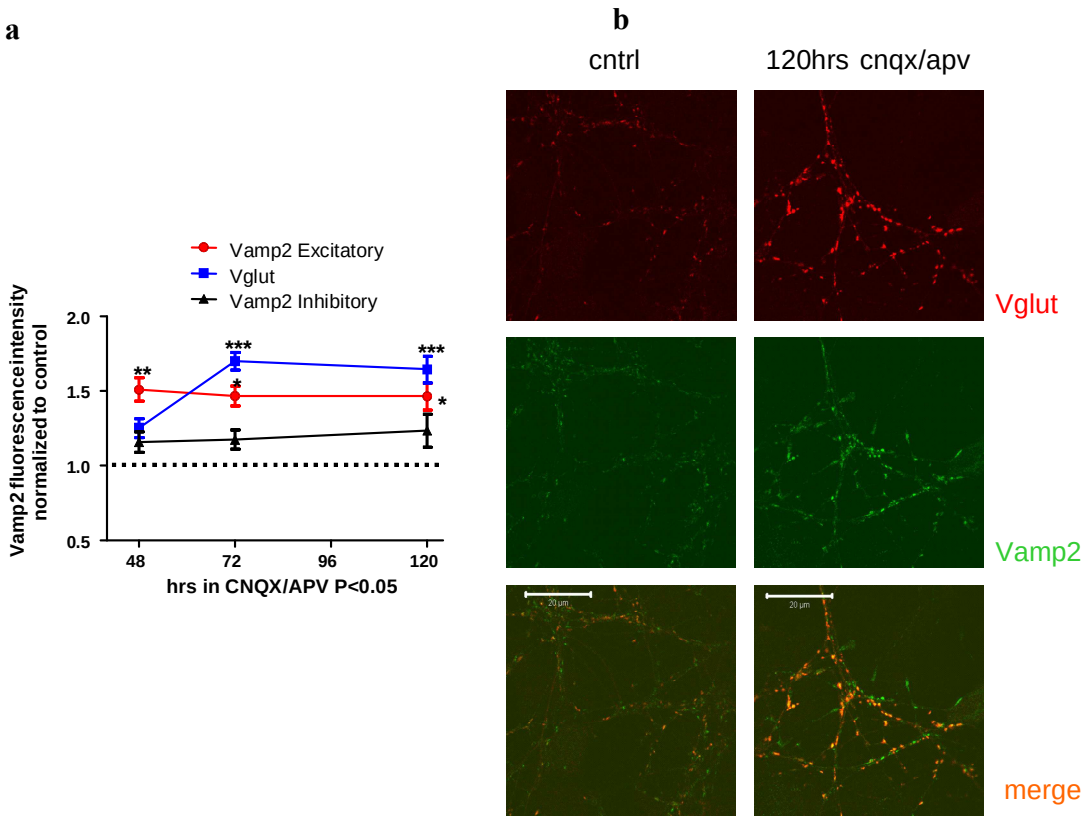

Fig.3.13 VAMP2 responds homeostatically in the face of chronic activity disuse

a. Hippocampal cultures were treated on with CNQX/APV for 48, 72 and 120hrs at which point they were fixed and stained on DIV 15 with antibodies against VAMP2. We observed significant increases in VAMP2 at 48hrs (1.51 ± 0.08 n=15, 450 synapses), 72hrs (1.47 ± 0.07 n=15, 450 synapses) and 120hrs (1.46 ± 0.09 n=15, 450 synapses) when compared to controls (1.00 ± 0.10 n=14, 420 synapses) $P<0.05$. The same cells were also stained with antibodies against vGlut1. After 48hrs we observed an increase in the levels of vGlut1 (1.25 ± 0.06 n=15, 450 synapses) although this did not reach statistical significance. However, after 72hrs we began to see significant increases in vGlut1 (1.70 ± 0.06 n=15, 450 synapses) which persisted until 120hrs (1.64 ± 0.13 n=15, 450 synapses) when compared to controls (1.00 ± 0.067 n=14, 420 synapses) $P<0.05$. We did not observe any significant changes in the levels of VAMP2 found in inhibitory neurons after 48hrs of drug treatment (1.16 ± 0.07 n=15, 450 synapses), 72hrs (1.18 ± 0.06, n=15, 450 synapses) or at 120hrs (1.24 ± 0.11 n=15, 450 synapses) when compared to controls (1.00 ± 0.12 n=13, 390 synapses). $P>0.05$. Dunn's multiple comparison test was used for all analysis. Fluorescence intensities were normalized to controls and expressed as mean and S.E.M from 3 different experiments.

b. Representative images of untreated control cultures (left panel) fixed or cultures treated with CNQX/APV for 120hrs (right panel) and stained on DIV15 with antibodies against VAMP2 (red) or vGlut (green). The bottom two images are merged. Scale=20µm.

In summary, synapses appear to respond to chronic and global changes in activity, structurally and functionally in a bi-directional manner. Increases in activity result in a decrease in both pre- and post-synaptic protein levels, whereas the reverse is seen upon reductions in network activity. Perhaps more intriguingly, we find that this form of plasticity is expressed during development, specifically during the period of synaptogenesis. Our findings suggest that neurons are capable of adjusting their input-output curves by changing the strength of synaptic connections in response to on-going levels of network activity. Such a mechanism will likely provide the necessary feedback for network stability.

3.11. Homeostatic plasticity at the electron microscopy level.

Having established that a variety of pre and postsynaptic proteins, directly involved in synapse function, are under homeostatic control, we sought for a more complete understanding of the structural changes that occur at the level of the synapse. To accomplish this we performed electron microscopy on hippocampal neurons, achieving high resolution characterisation of previously well defined synaptic structures (Shikorski & Stevens, 1997). We thus set out to examine if our reported immunohistochemical homeostatic changes translated into ultrastructural ones. We specifically focused on measuring the number and size of vesicles in presynaptic compartments and the size of the postsynaptic density on the opposing postsynaptic compartment.

Cells were either left untreated (controls) or treated on DIV 10 for 72hrs with either TTX or gabazine. We focused solely on excitatory synapses (Fig.3.14.a), which we differentiated from inhibitory boutons by the shape of the vesicles: spherical in excitatory synapses and more elongated and ovoid in inhibitory ones (Fig.3.14.b). We also excluded from our analysis postsynaptic boutons that had more than one presynaptic partner (Fig.3.15)

a Excitatory synapse

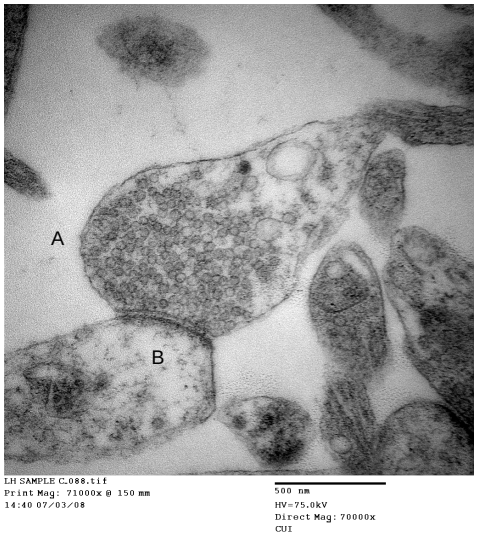

b Inhibitory synapse

Fig.3.14. Visual identification of excitatory and inhibitory neurons.
a. Image of an excitatory synapse taken at x 70000 magnification. Its excitatory nature is determined by the presence of spherical vesicles. Tissue samples were from E.17.5 hippocampal cultures at DIV13. Tissue was sectioned at 60nm thickness. (A) Axonal bouton (B) Dendritic spine. Scale=500nm.
b. Image of an inhibitory synapse taken at x 70000 magnification. Its inhibitory nature is determined by the presence of ovoid vesicles. Tissue samples were from E.17.5 hippocampal cultures at DIV13. Tissue was sectioned at 60nm thickness. (A) Axonal bouton (B) Dendritic spine. Scale=500nm.

Presynaptic bouton with several termination sites

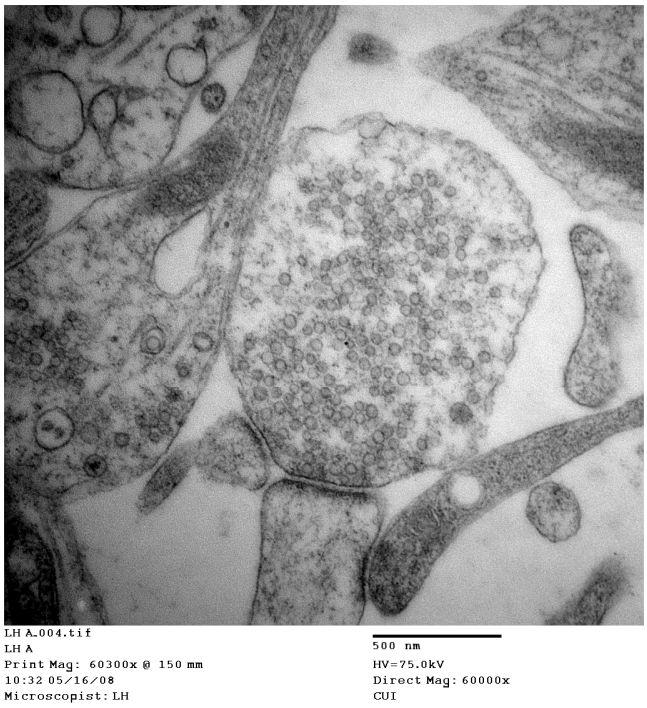

Fig.3.15. Example of an excitatory presynaptic terminal with several postsynaptic partners.
Image was taken at x 70000 magnification. Tissue was sectioned at 60nm thickness. Scale=500nm

A representative synapse we considered for analysis is shown in Fig.3.16. Two structures were taken into consideration. Firstly the vesicles, depicted by pink arrows, and secondly, the postsynaptic density defined by the electron dense material close to the membrane, as indicated by the red line. The active zone is not clearly defined in terms of where it begins and ends in comparison to the postsynaptic density which is evident as a dark stripe. However, the active zone has been previously described to directly oppose the postsynaptic density and has been shown to be highly correlated (>0.97) in rat cultures and slices (Shikorski & Stevens, 1997). Using the reconstruct software (Fiala, 2005) we first measured the area of every single vesicle within axonal termination zones. When we compared vesicular area between the three conditions we found no statistical difference between controls and cells treated with gabazine. However, we did observe that vesicles from neurons treated with TTX were statistically smaller when compared to controls and gabazine treated cells (Fig.3.17.a). Vesicles showed a 10% decrease in area, which is not likely to have crucial biological consequences on the synapse. The statistical difference measured is most likely due to

the large n number in each data set (in the order of thousands), but its biological significance is less clear.

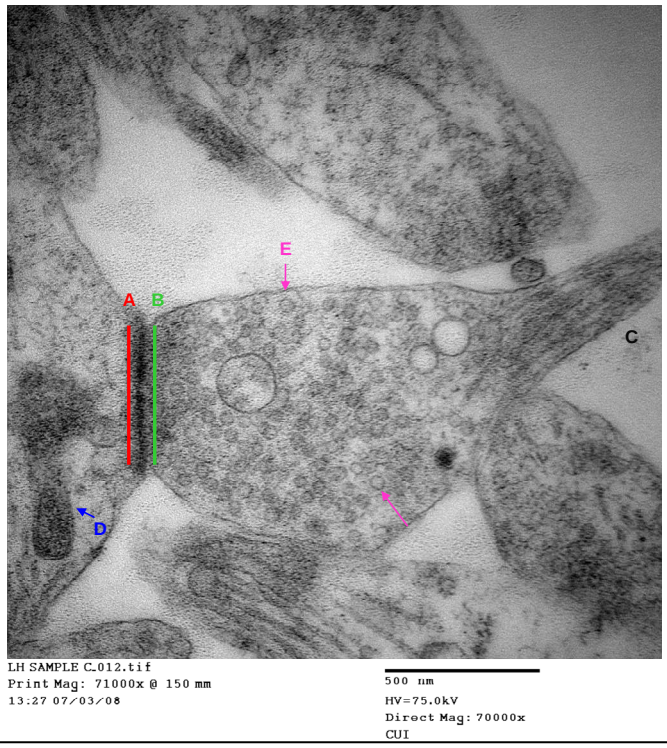

Fig.3.16. Basic structural components from an excitatory hippocampal synapse on DIV13. Image was taken at x70000 magnification (A) Post-Synaptic Density (B) Active Zone (C) Axon with visible microtubules (D) Mitochondria (E) Vesicles. Scale=500nm

Measurements of the length of the PSD in each of our three conditions revealed there was no observable difference in mean length between control cells and TTX treated cells. We did, however, observe a significant decrease in the length in gabazine treated synapses when compared to both other conditions (Fig.3.17.b).

a **b**

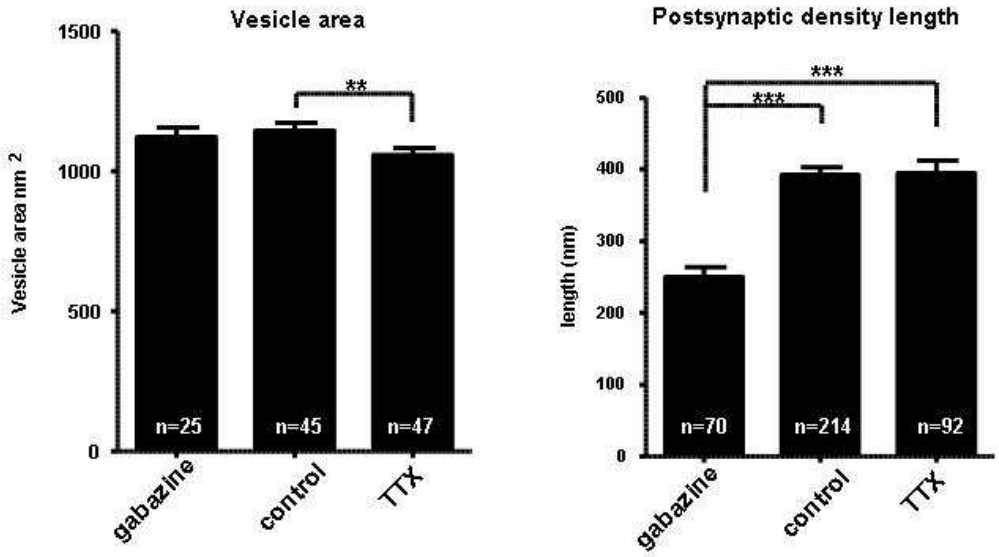

Fig.3.17. Homeostatic regulation of vesicular area and postsynaptic density length.

a. Measurement of vesicular area from hippocampal cultures on DIV13. Cells were left untreated or treated with TTX/Gabazine for 72hrs. We only observed a significant difference between controls and cells treated with TTX.
Gabazine n=25 synapses, mean area 1174nm^2 ± 35.76, 1236 vesicles. **Control** n=45 synapses, mean area 1198 nm^2 ± 30.21, 3358 vesicles. **TTX** n=47 synapses, mean area 1106 nm^2 ± 27.26, 3093 vesicles. Data from 2 separate experiments. Data expressed as mean and S.E.M. Kruskal-Wallis test P=0.01
b. Measurement of PSD length from hippocampal cultures on DIV13. Cells were left untreated or treated with TTX/Gabazine for 72hrs. Significant differences were observed between cells treated with gabazine compared to controls and cells treated with TTX. **Gabazine** n=70 mean length 256 nm ± 13.54. **Control** n=214 mean length 401.4 ± 10.95 **TTX** n=92 mean length 404.3 ± 17.34. Data from 2 separate experiments. Data expressed as mean and S.E.M, Kruskal-Wallis test P<0.0001.

Our results suggest that the system may respond to chronic heightened activity by reducing the size of the postsynaptic density. Previous reports have demonstrated that pharmacologically silenced neurons show increases in all measurements of synaptic size: the active zone length, postsynaptic density length and bouton volume.

Furthermore, the total number of vesicles as well as docked vesicles increased, although the number of docked vesicles per area of active zone remained unchanged (Murthy *et al.,* 2001).

Another possible outcome of altering presynaptic output homeostatically could arise through changes to the number of docked vesicles at the active zone. Thus, we counted the docked vesicles in each of our three conditions. As the readily releasable pool is defined as those vesicles that are immediately available for release we included not only vesicles where the separation between the vesicular and the plasma membrane is not resolvable, but also any vesicles within a distance of two vesicle diameters from the active zone. This analysis revealed that statistically there was a significant difference between control cells and cells treated with gabazine. There was no significant difference between cells treated with TTX and control (Fig.13.8). These results suggest that synapses may respond homeostatically by decreasing the amount of vesicles available for immediate release during prolonged hyperactivity.

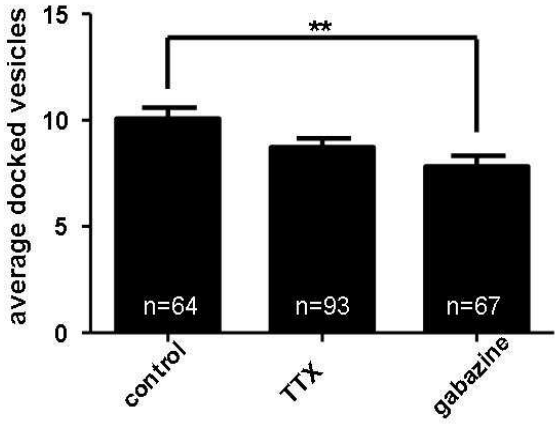

Fig.3.18. Homeostatic regulation of docked vesicles.
Measurement of the number of docked vesicles from hippocampal cultures on DIV13. Cells were left untreated or treated with TTX/gabazine for 72hrs. We only observed a significant diffference between cells treated with gabazine and controls. Kruskal-Wallis test, P=0.003. Data expressed as mean and S.E.M from 2 separate experiments.
Gabazine n=67 synapses, mean number of docked vesicles 7.87, ± 0.5.
Control n=64 synapses mean number of docked vesicles 10.09 ± 4.153.
TTX n=93 synapses, mean number of docked vesicles 8.73± 0.4.

Our finding of 10 docked vesicles in thin slices may be a little high in comparison to other reports which have shown 10 docked vesicles in 3D reconstructions (Shikorski & Stevens, 1997), which is most likely due to the fact that we defined and measured not only vesicles in which the separation between the vesicular and the plasma membrane is not resolvable, but also any vesicles within 80nm, i.e. 2 vesicle diameters, away from the cell membrane. Tissue sections were sliced at a thickness of 60nm as this was large enough to encompass the entirety of a single vesicle (40nm). Any sections larger than this would obscure the clarity of the images as vesicles tended to overlap one on top each other. Although tissue sections of this thickness allow for measurements of vesicular size they only reveal a small 2D representation of the entire 3D structure of the synapse. Thus, we did not measure vesicle number as any such measurements would not reveal the true total number of vesicles per vesicle. One possible method of circumventing this problem would be to carry out tomography on larger sections, 200nm in thickness, allowing for serial 3-D reconstructions. Thus, we were unable to draw any firm conclusions on the effects of chronic activity manipulations on postsynaptic density size and vesicle numbers.

In summary, we observed small changes to vesicle volume in response to chronic inactivity which may not have huge consequences on the functional output in terms of neurotransmitter release. As vesicle volume was not altered in a bidirectional manner it is most likely that vGlut numbers are unaltered per vesicle after chronic activity perturbations and that vesicle numbers are more likely regulated homeostatically, as has been suggested by others (Murthy *et al.,* 2001). Decreases in mEPSC amplitudes have been observed with knockout mice for vGlut1. Moreover, over-expression of vGlut 1 in cultured hippocampal neurons (Wilson *et al.,* 2005) or DVGLUT (a drosophila homologue) in flies (Daniel *et al.,* 2004) results in increased mEPSC and mEJP (miniature excitatory junction potentials) respectively. In the fly studies, genetically increasing the number of transporters per vesicle resulted in a 95% increase in vesicle volume. In addition, DVGLUT mutant flies with reduced transporter levels also exhibit smaller vesicles in size (Daniel *et al.,* 2006). Thus, as we did not observe such a robust change in vesicle volume after pharmacological treatment it is unlikely that vGlut numbers are altered homeostatically and that an

increase in vesicle numbers most likely explains the homeostatic regulation of vGlut1 we have observed immunohistochemically in Fig.3.4&3.6

4. Results Chapter.2-Cell autonomous homeostatic plasticity.

4.1. Manipulating activity in individual cells with genetically-encoded probes.

Neural networks are capable of responding homeostatically to persistently aberrant levels of activity to maintain circuit dynamics and plasticity. Such global scaling preserves the relative differences in synaptic weights while maintaining neuronal firing rates within an acceptable range. Investigation of homeostatic plasticity has typically involved the drastic alteration of activity in a network wide manner. Similarly, so far we have only addressed this phenomenon using pharmacological agents to alter activity throughout the entire network. Although useful as a strategy for studying this form of plasticity, it does not provide any spatial information: how many neurons in a network must be stimulated or silenced to observe compensatory synaptic changes? At its extreme, can a single neuron respond autonomously when subjected to extreme chronic changes in activity, or do homeostatic responses only emerge when the activity of the entire network is altered? To answer this question we set out to chronically manipulate the activity in single neurons within a network.

Previous findings using Kir2.1 to suppress activity in individual neurons, have already suggested that homeostatic plasticity is a cell autonomous feature, highlighting the differences between global and selective suppression of activity, as well as those between early and late manipulations (Burrone *et al.,*2002). There are even reports suggesting that homeostatic plasticity can emerge in individual dendrites when activity is suppressed locally (Sutton *et al.,* 2006, Branco *et al.,* 2008, Rabinowitch *et al.,* 2008). However, matters are complicated by evidence suggesting that, in some cases, homeostatic

plasticity only follows network-wide changes in activity. GABAergic synapses appear to fall into this category. Blocking activity globally, in hippocampal neurons, results in a reduction in mIPSC amplitude and frequency as well as in the number of GABAergic terminals. However, suppression of activity in individual neurons did not alter inhibitory synaptic inputs as seen during global network manipulations. These results suggest that GABAergic synapses are regulated by the level of activity in surrounding neurons (Hartman *et al.,* 2006).

More affirmation of network-wide effects has come from evidence that glial cells are involved in homeostatic responses (Stellwagen *et al.,*2005, Stellwagen & Malenka, 2006). Synaptic scaling of excitatory synapses was shown to be mediated by the pro-inflammatory cytokine, TNF-α, released by glia rather than neurons. This implies that glial cells are able to sense network activity and induce neural synaptic scaling through the release of TNF-α, which is generally thought to act in a global manner.

With evidence supporting both cell-autonomous and network-wide driven processes in homeostatic responses it is currently unclear which phenomenon is dominant. In addition, it is unclear what type of activity drives homeostatic plasticity, as most pharmacological manipulations push network activity to extremes. What levels of activity does a neuron consider to be aberrant? In addition, although there is a strong correlation between chronic changes in activity and synaptic homeostatic plasticity, a critical experiment is lacking: if activity is removed pharmacologically, but somehow put back into a neuron or network, in the presence of the pharmacological compound, are neurons prevented from undergoing a homeostatic program? This recovery experiment, which is key to any knock-down or knock-out experiment where a molecule is removed and then re-expressed to assess for specificity, is lacking for electrical activity in homeostatic plasticity. Here, we performed precisely this experiment to establish if neuronal activity is critical for homeostatic plasticity and if it is cell autonomous in nature.

Until now these experiments were hard to perform because tools were not available to precisely control the electrical activity of individual neurons for long periods of time (many days). For our experiments the temporal precision for manipulating activity within individual cells would have to be in the order of milliseconds and be able to persist for several hours to days. Extracellular electrodes have limitations in their spatial resolution

and other methods like intracellular electrophysiology rely on mechanical stability, are invasive and ultimately lead to cell death within minutes to hours. However, alternative methods of stimulating neurons have begun to emerge. Now, optogenetic approaches allow the possibility of manipulating activity within genetically-targeted single cells (Boyden *et al.,* 2005). Using light as a means of stimulation would meet our experimental requirements, providing sufficient temporal and spatial accuracy.

In mammals, specialized retinal cells (rods and cones) involved in vision have evolved to be photoresponsive. Retinal cells possess the photoreceptive protein rhodopsin that signals to ion channels indirectly and is therefore a relatively slow process (Burns & Baylor, 2001). Nonetheless, these cascades have been exploited to confer light-sensitivity to non photoresponsive cells. This was initially accomplished by taking advantage of the invertebrate phototransduction system. In invertebrates, light mobilizes a different class of G protein (Gq/11) which then activates phospholipase C. This results in cation channels in the plasma membrane opening which depolarize the cell (Ranganathan *et al.,* 1991). Thus, ectopic expression of the invertebrate transductions system could serve to stimulate excitable cells with light by expressing the minimum number of proteins needed for phototransduction. These include rhodospin, a G protein and arrestin, all of which, when expressed in neurons have been referred to as chARGe (Zemelman *et al.,* 2002). However, even with this cohort of proteins present in non retinal cells conveying photosensitivity, light responses are slow and small in magnitude and require the exogenous expression of three different genes making this specific optogenetic tool unsuitable for our purposes.

Alternative means of stimulating neurons also exist. Light can be used to directly photoisomerize the synthetic molecule azobenzene that is covalently attached to an engineered K^+ channel. Photoisomerization of an azobenzene enables neural control through chemical gating (Banghart *et al.,*2004). Long wavelength light drives the azobenzene into its *trans* configuration causing it to block the pore, while short wavelength light generates the *cis* configuration resulting in a removal from the pore allowing conduction. Light can also be used indirectly to activate a receptor through caged precursors. These include 'caged' forms of neurotransmitters such as glutamate and GABA, as well as intracellular signaling molecules such as calcium and cAMP

(Kantevari *et al.,* 2009). Uncaging of these compounds have been used to locally activate cellular processes, but are generally used acutely and not for long periods of time.

The approaches used to photostimulate can thus be placed into 3 categories: uncaging of chemically-modified signaling molecules, chemical modification of ion channels and the photosensitive proteins/channels. All these techniques ultimately allow modulation of the membrane potential of excitable cells or initiation of downstream signaling cascades with varying temporal and spatial control. The method we chose to photoactivate single cells was the introduction of a photosensitive cation channel, channelrhodopsin-2 (ChR2), as this tool did not have some of the limitations in temporal and spatial control that other techniques suffer from.

4.2. Channelrhodopsin-2.

Recently, two distant relatives of rhodopsin, Channelrhodopsin 1 (ChR1) and 2 were identified in the unicellular green algae *Chlamydomonas reinhadrtii*. Both these channels are gated by visible light and are thought to enable phototaxis by coupling to specific transducers. ChR1 has been shown to be selective towards protons (Nagel *et al.,*2002). ChR2 is activated by blue light (450-500nm wavelength; Fig.4.1.), which converts the dark adapted all-*trans* form of retinal into its *cis* isomer configuration after illumination, opening the channel. Recent findings have identified a four-state model in ChR2 composed of 2 closed (C1 and C2) and two open (O1 and O2) states suggesting that the C1-O1 represent dark-adapted and the C2-O2 light-adapted branches. In addition, the fact that ChR2 currents decay in a bi-exponentially can be explained by this four-state model (Nicolic *et al.,*2009*).*

Since the discovery of ChR2 there have been efforts to modify its properties. For example, modifications at the C128 position extends the life time of the open state making the protein more responsive to light at lower intensities in comparison to the wild type ChR2 (Berndt *et al.,*2009). In addition, an engineered opsin gene has been

constructed allowing for sustained spike trains of up to 200 Hz which exceeds the limits (30-40Hz) of the wild type version (Gunaydin *et al.,*2010).

Under normal conditions the inward flood of cations depolarizes the cell and, if the threshold for activating Na^+ channels is reached, this results in the generation of action potentials. As the channel can return to the all-trans ground state without the necessity for other enzymes, this tool is ideal for stimulating subset of neurons with millisecond precision. One important factor that directly influences the success of photostimulating cells is the expression levels of the channel in the cell membrane. It may be that cells expressing low levels are only depolarized at subthreshold levels rather than generating action potentials. However, when patching onto cells expressing low levels we were able to still generate action potentials reliably upon photostimulation (data not shown). Other advantages are also the apparent lack of toxicity to cells that over express ChR2 (Aravanis *et al.,*2007). The resting properties of neurons, as well as the shape and threshold of action potentials is normal in transgenic mice that express ChR2 (Wang *et al.,*2007), a feature that we confirm in rat cultures in this chapter. As a result, ChR2 has so far been expressed successfully in variety of different cells and species, including mammalian cells (Nagel *et al.,*2003, Ishizuka *et al.,*2006), *Drosophila* (Schroll *et al.,*2006), *C. Elegans* (Nagel *et al.,* 2005), as well as in the rodent retina (Bi *et al.,*2006), rodent motor cortex (Aravanis *et al*., 2007), spinal chord and hindbrain (Hagglund *et al.,*2010).

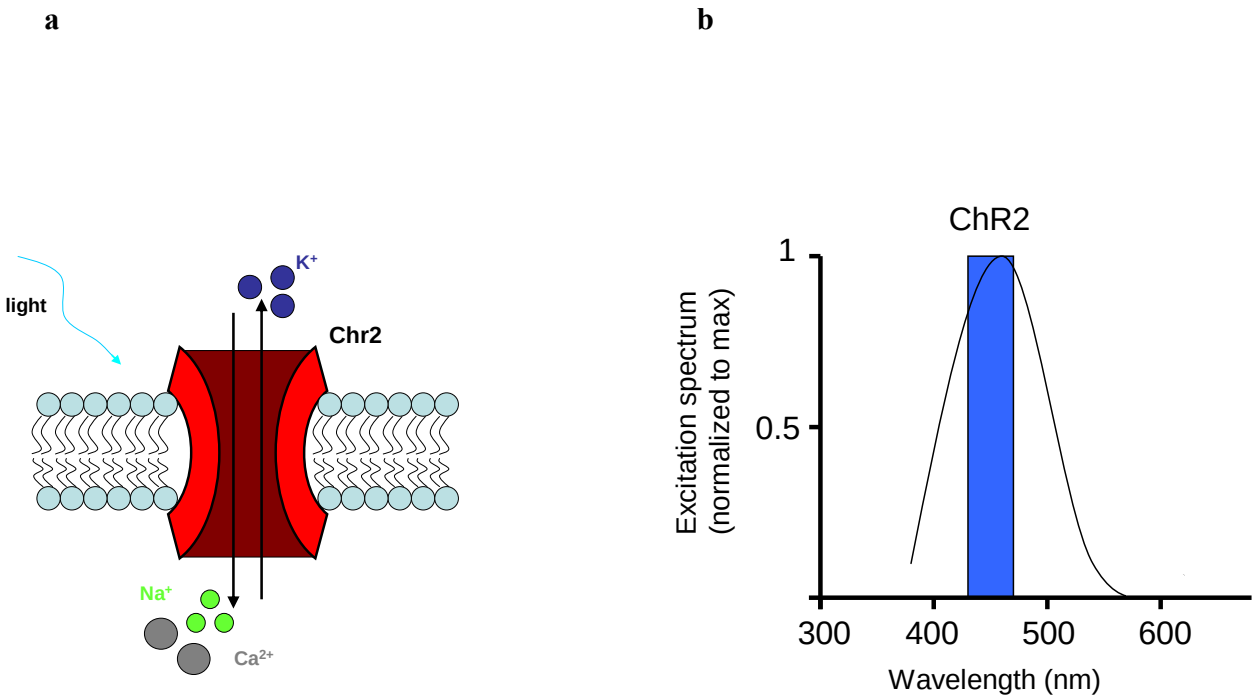

Fig.4.1. Photostimulation of Channelrhodopsin-2.
a. Illumination of ChR2 with blue light (bandwidth 450-500nm) activates the channel allowing cations to pass through resulting in depolarization of excitable cells.
b. Action spectra of ChR2.

4.3. *Exploring cell-autonomous homeostatic plasticity.*

We set out to establish whether we could reintroduce neuronal activity into a single neuron, in an otherwise pharmacologically silent network, and prevent that neuron from undergoing homeostatic plasticity. In other words, we aimed to trick a neuron into believing that it was normally active, despite being surrounded by inactive neighbors. To do this we aimed to express ChR2 in a small subset of neurons and photostimulate them for several days with short bursts of full field light pulses. The low efficiency of transfection using the lipofectamine method permitted us to minimize interactions between multiple transfected cells. By doing so we sought to increase the overall activity within these individual cells to explore homeostatic plasticity in individual neurons. We could then look for both structural and functional phenotypes at the synapse, by using immunohistochemical and electrophysiological means. Importantly, this would also allow us to probe the location of the sensor for homeostatic plasticity, by focusing on either the inputs or the outputs of a neuron with altered activity patterns. In other words, could we replicate homeostatic plasticity induced through global changes in activity by changing presynaptic or postsynaptic activity only (Fig.4.2.)?

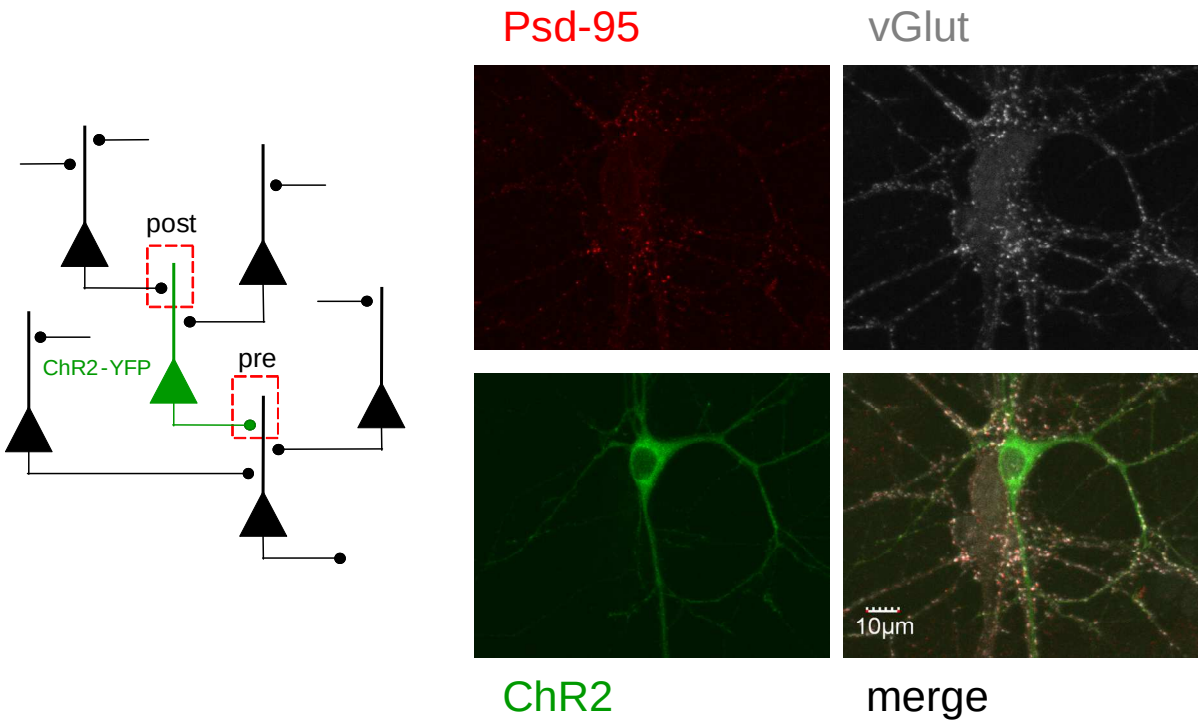

Fig.4.2. Schematic diagram illustrating a subset of neurons expressing ChR2 integrated within a network.

a. Illustration of experimental set up. Transfections yield a subset of cells expressing ChR2. In the presence of CNQX/APV these cells can have activity re-introduced into them through photostimulation preventing any homeostatic regulation. Using immunohistochemistry we can explore for any structural changes to specific pre and postsynaptic proteins within the axons and dendrites of these individual cells.

b. Representative images of a ChR2-eYFP (green) hippocampal expressing cell at DIV13 which has been fixed and stained with antibodies towards vGlut1 (grey) and PSD-95 (red). Scale =10 µm

We first set out to choose the correct pharmacological treatment for inducing homeostatic plasticity. From the previous chapter it became clear that blocking glutamate receptors with CNQX/APV was very effective in that regard and provided a means to silence the network. This would therefore allow us to reintroduce activity into a single neuron and drive it to fire action potentials when the blockers were present. The presence of glutamate receptor antagonists would also prevent the spread of activity along the

network, providing a means to precisely stimulate a single neuron in a network, without network-wide effects or recurrent excitation. In essence, each neuron became uncoupled from the network, at least at the level of excitatory transmission. Through long-term photostimulation we aimed to re-introduce activity in the ChR2+ive cells and effectively prevent them from drug-induced homeostatic regulation (Fig.4.3.). This approach would also allow us to explore whether homeostatic plasticity is cell autonomous in nature and whether pre- or postsynaptic activity (or both) is required. If individual cells were influenced by the activity of surrounding cells we would expect our ChR2+ive cells to up regulate their synaptic output in response to the drug treatment despite the presence of action potentials. However, if single cells regulate their synaptic output according to the activity they exhibit and sense, cells would not behave like their neighboring counterparts, more specifically we would not observe any homeostatic synaptic up regulation.

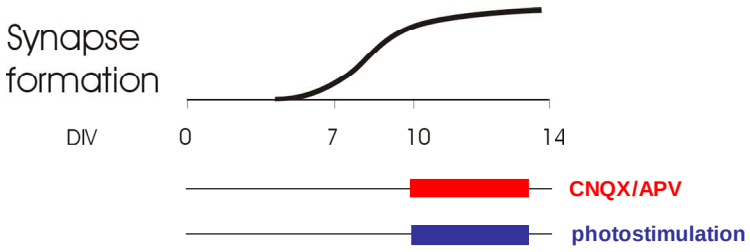

Fig.4.3. Experimental outline for the prevention of homeostatic plasticity using optogenetics.
A subset of hippocampal neurons transfected with ChR2 are treated on DIV10 with CNQX/APV until DIV13, inducing a homeostatic response. ChR2+ive cells are concurrently photostimulated with blue light through out their incubation time in the drugs, effectively rescuing them from inactivity and preventing a homeostatic response.

4.4. ChR2 expression does not alter the electrical properties of neurons.

First, it was essential that we verified that incorporation of the ChR2 into the membrane did not alter the electrical properties of transfected cells. As shown by other labs (Wang *et al.,*2007) we saw no difference in the electrical resting properties of the membrane of neurons expressing ChR2 recorded at DIV 13 (Table in Fig.4.4.e). We also recorded mEPSC from ChR2+ive and ChR2-ive neurons at the same stage, from cells from within the same coverslip (Fig.4.4.a). There was no significant difference in the mEPSC amplitudes or frequencies between the two groups, nor in the time of rise or decay and neither the area (Fig.4.4.a&b&e) We were thus confident that any possible differences seen in synaptic strength or properties in ChR2+ive cells after chronic photostimulations would be due to the induction of activity rather than any adverse effects from transfections or the actual expression of ChR2 on the cell membrane.

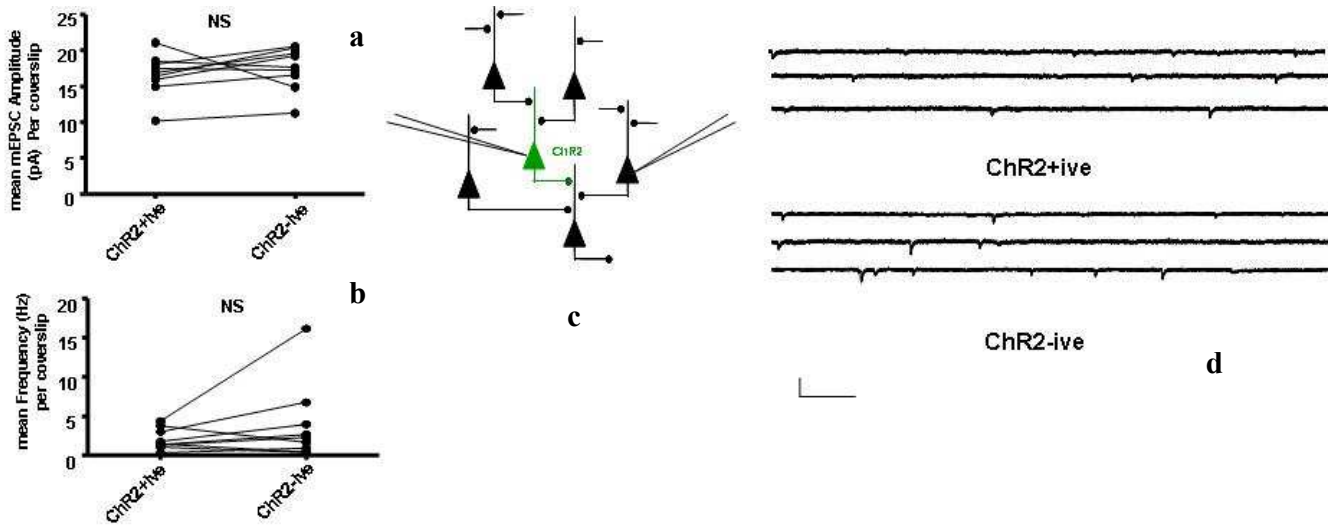

e

ChR2	Rm (MΩ)	Cm (pFa)	Amp. (pA)	Hz	Rise (ms)	Decay (ms)	Area (pA/ms)
+ive	321.6 ± 16.48	50.50 ± 2.97	16.64 ± 1.0	2.07± 0.45	1.69 ± 0.09	5.88 ± 0.41	68.31 ± 6.68
-ive	312.1 ± 41.41	50.50 ± 2.97	17.51 ± 1.0	3.94 ± 1.67	1.81 ± 0.07	7.99 ± 0.87	93.81 ± 10.19

Fig.4.4. ChR2 expression does not alter the electrical properties of neurons or quantal synaptic transmission.

- **a.** mEPSC recording were taken form ChR2+ive and ChR2-ive hippocampal DIV13 cells from within the same coverslip and the amplitudes were compared. These recordings were taken from 3 separate experiments and a total of 9 different coverslips. The values for either cells did not significantly differ (ChR2+ive = 16.64 ± 1.08 pA n =13 cells, ChR2-ive = 17.51 ± 1.73 pA n=14 cells, 9 coverslips, unpaired t-test P=0.55). Data is expressed as mean and S.E.M
- **b.** When we compare the frequencies between coverslips we did not observe a significant difference between ChR2+ive cells (2.07 ± 0.45, n=13 cells) when compared to ChR2-ive cells (3.94 ± 1.67, n=14 cells, 9 coverslips). Mann Whitney test P= 0.67. Data is expressed as mean and S.E.M.
- **c.** Schematic diagram of ChR2 +ive (green) and –ive (black) cells recorded form within the same coverslip.
- **d.** Representative mEPSC traces form ChR2 +ive (top) and –ive cells (bottom). Scale= 51.2 pA/106.5ms. Each trace is from a different cell.
- **e.** Table with cell electrical properties and mini properties. Cell membrane resistance and capacitance as well as mEPSC amplitude, frequency, mean rise, decay and area values showed not significant differences between ChR2+ive and –ive cells. All values were analyzed with an un-paired t-test P>0.05, except for the frequency and decays times which were calculated using a Mann Whitney test. Amp: P= 0.55, Hz: P=0.67 Rm: P=0.84, Cm: P=0.40, Rise: P=0.34, Decay: P=0.13, Area: P=0.05.

4.5. Successful induction of bursting activity in ChR2+ive cells.

To photostimulate in the incubator, for long periods of time (up to 2 days) we used blue LEDs (Light Emitting Diodes, wavelength 455 ± 10 nm). This was powered by a custom made driver and controlled by a Master-8 stimulator. Using a photometer we calculated that the LEDs emitted approximately ~1 $mW.mm^2$ at the coverslip surface which is sufficient to generate photocurrents large enough to induce action potentials in hippocampal neurons. These were placed directly under the 12 well transparent culture plates in adapted light stands. The distance between the cells and the LED was approximately 0.5cm.

To establish that these LED's could induce action potentials in our neurons, on-cell recordings were carried out by Mathew Grubb, where he delivered varying temporal patterns of 20 ms-duration light pulses in 12-14 DIV cultures. Cells were stimulated with the LEDs using a sparse regular pattern of 1 Hz (Fig.4.5.a) or by grouping the flashes into burst of 5 pulses at 20 Hz every 5 s (Fig.4.5.b). With both temporal patterns he was able to generate a minimum of one action potential per light pulse and in most cases even two. These results demonstrate that the light emitted from these LEDs were sufficient to drive action potentials in ChR2 expressing cells and are ideal for long-term photostimulations.

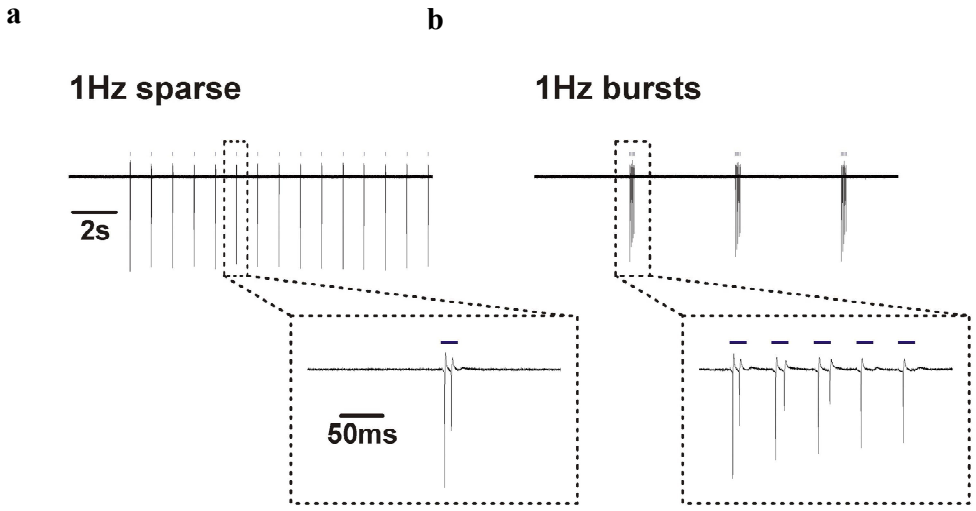

Fig.4.5. Successful generation of photocurrents in ChR2 cells using various temporal patterns of light emitted form an LED.

a. On-cell configuration recordings from a ChR2+ve neurons, DIV12-14, during 1Hz sparse (left) LED photostimulation (blue bars 20ms), demonstrating succesfull photoactivation, scale=2 &50ms.

b. On-cell configuration recordings from a ChR2+ve neurons, DIV12-14 during 1Hz burst (right) LED photostimulation (blue bars 20ms), demonstrating succesfull photoactivation, scale=2 &50ms.

4.6. Re-introducing activity into pharmacologically silenced ChR2+ive cells.

To re-introduce the neuronal activity that was removed by CNQX/APV treatment we first needed to establish what the baseline firing properties of our neurons was at DIV 10 (when treatment starts) and at DIV 12 (when treatment ends). We performed on-cell, patch-clamp recordings from hippocampal neurons at these two developmental stages, to record ongoing spontaneous activity in ChR2+ive cells (Fig.4.6.a). At DIV 10 neurons fired at a low frequency (0.12 Hz), which increased after two more days in vitro (0.33 Hz). Importantly, we found that neurons generally fired in bursts, with multiple action potentials (2-10) arriving at frequencies of 10 to 30 Hz. Acute addition of CNQX/APV dramatically decreased neuronal firing at both stages (DIV 10: 0.01 Hz; DIV 12: 0.0001 Hz) (Fig.4.6.b). The number of action potentials fired during a burst of 7 action potentials at 20Hz varied at the two different developmental stages. At DIV10, the average number of action potentials fired per burst was 2.6, whereas at DIV12 it was 7.55. The latter value indicates that in some cases a single light pulse elicited more than one action potential.

We therefore decide to re-introduce a form of activity that was similar to that recorded spontaneously. It consisted of seven 30 ms light flashes delivered at an overall frequency of 0.09 Hz. These light flashes were delivered in bursts (similar to the spontaneous firing described above) at 20 Hz each with an inter-pulse interval of 20ms every 75 sec. Using the same LED's employed for long-term photostimulation of neurons, we showed that we could successfully reintroduce activity levels that were similar to those recorded spontaneously (Fig.4.6.b). Overall, we noticed that ChR2-expressing cells responded better to light at DIV12 than at DIV10, which could results from changes in the intrinsic properties of neurons or simply due to the expression levels of ChR2 at these two different time points after transfection. These results also verify that at 5 days post-transfection there are sufficient levels of ChR2 in the cell membrane to elicit photocurrents, and that at this developmental time-point the overall neuronal activity is low in comparison to what has been observed later in development (Wagenaar & Potter,

2006). Therefore, preventing homeostatic plasticity in response to glutamatergic blockade should require relatively low levels of activity.

.

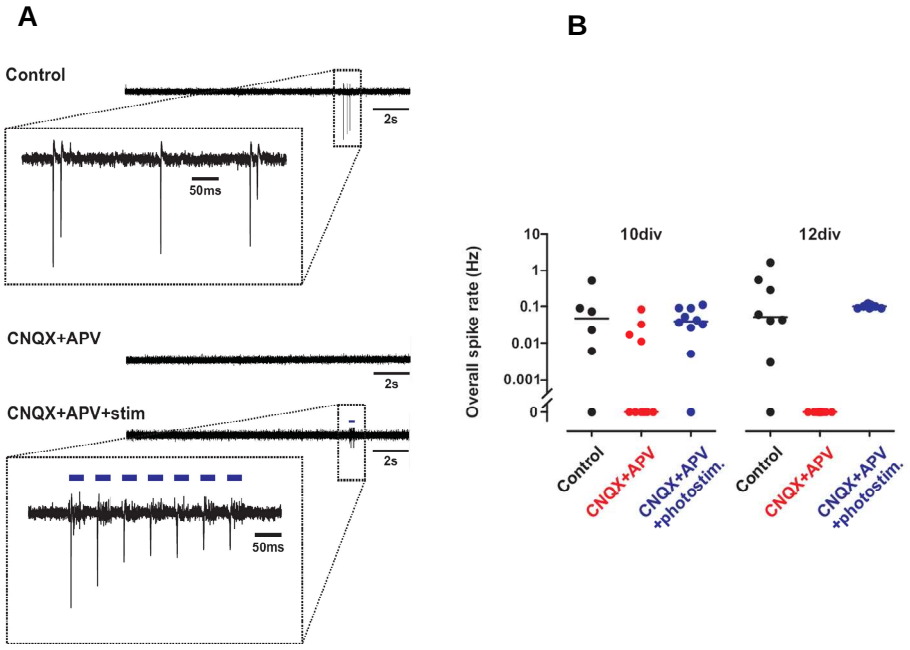

Fig.4.6. Photoevoked re-introduction of activity in pharmacologically silenced ChR2+ive cells.

a. Example traces of spontaneous events in ChR2+ive cells at DIV12 (top trace), after the application of CNQX/APV (middle trace) and then during concurrent photostimulation with a burst of seven 30ms light pulses at 20Hz (blue dashes) in the presence of drugs. Scale=2 sec (expanded traces scale=50ms)

b. Overall spike rate (Hz) of spontaneous activity in ChR2+ive cells (Black, median= 0.05), after the application of CNQX/APV (Red, median = 0.0001) and during concurrent photostimulation in CNQX/APV (Blue, median = 0.04) at DIV10 and DIV12 (Black, median= 0.053, Red = 0.0001, Blue = 0.10).
These recordings where performed byDr. Matthew Grub

4.7. Prevention of homeostatic plasticity: structural measures.

Having verified that photostimulation of ChR2 cells could chronically reintroduce electrical activity into individual neurons in the presence of glutamate receptor blockers; we then proceeded to look for any structural changes at synapses formed onto the dendrites of ChR2+ive cells after a 72hr photostimulation protocol mentioned previously. These cells were then compared to ChR2+ive cells which had just been incubated in the drugs but were not photostimulated, or to cells left untreated. In agreement with our previous findings, we found that the fluorescence intensities of both vGlut1 and PSD-95 puncta on non-stimulated cells increased after chronic treatment with CNQX/APV when compared to untreated cells. However, when we looked at the intensities of these proteins in cells which had been photostimulated while incubated in drugs, we did not observe any significant increases in fluorescence levels, when compared to untreated controls (Fig.4.7.a&b). These results demonstrate that we were able to prevent ChR2+ive cells from drug induced homeostatic up-regulation. This also suggests that single cells are able to cell-autonomously regulate their synaptic inputs and were not influenced by the activity (or lack of activity) in the network. In addition, when we looked at synapse density we did not observe any change in ChR2+ive cells when treated with CNQX/APV (0.37 ± 0.02 synapses/μm, n=42) when compared to controls (0.35 ± 0.02 synapses/μm, n=43). Similarly, cells photostimulated in the presence of CNQX/APV did not differ significantly (0.37 ± 0.02 synapses/μm, n=51), Kruskal-Wallis test P=0.74. Together these findings show that neither chronic drug treatment nor photostimulation affected synapse density within our cells.

However, although these results confirm the existence of cell autonomous homeostatic regulation they do not rule out the possibility that additional network wide influences, such as TNF-alpha, can also modulate synaptic strength. Importantly, our rescue data showed a strong presynaptic phenotype. This is particularly interesting because presynaptic axons will belong to ChR2 -ive neurons in the network, which remained

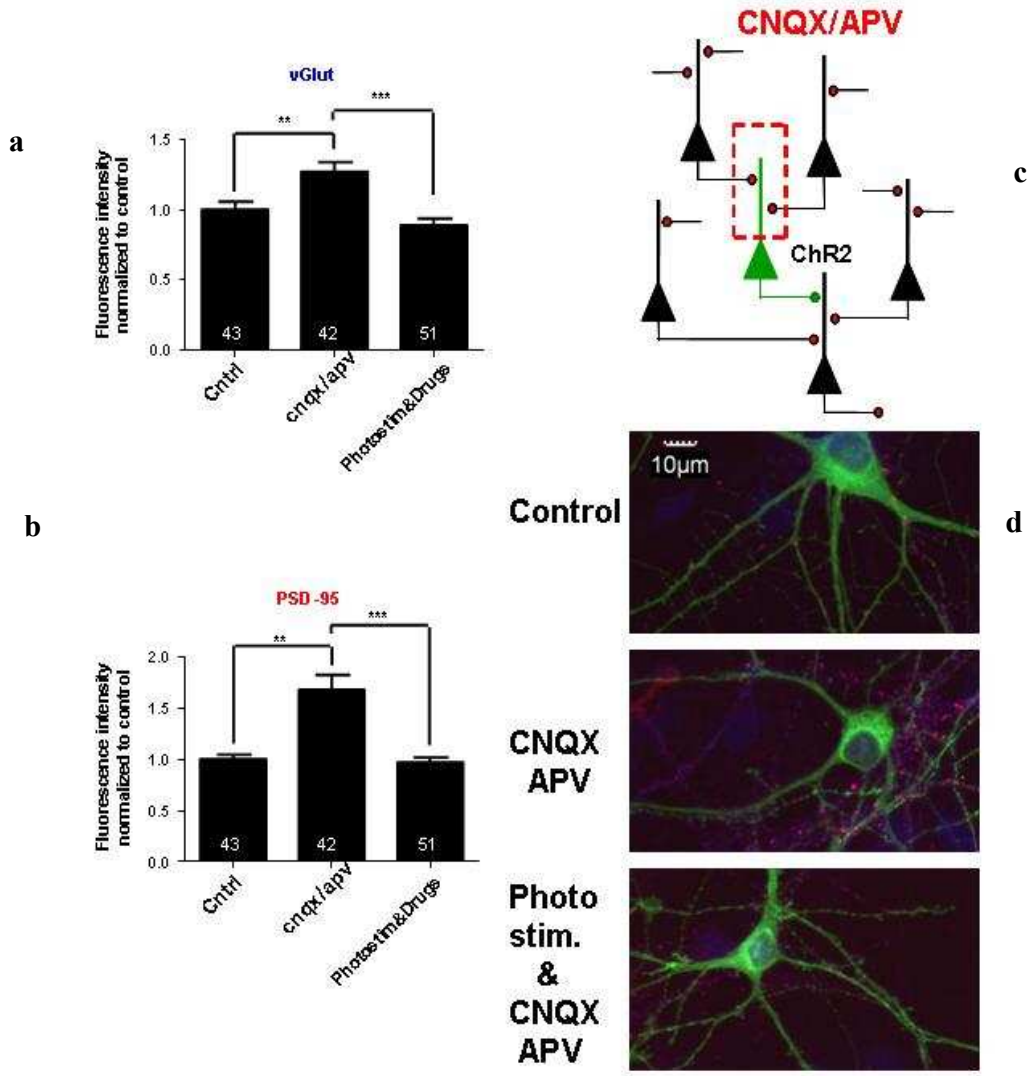

Fig.4.7. Structural prevention from homeostatic plasticity.

a. Synaptic fluorescence intensities for vGlut1 on DIV13 in ChR2+ive cells were significantly larger in cells treated with CNQX/APV (1.27 ± 0.07, n=42 cells, 1260 synapses) while cells photostimulated in the presence of CNQX/APV were not (0.89 ± 0.05 n=51 cells, 1560 synapses) when compared to untreated controls (1.00 ± 0.06 n=43, 1290 synapses), Bonferroni's multiple comparison test ($P<0.05$) 4 separate experiments. Data expressed as mean and S.E.M.

b. Synaptic fluorescence intensities for PSD-95 in ChR2+ive cells were significantly larger in cells treated with CNQX/APV (1.67 ± 0.15, n=42, 1260 synapses) while cells photostimulated in the presence of CNQX/APV were not (0.97 ± 0.05 n=51 cells, 1560 synapses) when compared to untreated controls (1.00 ± 0.04 n=43, 1290 synapses), Dunn's Multiple Comparison Test $P<0.05$, 4 separate experiments. Data expressed as mean and S.E.M.

c. Experimental setup. Fluorescence intensities on dendritic synapses in ChR2 +ive cells are selected and compared between three conditions: untreated controls, cells treated with CNQX/APV and cells photostimulated for 3 days with a burst of seven 30ms light pulses at 20Hz. Black neurons represent untransfected cells synapsing onto green transfected ChR2+ive cell dendrites.

d. Images of ChR2+ive cells for each three conditions fixed/stained with antibodies against PSD-95 (red) and vGlut1 (blue). Top image is an untreated control cell. Middle image is a cell treated with CNQX/APV for 3 days and the bottom image is of a cell photostimulated for 3 days in the presence of CNQX/APV. Scale=10µm

results also suggest that a sensor for chronic perturbations in activity, which initiates the induction of a homeostatic response, exists in the postsynaptic compartment.

4.8. Functional homeostatic rescue.

To establish if these cell-autonomous structural synaptic changes also manifested into functional changes we also performed whole-cell patch clamping to measure excitatory mEPSCs. As above, ChR2+ive neurons were photostimulated in the presence of CNQX/APV for 72hrs. Once again, we compared ChR2+ive cells which had been photostimulated with or without CNQX/APV to ChR2+ive cells left untreated. Cells treated with CNQX/APV exhibited a significant increase in mEPSC amplitudes when compared to untreated controls (Fig.4.8.a). However, recordings from photostimulated neurons, which had been incubated in CNQX/APV, showed no increase in mEPSC amplitude when compared to untreated cells. Additionally, when compared to cells treated with CNQX/APV we observed a significant decrease in mEPSC amplitudes (Fig.4.8.a). On the other hand, the frequency of mEPSCs was not significantly different between groups, except for a decrease in frequency in cells that had been photostimulated in the presence of CNQX/APV (Fig.4.8.b). The decrease could have resulted if our manipulation led to a decrease in synapse density. However, as noted before this possibility was ruled out as we found no change in synapse density between conditions. Together, these results show that we were able to rescue individual neurons from homeostatic changes to synaptic strength after prolonged activity disuse. This rescue phenotype was observed structurally as well as functionally.

Finally, the electrical properties of all ChR2+ive cells were generally unaltered for each condition as shown in the table in Fig.4.9. However, we did observe a small significant difference in the Cm values between cells incubated in CNQX/APV and those concurrently photostimulated.

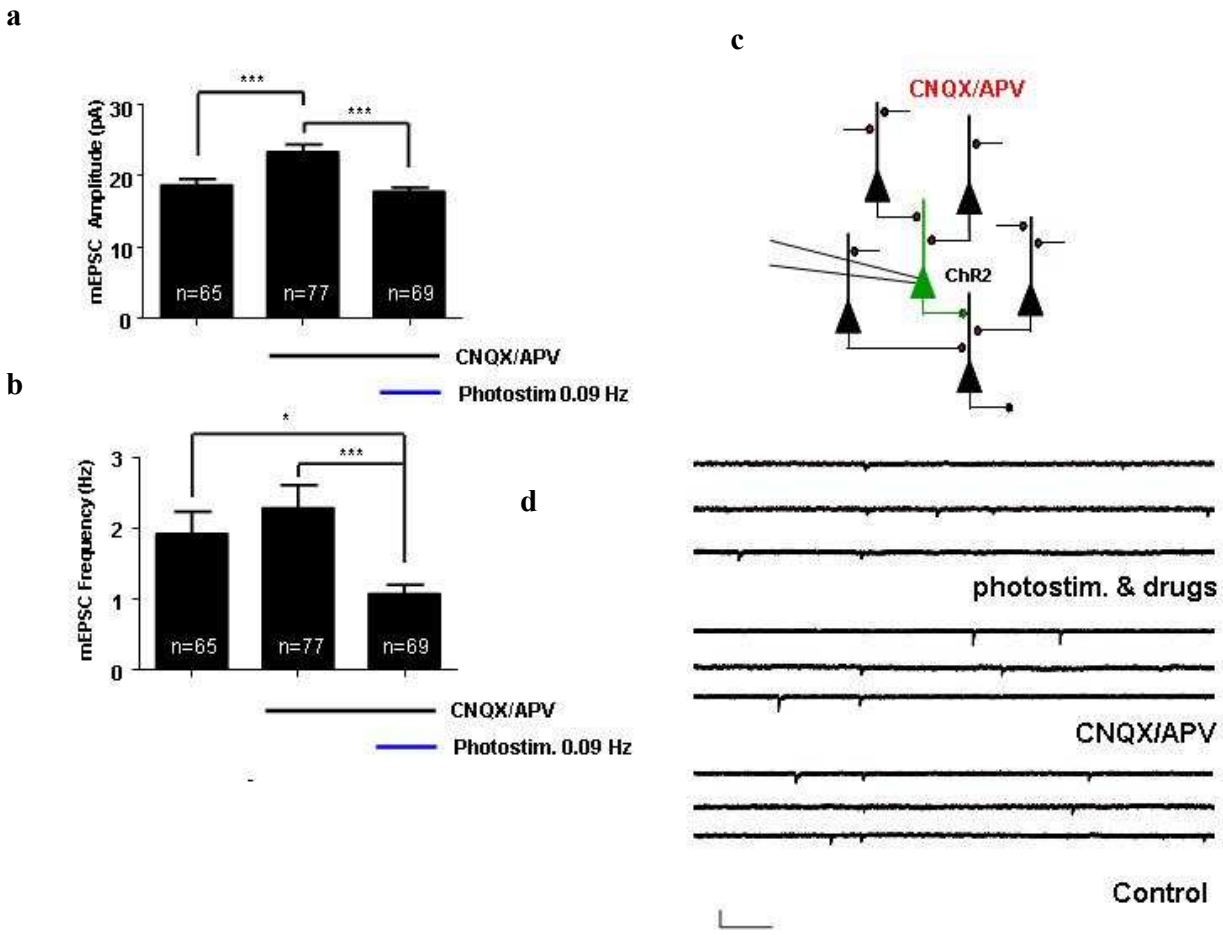

Fig.4.8. Cell autonomous functional homeostatic plasticity in single cells.

- **a.** ChR2+ive hippocampal cells were photostimulated on DIV 10 (3days post transfection) in the presence of CNQX/APV for 72hrs with a burst protocol of seven 30ms pulses of blue light every 75seconds (burst frequency = 20Hz). Cells were then visually identified and whole cell mEPSC recordings were taken. mEPSC amplitudes from cells in the presence of CNQX/APV which had or had not been photostimulated were compared to untreated controls. Cells treated with CNQX/APV exhibited significant increases in amplitude (23.36 pA ± 1.02, n=77) when compared to controls (18.70 pA ± 0.86, n=65). Interestingly cells photostimulated through out their incubation in drugs exhibited a preventative phenotype (17.77 pA ± 0.60, n=69) with amplitudes remaining at control levels (Kruskal-Wallis test $P<0.0001$). Data expressed as mean and S.E.M
- **b.** Whole cell recordings from ChR2+ive cells incubated in CNQX/APV for 72hrs did not exhibit significantly different frequencies in mEPSCs (2.29 Hz ± 0.32, n=77) when compared to controls (1.93 Hz ± 0.32, n=65, $P < 0.05$). However both these conditions exhibited significantly higher frequencies when compared to cells which had been photostimulated throughout their incubation in drugs (1.08 Hz ± 0.13, n=69, Kruskal-Wallis test $P=0.001$). Data expressed as mean and S.E.M
- **c.** Schematic diagram illustrating whole cell recordings from photostimulated ChR2+ive cells after they had been incubated in CNQX/APV.
- **d.** Traces of mEPSC recordings for each condition. Bottom traces are untreated controls, middle traces are from cell treated with CNQX/APV and top traces are from cells photostimulated in the presence of drugs, scale= 51.20 pA, 106.5ms

	Electrical properties		mEPSC properties				
ChR2	**Rm (MΩ)**	**Cm (pFa)**	**Amplitude (pA)**	**Frequency (Hz)**	**Rise (ms)**	**Decay (ms)**	**Area (pAms)**
Untreated controls	280.3 ± 20.27	55.42 ± 2.27	18.70 ± 0.86	1.93 ± 0.32	1.676 ± 0.05	6.06 ± 0.22	81.93 ± 4.16
CNQX/APV	239.2 ± 17.59	62.85 ± * 2.330	23.36 ± 1.02	2.29 ± 0.32	1.64 ± 0.04	6.38 ± 0.24	97.91 ± * 4.89
Photostimulation & CNQX/APV	251.7 ±13.80	53.18 ± 2.00	17.77 ± 0.6	1.08 ± 0.13	1.75 ± 0.05	6.52 ± 0.54	85.70 ± 7.75

Fig.4.9. Electrical properties of ChR2+ive cells in three conditions and mEPSC properties.
Average membrane resistance and capacitance values as well as the amplitude, frequency, rise, decay and area values of mEPSCs from each condition. No significant changes were observed in most parameters for all three conditions, Rm: P=0.25, Rise: P=0.12, Decay: P=0.75. However, significant differences were observed in the Cm: P=0.02 between CNQX/APV treated cells and those photostimulated in the presence of CNQX/APV, and not surprisingly in the area: P=0.01 between cells incubated in CNQX/APV and those concurrently photostimulated in CNQX/APV and untreated cells, Kruskal-Wallis test was used in all conditions. Data expressed as mean and S.E.M.

4.9. Additional verification of cell autonomous functional homeostatic plasticity.

Our experimental approach compared neurons from different coverslips which would inevitably increase the variability within the data set. We therefore exploited our experimental setup, which allowed us to record from ChR2+ive and neighbouring ChR2 -ive cells in the same coverslip. In the presence of CNQX/APV, ChR2-ive neurons should undergo homeostatic plasticity, but not ChR2+ve cells (Fig.4.10.c). We thus recorded from a total of 10 different coverslips, obtained from three different culture preparations. When comparing mEPSCs we observed a significant decrease in amplitude for photostimulated ChR2+ive cells when compared to surrounding ChR2-ive cells (Fig.4.10.a). However, we found no difference in mEPSC frequency (Fig.4.10.b). Importantly, we did not observe any changes in the electrical properties of these cells, except for a small significant change in Cm (Fig.4.11). These results further corroborate our previous findings as we not only observed a prevention of homeostatic regulation in photostimulated ChR2 +ive cells in the presence CNQX/APV when compared to ChR2 +ive cells only treated with CNQX/APV from different coverslips, but we also observed a similar phenotype when comparing photostimulated ChR2+ive cells when compared to surrounding non ChR2-ive cells within the same coverslip.

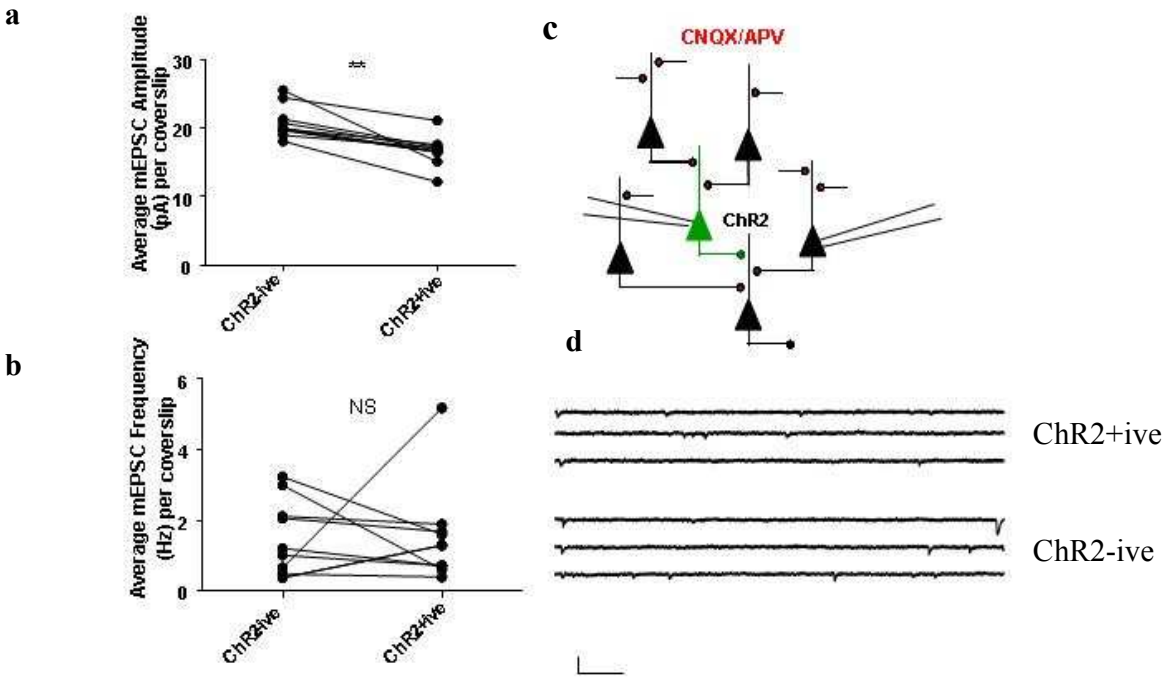

Fig.4.10. Cell-autonomous homeostatic regulation of quantal amplitude.

- **a.** Whole cell recordings were taken from ChR2+ive and –ive cells from the same coverslip after 72hr photostimulation DIV10-13 in the presence of CNQX/APV. mEPSC recording revealed that ChR2+ive cells displayed reduced amplitudes (16.71 ± 0.70 pA, n=10 coverslips & 24 cells) when compared to surrounding ChR2-ive cells (20.86 ± 0.75 pA, n=19 cells, Mann Whitney test P=0.0005. Data expressed as mean and S.E.M.
- **b.** mEPSC frequencies from ChR2+ive cells were not different (1.53 ± 0.44Hz) to surrounding ChR2-ive cells (1.45 ± 1.45 Hz), Mann Whitney test P=0.85. Data expressed as mean and S.E.M.
- **c.** Schematic diagram illustrating whole cell recordings from ChR2+ive and –ive cells from within the same coverslip.
- **d.** Representative mEPSC traces for each condition. Top trace is from a ChR2+ive cell and the bottom trace is from a ChR2-ive cell. Scale= 51.2pA, 106.5ms

ChR2	Rm	Cm (pFa)	Amplitude (pA)	Frequency (Hz)	Rise (ms)	Decay (ms)	Area (pAms)
+ive	299.6 ± 32.37	51.90 ± 4.07 *	16.71 ± 0.70 *	1.53 ± 0.44	1.74 ± 0.10	6.54 ± 1.04	90.21 ± 13.13
-ive	235.1 ± 27.81	73.08 ± 6.75 *	20.86 ± 0.75 *	1.45 ± 1.45	1.854 ± 0.09	6.12 ± 0.31	79.78 ± 5.06

Fig.4.11. Electrical properties of ChR2 +ive and –ive photostimulated cells from within the same coverslip.
Electrical properties of cell, as well as mEPSC porperties from ChR2 +ive and –ive hippocampal cells which had been photostimulated for 72hrs on DIV10 were determined. Mean membrane resistance, capacitance values as well as the mean rise, decay and area values overall showed not significant differences between ChR2+ive and –ive cells from the same coverslip. All values were analyzed with an un-paired t-test except for the area which was calculated using a Mann Whitney test. Most values did not significantly differ. Rm P=0.15, Rise P= 0.39, Decay= 0.35, Area P= 0.92, Hz P=0.85. However, we did observe a significant difference in Cm values P= 0.015 unpaired t-test and in mEPSC amplitudes Mann Whitney test P=0.0005.

4.10. Chapter synopsis.

Here we give evidence in support of cell autonomous homeostatic plasticity. By exploiting optogenetics we were able to manipulate electrical activity within individual neurons, over many days. This allowed us to re-introducing electrical activity into single neurons and was therefore able to prevent the drug-induced up-regulation of synaptic strength observed in response to decreases in activity. Interestingly, this rescue phenotype was observed structurally in both the active postsynaptic ChR2+ive compartment as well as in electrically inactive presynaptic terminals from ChR2-ive neighbouring cells, suggesting the involvement of some retrograde signal.

Although this retrograde signal has not yet been identified there are many possible candidates that include neuroligin, which binds to PSD-95 and connects the postsynaptic density to the presynaptic machinery through its transynaptic partner β-neurexin, nitric oxide and arachidonic acid as all are membrane permeant factors (Tao & Poo, 2001). In addition, brain derived neurotrophic factor (BDNF) which has been implicated in homeostatic plasticity (Thiagarajan *et al.,*2002) could prove to be a strong candidate.

Our results have shown that re-introducing activity in single cells was sufficient to prevent them from the pharmacological induced homeostatic up regulation of synaptic gain. However, one drawback for our experimental approach is the way in which available optogenetic tools deliver activity into neurons. By using a full field flash of blue light to introduce activity into neurons expressing ChR2 over their entire membrane, we consistently depolarize the entire neuron. It is still unclear from our data whether this level of depolarization is sufficient to rescue neurons from homeostatic plasticity or whether it is the action potentials that are actually needed. A possible experiment to resolve this issue would be to repeat our photostimulations in the presence of TTX rather than CNQX/APV. With CNQX/APV, ChR2+ive are able to fire action potentials upon photostimulation. In TTX, cells would be unable to fire action potentials but would still depolarize in response to blue light stimulation. If a homeostatic rescue was not observed in the presence of TTX, it would suggest that some readout of spike frequency/pattern was monitored. However, if cells were rescued by subthreshold depolarization through

ChR2, it would suggest membrane depolarization, but not through activation of Na^+-channels, is important. For example, it may be the case that ChR2 depolarization may induce calcium influx through activation of voltage-gated calcium channels. Regardless of this, our data shows that homeostatic plasticity is cell autonomous and that stimulating a single neuron within a silent network can prevent homeostatic plasticity

Our choice of stimulation paradigm was loosely based on the on-going activity patterns observed in neurons at rest. Our experimental approach will allow us explore the vast domain of frequencies and activity patterns that drive homeostatic plasticity. This technique can be used to test different stimulation paradigms to establish what frequencies and patterns of activity are needed. Here, we have shown one possible paradigm that the neuron takes as normal levels of activity. But we could equally increase the levels of activity re-introduced into a neuron and, in this way, begin to understand how large the range of 'normality' really is. At what point does activity become too large and therefore result in decreases in synaptic gain? By implementing our approach we can begin to get a handle on these unanswered questions.

However, there are some limitations to optogenetic approaches used here, since frequencies higher than 20 Hz become less reliable, with many failures appearing during a burst. More recent studies have shown that higher frequencies may be possible to attain with the emergence of channelrhodopsins that can reach firing frequencies of up to 200 Hz (Gunaydin *et al.,*2010).

Our approach could also determine the time required for the reversal of homeostatic plasticity. For example, if we induced a homeostatic response in ChR2+ive cells with a 24hr treatment with CNQX/APV and then began to photostimulate we could determine how long would it take for a reversal of up regulation? This experiment could shed some light on whether we could speed up the reversal of homeostatic up regulation as well as identify the minimum time required. Clearly all these questions are of interest, and given more time can be resolved.

Efforts were made on our part to photostimulate neurons at higher frequencies of 1 pulse every second. However, after several repetitions it became apparent that this manipulation was lethal to our cultures. Attempts to shorten the duration of the stimulation also proved to be fruitless as cells driven with light for 24hrs also appeared

poor in health. As cells have previously been incubated in CNQX/APV for up to 120hrs without any adverse effects to cell health we ruled out the possibility that the drugs could be having some effect. It became apparent to us that ChR2+ive and –ive cells were dying after chronic photostimulation. This then excluded the possibility of excitotoxicity through ChR2 photostimulation. If we were indeed releasing dangerous levels of glutamate due to our photostimulation, the presence of CNQX/APV would have dampened any excitotoxic effects. Likewise, any glutamate overspill would be localized in the vicinity of ChR2+ive cells and so, any cell death would be confined in certain areas rather than be ubiquitous. As this was not observed this lead us to believe that the deleterious effects must have originated from the light itself.

It has long been known that ultraviolet light radiation can lead to photochemical damage in living cells. Could persistent exposure to blue light be toxic to our cultures? Exposure to visible light (390-550nm) has been shown to generate reactive oxygen species (ROS) such as hydroxyl radicals, superoxide anions and singlet oxygen which can lead to mitochondrial damage (Godley *et al.,*2005). Although low levels of ROS are required for microdomain signalling they also display high reactivity with lipids, nucleic acids and proteins and excessive ROS generation can lead to apoptosis (Brookes *et al.,* 2002). It is thus not surprising that our cultures were not viable after 72hrs of photostimulation. Thus, as increasing the number of flashes led to cell death we only used the physiological stimulation measured electrophysiologically (Fig.4.6) which did not result in cell death. This was confirmed as cells which had been chronically photostimulated in the presence of CNQX/APV exhibited normal cell and mEPSC properties (Fig.4.9.).

Having observed a structural up-regulation in ChR2 cells in the presence of CNQX/APV and a rescue phenotype upon concurrent photostimulation, would these changes translate at the ultrastructural level which could be assessed with electron microscopy? More specifically does the postsynaptic up regulation of PSD-95 result in a larger spine size? Also how does the retrograde messenger from the postsynaptic compartment control the levels of vGlut? Does it alter the number of vesicles, the number of transporters per vesicle or both? If we identified the retrograde signal and disrupted it, could we de-correlate pre- and postsynaptic gain, which we have been unable to do so

pharmacologically? Would the changes in synaptic gain measured with spontaneous events also be observed with evoked transmission?

Although we saw a rescue in the synapse made onto ChR2+ive dendrites would we observe a similar outcome if we had looked at the synapses made by ChR2+ive axons i.e. would we observe an down regulation of PSD-95 on the inactive postsynaptic side of neighbouring dendrites suggesting the existence of an anterograde signal as well?
Our experiments were done *in vitro*, would a similar phenotype be seen *in vivo*?

Recently, a paper was published in which ChR2 was expressed in organotypic hippocampal slices. A 24hr, 3 Hz photostimulation resulted in depressed AMPAR and NMDAR responses in compound EPSCs (Goold & Nicoll 2010). In addition, they did not observe homeostatic regulation in inhibitory responses as GABAR IPSCs in photostimulated neurons did not exhibit any functional changes. Also mEPSCs showed a small decrease in amplitude and significant reduction in frequency. This was attributed to an elimination of synapse rather than to presynaptic release probability. It was also established that Glu2A knockout mice were able to undergo photostimulation-induced depression of NMDAR responses but that GluA2 knockout mice were not. Also, the addition of nifedipine blocked EPSP depression suggesting that L-type calcium channels are necessary for this homeostatic regulation. These results are interesting as they in agreement with our conclusions towards the cell autonomous nature of homeostatic plasticity and the involvement of GluR2. Similarly they did not observe inhibitory responses being homeostatically regulated. However, their finding that L-type calcium channels antagonist, nifedipine, blocked photostimulation induced depression of AMPAR and NMDAR synaptic currents may be specific in homeostatic regulation induced by enhancing activity, or may be due to the *in vivo* nature of their experiments. Although they draw conclusions that chronic heightened calcium influx through L-Type calcium channels drives the synaptic depression, they could not rule out the possibility that some calcium influx through the ChR2 channel itself may contribute to the process.

ChR2 has proven to be a powerful tool with which to explore the nature and properties of homeostatic plasticity. Permutations on the experiments we have carried out can and will progress the understanding we have on homeostatic regulation in neurons. Here we

have added to the understanding of this phenomenon and strengthened the hypothesis that homeostatic plasticity is indeed a cell autonomous feature.

5.DISCUSSION

5.1. Stuctural and developmental correlates of homoestatic plasticity.

Our knowledge in the field of homeostatic plasticity has advanced through various experimental efforts in various organisms including fruit flies (Davis *et al.,* 2001), rodents (Turrigiano *et al.,* 1998), chicken (Borodinsky *et al.,* 2004), nematodes (Grunwald *et al.,* 2004) as well as from various central regions such as the hippocampus (Burrone *et al.,* 2002), visual cortex (Desai *et al.,* 2002), Nucleus accumbens (Sun &Wolf, 2009), spinal cord (Borodinsky *et al.,* 2004) to name a few. In addition, homeostatic plasticity has been observed both *in vivo* (Echegoyen *et al.,* 2007) and *in vitro* (Turrigiano *et al.,* 1998, Burrone *et al.,* 2002). However, there still remain a lot of uncertainties. This is partly due to the experimental differences within the literature and partly due to the absence of a clear understanding of the underlying mechanisms.
It is thus difficult at times to bring together and reconcile the abundance of experimental evidence, which more often than not, is contradictory. However, there are certain accepted concordances within the literature.

Most studies have demonstrated that the standard response of neurons within a network, to abnormal chronic activity, is the regulation of synaptic inputs. This is accomplished in a homeostatic manner, maintaining neuronal firing within appropriate operating levels. At the level of the synapse, adjustments are made that modify the overall structure of the synapse (Murthy *et al*., 2001), the postsynaptic receptor numbers (Wierenga *et al.,* 2005, Ibata *et al.,* 2008, Gainey *et al.,* 2009) and the level of presynaptic proteins (Wilson *et al.,* 2005, De Gois *et al.,* 2006). This results in changes in postsynaptic gain, changes in presynaptic release probability (Bacci *et al.,* 2001) and vesicle priming (Moulder *et al.,* 2006) as well as synaptic size (Murthy *et al.,* 2001). Overall, it is generally thought that global pharmacological manipulations of activity do not appear to alter synapse density

along a dendrite, which we also did not observe with our single (Fig.3.6.) or global activity manipulations (Fig.4.7.)

Postsynaptically, the receptors which are homeostatically altered appear to be AMPA (Ju *et al.,* 2004) and NMDA (Rao *et al.,* 1997) receptors. In fact, work in dissociated cortical neurons has shown that AMPA and NMDA receptor were co-regulated at the synapse (Watt *et al*., 2000). Here, we also give evidence in support of an increase in AMPA receptor numbers at the synapse in response chronic alterations to activity. Firstly, we demonstrated that PSD-95, a scaffolding protein known to traffic and stabilize receptors to the cell membrane (El- Husseini *et al.,* 2000, Shnell *et al.,* 2002, Ingrid & Malinow, 2004) is homeostatically regulated (Fig.3.4&3.8.). This activity-dependent alteration in the levels of PSD-95 is suggestive of a larger postsynaptic density and therefore an increased number of glutamate receptors. Indeed, we found that GluR2 receptor numbers were up-regulated at dendritic arbors in parallel with PSD-95 (Fig.3.6.).

Presynaptically, we observed homeostatic regulation of a variety of synaptic and vesicular proteins and including vGlut (Fig.3.6&3.8.), synaptotagmin, synapsin (Fig.3.12.) and VAMP2 (Fig.3.13.) involved in neurotransmitter loading and release. Previous reports have shown corroborating results in that, rat neocortical neurons treated on DIV19, with TTX or bicucculine, exhibited activity-dependent regulation of vGlut 1 protein and mRNA (De Gois *et al.,* 2006).

Here, we also determined that the rate of homeostatic induction depended on which drug we used to alter activity globally. We found that chronic inactivity produced a faster onset of homeostatic plasticity (Fig.3.4.), compared to increases in activity (Fig.3.8.). Treatment with gabazine exhibited a more stalled onset requiring up to 96 hrs for any structural alterations to appear. As we do not know how gabazine treatment changes network activity in our system, it is possible that only mild increases in neuronal firing are achieved with this pharmacological approach. Unfortunately, there is little information in the literature regarding this treatment. Possible future experiments would include assessing the ongoing changes in network activity during treatment with gabazine by performing long-term recordings with micro-electrodes (Hennig *et al.,* 2011). Some of the experimental discrepancies on the synaptic locus of homeostatic plasticity reported between different labs have been reconciled by attributing these differences to the

developmental time point at which activity is perturbed and the duration of the perturbation. Changes in activity, at early developmental time-points, result in predominantly postsynaptic alterations while ones later on in development result in both pre- and postsynaptic changes (Turrigiano *et al.,* 2006, Han & Stevens, 2009).

We attempted to repeat similar experiments and assess for the synaptic locus in response to activity perturbations at various developmental time-points. Our assessment of the homeostatic locus was performed once more through visualization of the pre- and postsynaptic markers vGlut1 and PSD-95. Our experiments revealed that pharmacological manipulations to activity late in the development in cultures (DIV 10 and onwards) results in both pre- and postsynaptic modifications to our protein markers (Fig.3.4.&3.8.). When we decreased activity just before the onset of synaptogenesis and throughout development (DIV3-13), here we observed a similar phenotype with both pre- and postsynaptic alterations (Fig.3.7.a&b). When we next decreased activity only during the onset of synaptogenesis (DIV3-7) we observed once more changes to both pre- and postsynaptic markers (Fig.3.7.c&d). These results suggest that there may be presynaptic homeostatic modifications at earlier developmental time points in response to activity perturbations previously not reported.

When we plotted the fluorescence intensity of PSD-95 as a function of vGlut1 fluorescence intensity for cultures left untreated at DIV13, this revealed a high correlation between the two (Fig.3.3.) which remained correlated despite chronic pharmacological treatment (Fig.3.4.). This leads us to believe that there is a tight interaction and communication between the presynaptic and the postsynaptic compartment, rather than each side being two completely separate and isolated structures. In addition, we found that this correlation was already apparent at earlier time points, as early as 7 DIV, a time when synapses are just beginning to form in our hippocampal cultures. Also, blocking action potentials in the entire network, from 10 to 14 DIV, by incubating neurons with TTX, had no effect on this correlation (Fig.3.5.a-d).
This strong correlation isn't surprising as there are a myriad of different forms of communication between the two synaptic compartments other than neurotransmission. For example, the binding partner of PSD-95, neuroligin (NLG) provides a direct link to the presynaptic compartment and the vesicular release mechanisms via β-neurexin which

binds presynaptically to calcium/calmodulin-dependent serine protein kinase 3 (CASK) which in turn binds to the mammalian uncoordinated-18 (Munc18) which regulates neurotransmitter release (Kensuke *et al.,* 2007). Another candidate, nitric oxide, is produced in neurons by nitric oxide synthase. Nitric oxide is synthesized in response to the excitation of a neuron by glutamate and can influence synaptic vesicle docking fusion reactions and LTP (Meffert *et al.,* 1996, Schulman, 1997). The tight correlation we observed between our pre- and postsynaptic markers could be maintained through these tran-synaptic forms of communication or through others yet to be discovered.

The total levels of these synaptic proteins which are homeostatically regulated will depend on the rate of production and degradation (turnover). As a result, increases in protein levels could arise from either an increase in gene transcription or a decrease in protein degradation. Altering the equilibrium between the two will have important effects on protein abundance. It is perhaps not surprising that protein degradation pathways have also been shown to be involved in homeostatic synaptic remodeling.

Ubiquitin is a 76 amino acid polypeptide which is linked covalently to proteins through various ubiquitin enzymes (E1-3) tagging them for degradation by the ubiquitin-proteasome complex. Ubiquitin has been shown to control the activity dependent remodeling of the postsynaptic density. Cells treated with TTX or bicucculine for 48hrs exhibited bi-directional changes in ubiquitin conjugates in the PSD. More specifically, ubiquitination of postsynaptic scaffolding proteins Shank, GKAP and AKAP79/150 were decreased at synapses treated with TTX. Equally treatment with proteasome inhibitors mimicked the effects of synaptic blockade. Shank and GKAP are multivalent adaptors which can bind to each other and various other PSD proteins. AKAP79/150 anchors various other proteins to glutamate receptors. In response to elevated levels of activity the turnover of these PSD affiliated proteins is enhanced through de-ubiquitination. The removal or addition of these proteins probably affects the stability of the PSD at the synapse (Ehlers 2003). In addition, glutamate receptors have also been shown to be ubiquitinated (Burbea 2002). In cultures containing a mix of Nuclear accumbans and prefrontal cortex, the addition of the proteosome inhibitors, MG13 or lactacystin, for 24 hrs increased the levels of GluR1 and 2 to the same degree seen after CNQX treatment. However, when they added leupeptin which inhibits lysosome degradation they did not

see any changes to GluR levels (Sun & Wolf 2009). These results thus suggest that the removal and degradation of postsynaptic proteins associated with the PSD are under activity dependent control via the ubiquitin-proteasome system.

5.2. The level of presynaptic proteins is controlled in a homeostatic manner and may represent changes in the number of presynaptic vesicles.

We used immunohistochemistry to investigate how other presynaptic markers involved in neurotransmission behave in response to chronic activity perturbations. These include the vesicular proteins, VAMP2 and synaptotagmin, and synaptic protein synapsin. We reasoned that if we only observed an increment in vGlut1 with the other vesicular proteins remaining unaffected, this would be strong evidence towards a model in which chronic inactivity results in the up regulation of presynaptic gain through increased neurotransmitter release as a direct result of more transporter insertion per vesicle. Alternatively, an up regulation of all vesicular proteins may suggest an increase in the total number of vesicles at the synapse.

Our results show that chronic activity reduction results in the up regulation of all the vesicular proteins we looked at (Figs.3.4 & 3.12 & 3.13.). This suggests that excitatory neurons regulate the number of vesicles rather than the number of transporters per vesicle during homeostatic compensation. However, it must be pointed out that it may be possible that neurons, in the face of chronic disuse, may increase the number of vesicles as well as the number of transporters per vesicle making such an occurrence difficult to distinguish from alterations solely to vesicle number.

We set out to reveal if vesicle numbers or transporter numbers are indeed altered after homeostatic regulation. This was done by pharmacologically increasing or reducing activity in mature hippocampal cultures and then taking high magnification electron microscopy images which we compared to untreated controls. We focused on excitatory synaptic contacts and looked in detail at the pre-and postsynaptic compartments and measured the average vesicular area. We reasoned that if transporter numbers are altered homeostatically, the amount of neurotransmitter packed within each vesicle should result

in a change to its size as observed when over expressing or reducing the vGlut homologue in flies (Daniels *et al.,* 2004 & 2006).

Our results revealed a small but significant reduction in vesicle size in cells treated with TTX when compared to controls. Also, there was no observed change to vesicle size in response to chronic hyperactivity (Fig.3.17.a). This came as a surprise to us. After chronic disuse if neurotransmitter release was altered homeostatically, as suggested by the up regulation of vGlut1, one might expect the size of vesicles to increase to oppose the drop in neural activity. However, the change on vesicle size although significant, was relatively small ($98nm^2$, about 10%) and probably has no effect on quantal size or biological effect at the synapse. Previous reports have indeed shown that quantal and vesicle size changes with genetic regulation of transporters (Karunanithi *et al.,* 2002, Daniels *et al.,* 2004 & 6, and Wilson *et al.,* 2005). However, our manipulations were pharmacological rather than genetic which may explain why we did not observe large changes to vesicle size. Thus, our results suggest that as chronic perturbations to activity have very little, if any, effect on vesicle size, the system responds homeostatically through regulation of vesicle number rather than changes to transporter number per vesicle. Similar to what our results suggest, others have reported evidence to vesicle numbers being modified homeostatically in response to chronic activity perturbations (Murthy *et al.,* 2001).

Additionally, we looked for any changes to docked vesicles after drug treatment (Fig.3.18.). We found that cells treated with TTX exhibited no difference, when compared to control neurons. However, gabazine-treated neurons showed significantly less docked vesicles when compared to either controls or TTX-treated neurons. These results may suggest that after prolonged hyperactivity, cells reduce the amount of primed vesicles available for release but do not increase them after prolonged inactivity.

It should be noted that our measurements were taken from single sections rather complete 3D reconstructions. Thus, they may not reveal the full extent of this phenotype and thus firm conclusions cannot be drawn. However, previous 3D modeling of synapses has shown a tight relationship between the active zone size and the number of docked vesicles (in the order of around docked 10 vesicles per active zone) (Schikorski & Stevens 1997). Additionally, it was shown the size and shape of the active zone, the area

of the PSD, the number of docked vesicles per active zone, and the size of the reserve pool of undocked vesicles all vary greatly from synapse to synapse (Schikorski & Stevens 1997). Even if our results are somewhat inconclusive on this matter, taken together with previous findings (Murthy *et al.,* 2001) they do provide some evidence that vesicle number is homeostatically controlled in hippocampal neurons.

5.3. Inhibitory synapses do not appear to be under the same homeostatic influence as excitatory synapses.

When we turned our attention to inhibitory synapses and assessed whether they too were regulated homeostatically as seen in excitatory synapses in response to chronic activity perturbation. This was assessed structurally by looking at two inhibitory protein found at either side of the synapse: vGAT on presynaptic vesicles and gephyrin on postsynaptic densities. Our results showed that inhibitory synapses, at least structurally, do not appear to follow the same homeostatic conventions of excitatory synapses (Fig.3.9.). These results are in agreement with previous reports (Thiagarajan *et al.,* 2005). However, our results are in contrast to other findings that show inhibitory neurons rapidly scale up there transmitter content in response to potentiation in the afferent fibers of the CA1 region in mouse hippocampal slices (Hartmann *et al.,* 2008). These contradictions may be attributed to the different models used to investigate homeostatic plasticity in inhibitory neurons as well as the method used to increase activity. The increase in vesicular GABA content observed by Hartmann *et al.,* (2008) was attributed to enhanced uptake-mediated plasticity through the transporters for GABA and glutamate. We did not look at transmitter content in inhibitory neurons or take any functional read outs after prolonged hyperactivity. It is feasible that although we did not see any changes in the levels of vGAT or gephyrin that we may have been looking at the wrong place if we are to go by others findings. Thus, if inhibitory synapses respond homeostatically it may be that they recruit completely different mechanisms to those used by excitatory synapses. On the other hand previous findings have shown that the specific synaptic changes triggered in inhibitory neurons depend on the developmental stage at which activity is

altered. (Hartman *et al.,* 2006). Density measurements of GAD65 puncta from cells treated at DIV10 to DIV14 with TTX were unchanged in comparison to controls. However, treating cells from DIV 5 for 9 days resulted in a marked reduction in the amount of GAD65 labeled boutons when compared to controls. These results are in support of our findings as they saw no change at around the same developmental time point but rather only early in development.

5.4. Functional correlates of homeostatic plasticity.

To confirm if the structural changes to excitatory cells, which arise from homeostatic synaptic mechanisms, manifest directly into functional changes, we carried out whole-cell patch electrophysiology on hippocampal pyramidal neurons, which had their activity chronically manipulated pharmacologically. Functional changes were assessed through measurements of mEPSCs. Overall, we observed increased mEPSC amplitudes in cells which had their activity reduced and vise versa when activity was enhanced. mEPSC frequencies however, remained unaltered throughout all conditions (Fig.3.10.). Increases in mEPSC amplitudes are consistent with the observed increases we registered with vGlut and PSD-95/Glur2 (Fig.3.4 & 3.5.) in response to chronic inactivity.

The increase in presynaptic synapsin we observed after chronic activity reduction could increase the facilitation of vesicles to the cell membrane. In addition, if the number of vesicles is also increased this could manifest into a functional change in mEPSC frequency. However, as we saw no significant changes to the frequency these results imply that the kinetics of release is not altered. One possibility is that, as spontaneous vesicles have been shown to belong to a distinctly separate pool from evoked vesicles (Fredj & Burrone, 2009), the reported increases in vesicle number (Murthy *et al*., 2001) may only have occurred in the evoked pool. As we did not test for evoked responses, we are unable to evaluate this possibility. Therefore, these results demonstrate that the blockade of ionotropic receptors or sodium channels for several days in mature cultures, results in corresponding structural and functional changes at the level of the synapse such

that they oppose the perturbation in activity. In addition, we observed an opposite effect structurally and functionally when we increased overall activity with GABAA blockers.

There have been reports that the application of glutamatergic receptor blockers during synaptogenesis, results in an increase in mEPSC frequency but not amplitude. This increase was not due to an increase in synaptic contacts, rather due to an increase in the rate of exo-endocytic recycling. More specifically, glutamate blockade down regulated the synaptophysin synaptobrevin-VAMP2 complex (Bacci *et al.,* 2001). As axons attempt to find a synaptic partner there is a large amount of membrane insertion necessary for growth and exploratory behaviour. However, during synaptic contact this high rate of exocytosis is down-regulated. The blockade of glutamate receptors during this period may prevent this down-regulation in a compensatory fashion by affecting these presynaptic mechanisms resulting in the observed frequency in spontaneous release.

The fact that we blocked glutamate receptors after synapses had formed and that this down-regulation of presynaptic vesicle recycling had already occurred might explain why we did not observe any differences in mEPSC frequencies. If we had carried out our pharmacological manipulations prior to synaptogenesis we may have seen a similar result.

5.5. L-type calcium channel blockade does not induce functional homeostatic regulation.

Wanting to reveal if blockade of L-type calcium channels results in a homeostatic induction we set out to block them with nifedipine in mature cultures and record for any functional changes. Our results side with those who have reported that their blockade does not appear to have any significant effect on inducing any homeostatic mechanisms (Leslie *et al.,* 2001, Sun & Wolf *et al.,* 2009) as demonstrated by a lack of change to mEPSC amplitudes or frequencies (Fig.3.11.).

Our results however, are in contradiction with results obtained by others (Gong *et al*., 2007) who have reported that application of nifedipine mimicked the effect of

CNQX/APV by increasing mEPSC amplitude and frequency in culture. This may be due to differences in the time cultures were treated, for example Gong treated cells on DIV13 rather than DIV10 like in our preparations and for only 24hrs. Also the sample numbers for where almost 3 times smaller than ours. A recent paper also demonstrated that changes in activity can alter the axon initial segment (AIS) location in a homeostatic manner with increased activity moving it away from the soma. Importantly, this movement was shown to depend on T-and/ or L-type voltage gated calcium channels (Grubb & Burrone, 2010). In addition, it has been reported that addition of nifedipine to organotypic slices, prevented photostimulation induced depression of AMPAR and NMDAR responses in compound EPSPs in ChR2 +ive cells (Goold & Nicoll, 2010)

Our results indicate that blockade of L-type calcium channels do not induce homeostatic mechanisms. However, it may have been interesting to explore if it prevented homeostatic regulation had we concurrently treated our cells with nifedipine and other activity blockers or enhancers. In addition, going by others results (Grubb & Burrone 2010) blockade of voltage gated calcium channels may influence homeostatic regulation in other non-synaptic sites which we did not look for.

5.6. Cell autonomous homeostatic plasticity: Optogenetic means of precisely controlling activity in individual neurons.

Our observations of structural and functional homeostatic plasticity at the synapse have predominantly been made within the context of global activity perturbations to the network through pharmacological blockade. Therefore, they do not address whether this phenomenon ultimately depends on the overall activity of the network or whether single cells can behave autonomously in response to chronic perturbations. Some efforts have been made towards answering this question (Burrone *et al.,* 2002, Ibata *et al.,* 2008) providing evidence for cell autonomy, while others have even gone as far as suggesting that it can emerge locally at the level of individual dendrites and synapses (Sutton *et al.,* 2006, Branco *et al.,* 2008, Rabinowitch & Segev, 2008). Here, we have attempted to address this question by chronically manipulating the activity of single cells through

optogenetic means. Initially, our experimental paradigm was to transfect a subset of neurons and, by means of blue light emitted from LEDs, to increase their overall activity chronically. We would then explore if this increase in activity within individual cells led to homeostatic changes at the level of the synapse when compared to surrounding untransfected neurons. This approach however, has its caveats as stimulation of ChR2 +ive cells would inevitably activate cells on which they synapse on to. Thus, in practice we would not be modulating the activity of single cells. We therefore attempted a different approach in which ChR2+ive cells were photostimulated in the presence of CNQX/APV. This allowed us to reintroduce activity back into ChR2 +ive cells through photostimulation, effectively preventing homeostatic regulation induced by CNQX/APV which surrounding cells will experience. If these cells do not undergo homeostatic regulation this would demonstrate a cell autonomous homeostatic regulation. Should we observe in photostimulated ChR2 +ive cells, an up regulation of synaptic gain, this would imply a network dependent form of homeostatic plasticity, possibly through some diffusible factor.

Initially, we first set out to prove that the insertion of ChR2 channel did not alter the electrical properties of the neurons. For these purposes we carried out whole cell recordings of mEPSC and compared those of ChR2+ive and -ive cells. These results validated that the insertion of ChR2 did not alter the electrical properties of the cells or the properties of minis when compared to untransfected controls cells (Fig.4.4.).

Next we established that ChR2 +ive cells were capable of generating photocurrents at various temporal patterns using the LEDs (Fig.4.5.), which enabled stimulation of cells chronically. As chronic photostimulations of ChR2+ive cells for such extended periods of time have been only recently attempted by few labs (Grubb & Burrone, 2010, Goold & Nicoll, 2010) it was necessary to verify that the ion channel was still expressed in sufficient levels 3 and 5 days post transfection. These experiments provided a measure of the spontaneous firing rate at DIV10 and 12, which was on average very similar and showed action potentials arriving in bursts. Importantly, we also showed that the application of CNQX/APV drastically reduced the spontaneous firing at both time points, as expected. Finally, we showed that we could successfully reintroduce activity levels that were similar to those recorded spontaneously, by using optogenetics (Fig.4.6.).

5.7. Preventing homeostatic regulation in single cells: structural measures at the synapse.

Having made sure that chronic photostimulation was possible; we then proceeded to characterize structurally any synaptic preventative phenotype in the ChR2+ive cells with our immunohistochemical assay. We measured fluorescence intensities of the synaptic markers vGlut1 and PSD-95 in the dendrites of ChR2+ive. Cells were photostimulated with a burst stimulation for 72hrs in the presence of CNQX/APV and compared to cells treated with CNQX/APV but not photostimulated or to untreated controls. Here we establish a structural prevention from homeostatic regulation (Fig.4.7.). Levels of PSD-95 remained similar to control levels in photostimulated cells and did not become up regulated as observed in cells treated with CNQX/APV. Interestingly when we looked at the levels of presynaptic vGlut1 in axonal contacts onto ChR2+ive photostimulated dendrites, they too appeared to remain comparable to control levels. Even though the presynaptic contacts remained reduced in activity during photostimulations, they too exhibited a structural prevention from the effects of CNQX/APV. Thus, this suggests that the postsynaptic compartment has sway over the presynaptic compartment influencing its presynaptic counterpart . This communication is most likely through some transynaptic signal which instructs the presynaptic compartment to maintain an output appropriate to that exhibited postsynaptically.

5.8. Preventing homeostatic regulation in single cells: functional measures.

Next we wanted to establish that this structural prevention phenotype also manifested into a functional prevention. We thus replicated the previous experiments and assessed for a functional prevention with whole cell mEPSC recordings. Here, we validated that

ChR2+ive cells in the presence of CNQX/APV exhibited increased mEPSC amplitudes when compared to control untreated ChR2+ive cells. However, cells photostimulated in the presence of CNQX/APV exhibited mEPSC amplitudes similar to controls demonstrating a functional prevention of homeostatic regulation had occurred. Interestingly, photostimulated cells had reduced mEPSC frequencies when compared to controls and to a larger extent when compared to CNQX/APV treated cells (Fig.4.8.). This reduction is not attributed to a decrease in synapse number as ChR2+ive cells had similar synapse density throughout all conditions.

Recordings of ChR2+ive cells from each condition were compared from different coverslips. Measurements comparing cells from different coverslips will inevitably exhibit larger variances due to differences in cell density and ratio of inhibition to excitation. We thus set out to ensure that our preventative phenotype was real. For these purposes we proceeded to measure mEPSCs from ChR2+ive cells treated as mentioned before but now compared them to ChR2-ive cells from within the same coverslip. We validated our preventative phenotype by demonstrating that ChR2+ive cells photostimulated in the presence of CNQX/APV had statistically smaller mEPSC amplitudes than surrounding ChR2-ive cells while frequencies when comparing cells from the same coverslip did not differ (Fig.4.10.).

Thus, these measurements from cells within the same coverslip provide more compelling evidence towards our cell autonomous phenotype as cell density and properties should be less variable. We have also shown previously that the expression of ChR2 does not alter the electrical properties of cells making comparisons between +ive and negative cells possible. We are tempted to assign the differences to frequency between conditions previously reported (Fig.4.8.) down to environmental differences between coverslips as cells from within the same coverslip did not exhibit this difference. These results reinforce our findings which demonstrate the existence of cell autonomous homeostatic mechanisms. Thus single cells are able to regulate their own synaptic output homeostatically according to the activity they exhibit.

5.9. Future experiments.

Here, although we provide compelling evidence towards cell autonomous homeostatic regulation, more facets of this homeostatic plasticity remain to be explored. For example, we would have liked to have used genetically encoded optical indicators such as synaptopHluorins (Miesenböck *et al.,* 1998), which reports vesicle cycling in presynaptic terminals. Using this method it would be possible to visualize if chronic activity perturbations also induce homeostatic alterations to the mechanisms of vesicle release and recycling in individual synapses. Along similar lines, it would also be important to measure changes in the levels of calcium influx at the synapse. New calcium reporters, such as GCAMP2 or 3 (Nakai *et al.*, 2001) measure overall neuronal activity. More recently, these calcium reporters have been targeted to the presynaptic terminal by fusing them to synaptic vesicle proteins, such as synaptophysin. Using both probes it would be possible to establish if there are any changes in release probability at the synapse and, if so, whether this arises from changes in the levels of calcium influx or not.

Most of the electrophysiology we carried after chronic pharmacological manipulations was on single cells. However, with the use of microelectrode arrays it would be possible to monitor the activity of a network of cells concurrently, with high throughput, for prolonged periods of time and in a non-invasive manner. Some efforts have already been made with a short treatment of 4 hours with TTX which has been shown to induce homeostatic responses in hippocampal cultures grown on MEAs. Neurons exhibited an increase in spontaneous firing as well as synchronized busting oscillation once the TTX had been washed off. This effect lasted for 4 hours at which point activity returned to normal basal levels (Zhou *et al.,* 2009). It would be of interest to ascertain if longer drug treatments would lead to a longer induction of homeostatic plasticity. Furthermore, what would be the outcome after chronic hyperactivity? Would spontaneous activity decrease and action potential amplitudes be reduced? Hippocampal neurons grown on MEAs which have been treated with bicuculline resulted in increased bursting and activity (Arnold *et al.,* 2004). However the time of treatment was only 15 minutes and probably was not sufficient in inducing homeostatic plasticity and therefore this manipulation most likely led to potentiation. Similarly, the lack of a homeostatic phenotype in these

experiments may also be attributed to the slower induction mechanisms induced by gabazine that we have previously reported.

Additionally, MEAs could be utilized once more to visualize the evoked activity of ChR2+ive cells which had been incubated in CNQX/APV throughout our photostimulation protocol and then compared for any differences to surrounding ChR2-ive cells once the drugs had been washed off. In comparison to whole cell electrophysiology, MEAs would permit the noninvasive measurement of electrophysiological activity on the same cells at different developmental time points.

We were able to successfully prevent pharmacological induced homeostatic regulation in single cells. This was done by re-introducing similar levels of activity normally observed on DIV10-12 through photostimulation. However, a plethora of options exist in the ways we could alter our photostimulation protocol. For example, we could alter the inter burst interval, the inter stimulus interval, the pulse duration and the number of pulses per burst. In doing so we could explore for the minimum amount of activity which is needed to prevent homeostatic regulation. Similarly, we could explore what types of activity produce the most robust prevention. Thus, we could start to answer what are the essential requirements for this phenotype. Is there a threshold which needs to be reached in terms of action potentials? Would we see a similar phenotype if we kept the frequency the same but spread out the light pulses rather than have them clustered in bursts? Alternatively, if we now incubated our cells in gabazine and photostimulated our ChR2+ive cells would we see an even larger down regulation in synaptic output in comparison to neighboring cells? Would photostimulation in the presence of TTX also result in a preventative phenotype? If so, this would demonstrate that action potential firing is not the parameter which is sensed during homeostatic plasticity. In addition, this would also show that that depolarization of cells is sufficient in inducing a response. Finally, one experiment which we did not carry out was an assessment of the axons in ChR2+ive cells which had been chronically photostimulated in the presence of CNQX/APV, with our synaptic markers. Here, the photostimulated presynaptic axon will exhibit normal levels of activity while its postsynaptic partner will exhibit reduced levels through the effects of CNQX/APV. Would we see a structural prevention of homeostatic regulation in both sides of the synapse as observed in the dendrites or just in the

presynaptic compartment? Thus, it is apparent, that using these optogenetic tools and our setup a more detailed exploration of the different facets of homeostatic plasticity is possible.

5.10. Underlying mechanisms of homeostatic plasticity.

How homeostatic plasticity manifests itself at the level of the synapse, in terms of pre- and postsynaptic mechanisms, has been relatively easier to visualize and demonstrate than the underlying mechanisms. For example, the mechanisms involved in sensing these perturbations are still actively pursued, with most emphasis placed on some readout of calcium levels being involved, with proteins kinases like CAMKII (Thiagaragan *et al.,* 2002) and CAMKIV (Ibata *et al.,* 2008) as potential protagonists. Similarly, another kinase, Polo-like kinase 2 (Plk2), has recently been implicated in homeostatic regulation during epileptiform activity. Plks are normally involved in the regulation of the cell cycle (van de Weerdt & Medema, 2006). However, dominant-negative or RNA interference approaches which disrupt Plk2 function has been shown to prevent the down regulation of membrane excitability in pyramidal neurons during increased activity. Activity induced weakening of synapses by Plk2 is achieved through the phosphorylation and degradation of SPAR, a postsynaptic Rap GAP (GTPase-activated protein) and scaffolding protein (Seeburg & Sheng, 2008) as well as through a loss of PSD-95 clusters (Pak *&* Sheng, 2003). These results suggest that Plk2 plays a homeostatic role in preventing epileptiform potentiation (Seeburg & Sheng, 2008). Other kinases which have been shown to be involved in homeostatic regulation include the phosphoinositide-3 (PI3) kinase signaling system. Addition of wartmannin, a PI3 kinase inhibitor prevented the homeostatic up regulation of GluR1 in Kir2.1 synapses (Hou *et al.,* 2008)

In addition, in *Drosophila,* it has been shown that during homeostatic plasticity presynaptic ephexin, a Rho-Type guanine nucleotide exchange factor, functions primarily via Cdc42 (cell division control protein 42 homolog) and converges upon the Cav2.1 calcium channel. These results suggest that the homeostatic retrograde signal may be in

the form of ephexin through the activation of presynaptic Eph receptors (Frank *et al.,* 2009)

Advancements have also been made in identifying more of the genes involved in homeostatic plasticity. In *Drosophila* gooseberry (gsb), a transcription factor which normally determines cell fate, has been shown to be necessary in post-mitotic neurons for the sustained expression of a homeostatic increase in presynaptic neurotransmitter release (Marie *et al.,* 2010). It has also been demonstrated that in null mutants for GluRIIA, the subsequent decrease in spontaneous mEPSCs amplitudes, are homeostatically countered by a corresponding increase in presynaptic vesicle release at the NMJ (Frank *et al.,* 2006). If gooseberry, which is the homolog of vertebrate pax3/pax7, is deleted in conjunction with GluRIIA, this presynaptic expression of synaptic homeostatic in hindered. However, the rapid protein synthesis-independent induction of synaptic homeostasis, as a result of glutamate receptor blockade with philanthotoxin application, in gsb mutants is normal. Therefore, it has been suggested that deletion of gsb does not affect the induction of homeostatic plasticity but rather is involved in the sustained maintenance of its expression. Gsb has been shown to inhibit wingless (Baht *et al.,* 2000). Therefore, a loss of wingless should restore the homeostatic compensation in GlurIIA gsb double mutants, which indeed appears to be the case (Marie *et al.,* 2010). Thus, wingless acts as an antagonist towards homeostatic plasticity. It will be important to assess if the vertebrate homologs retain the same role in the sustained maintenance of the expression of homeostatic plasticity.

Although some of the underlying mechanisms are now beginning to be unraveled, in the future, a more detailed molecular characterization of homeostatic signaling is essential before clear links to neurological disease, such as epilepsy, can be established.

5.11. Synapse specific homeostatic plasticity.

Although this body of work we have presented here reveals the cell autonomous nature of homeostatic plasticity and that of others, the underlying mechanisms (Marle *et al.,* 2010, Frank *et al.,* 2009), it still remains unclear as to the timescale required to induce it

and also whether this phenomenon can be observed in distinct cellular processes such as individual synapses. The notion that homoestatic plasticity is a cell wide feature is beginning to be contested. Moreover, new experimental findings suggest that homeostatic plasticity can act locally and control individual synapses individually.

Experiments have shown that mild depolarization through increased extracellular K^+ led to presynaptic adaptations. Hippocampal cultures were treated with TTX and NBQX/APV for 6-10 days and assessed for RRP adaptation by testing the mismatch between FM1-43 uptake and vGlut-1 immunoreactivity. Uptake was stimulated with strong depolarization by increasing extracellular potassium followed by fixation. Untreated cultures exhibited 20-30% vGlut-1 positive terminals that were devoid of FM1-43 labeling. However, in chronically inactive cells there was an increase in the number of functionally presynaptic elements (Moulder *et al.,* 2006). Conversely, a 16hr elevation of activity with increased extracellular potassium resulted in less vGlut-1 puncta positive for FM1-43 uptake. However, concurrent TTX treatment prevented this effect suggesting that spiking behavior is important for the effect observed with increased potassium. In addition, they suggest that the presynaptic depression they observe after chronic elevation in potassium is due to alterations to RRP size (and/or availability). However, this seemed to happen in an all or nothing fashion with some synapses becoming completely inactive while the remaining ones maintained their original strength. These findings contradict cell wide homeostatic scaling as different synapses responded homeostatically while others remained unaffected suggesting that homeostatic mechanisms can occur in a synapse specific manner.

Recent evidence suggests that local dendritic activity may regulate presynaptic release probability in a homeostatic manner. It has been demonstrated that synapses on a given dendritic branch have a similar release probability than synapses from the same axon on different dendritic regions of the same postsynaptic cell. Increasing network activity by delivering APs at 1–2 Hz throughout the entire network, for 2 hours, resulted in an increase in the pair pulse ratio (PPR), which is thought to correlate with a decrease in release probability. When a restricted number of synapses are stimulated locally with an identical protocol, a similar decrease in release probability is observed only on the stimulated synapses, suggesting local homeostatic regulation (Branco *et al.,* 2008).

These recent findings which give momentum to the concept of synapse specific homeostatic plasticity however, also imply that they could abolish any synaptic modifications made by Hebbian plasticity. Theoretical solutions however, have been provided to answer this paradox (Rabinowitz & Segev, 2008) in which it has been proposed that neurons can sustain changes in synaptic strength through Hebbian mechanisms even in the face of local homeostatic mechanisms. It has been suggested that neighboring synapses on a dendritic branch are intimately interlinked through electrical interactions and calcium fluctuations rather than exist as discrete isolated structures. A potentiated synapse will also result in an increase in activity to surrounding synapses. Thus local homeostatic mechanisms which will attempt to weaken not only the potentiated synapse, but also surrounding ones. This will bring about a local decrease in activity of adjacent synapses in a dendritic branch opposing the initial potentiation of the synapse. Thus, a potentiated synapse can maintain a significant fraction of its potentiation with the support of the surrounding non potentiated synapses that have been weakened resembling a "mexican-hat" like configuration which is resistant to the canceling actions of local homeostatic plasticity. Although these theories have been shown to be plausible in theory through computational modeling, biological existence of this phenomenon is still lacking.

Finally there have been several reports of numerous GABAergic, glutamatergic and voltage gated receptors which induce a homeostatic response after their blockade. However, there has been one report of one blocker resulting in an anti-homeostatic response. When strychnine but not bicuculline or CNQX was added to neurons, this led to an increase in spontaneous events, amplitudes, calcium transients and an overall network hyperexcitability and enhancement in glycinergic transmission (Carrasco *et al.,* 2006). It must be noted thought that these cells were from embryonic spinal neurons on DIV 5, a timepoint were the primarily display glycinergic neurotransmission and is depolarizing in nature. The anti-homeostatic effects of glycinergic blockade was also shown to be dependent on BDNF as blockade of the neurotrophin with antibodies or application of K252a, a tyrosine kinase inhibitor prevented this network enhancement (Carrasco *et al.,* 2006). These results are interesting as they imply homeostatic plasticity may be observed in certain neural systems and with certain receptors and not in others.

These differences in spinal chord may be most likely due to glycinergic transmission predominating over GABA and glutamatergic neurotransmission in immature neurons. However, these are in contradiction with others who have observed that the application of strychnine in rat organotypic spinal chord resulted in reduction postsynaptic current frequency and amplitude and a decrease in frequency of spontaneous events (Galante *et al.*, 2000). However, these manipulations were made on 13-14 DIV which might explain the differences.

Finally we would like to summarize by saying that with this work we provide evidence towards the structural and functional characterization of homeostatic mechanims in response to global chronic activity manipulations. Moreover, we show how pre- and postsynaptic proteins involved in neurotransmission are regulated homeostatically so as to oppose and compensate for chronic detrimental activity. Consequently, postsynaptically glutamatergic receptors are critical for adjusting synaptic output while presynaptically vesicles, vesicular components and proteins involved in recycling are adjusted accordingly depending on the systems demands. To our knowledge, this study and one more lab have attempted to use optogenetics to verify the cell autonomous nature of homeostatic plasticity (Goold & Nicoll, 2010) and the location of its sensor, which we demonstrated with the structural and functional prevention in individual neurons from drug induced perturbations. This dendritic postsynaptic sensor also appears to determine the output of its presynaptic counterpart possibly through some retrograde signal.

Finally, optogenetics has proven to be a powerful tool, and its applications in exploring homeostatic plasticity have been fruitful with the potential for even more revelations. We predict that ChR2 in the future will not only contribute as an exploratory tool but also prove vital in therapeutic rehabilitation, reintroducing activity to effected areas such as spinal cord injuries and visual deficits.

6.REFERENCES

A

Araque A, Parpura V. Sanzgiri RP, Haydon PG.
Tripartate synapses: glia, the unacknowledged partner.
Trends in Neuroscience, May 22, 1999, (5):208-15.

Arnold FJ, Hofmann F, Bengston CP, Witmann M, Vanhoutte P, Bading H.

Microelectrode array recording of cultured hippocampal networks reveal a simple model for transcription and protein synthesis-dependent plasticity

Journal of Physiol. 2005 Apr. 1;564(Pt 1):3-19.

Aoki C, Miko I, Oviedo H, Mikeladze-Dvali T, Alexandre L, Sweeney N, Bredt DS.
Electron microscopic immunocytochemical detection of PSD-95, PSD-93, SAP-102, and SAP-97 at postsynaptic, presynaptic, and nonsynaptic sites of adult and neonatal rat visual cortex.
Synapse, 2001, June 15, 40 (4):239–257.

Chiye Aoki, Sho Fujisawa, Veera Mahadomrongkul, Priti J. Shah, Karim Nader and Alev Erisir.
NMDA receptor blockade in intact adult cortex increases trafficking of NR2A subunits into spines, postsynaptic densities, and axon terminals.
Brain Research, 2003, Feb. 14, Volume 963, Issues 1-2, 139-149

Caitlin O. Aptowicz, Phillip E. Kunkler, Richard P. Kraig.

Homeostatic plasticity in hippocampal slice cultures involves changes in voltage-gated Na+ channel expression.
Brain Research, 2004, Feb. 20, 998, 155– 163.

Alexander M Aravanis, Li-PingWang, Feng Zhang, Leslie A Meltzer, Murtaza Z Mogri, M Bret Schneider and Karl Deisseroth.
An optical neural interface: in vivo control of rodent motor cortex with integrated fiberoptic and optogenetic technology.
J. Neural Eng, 2007, Sep. 4, (3) S143–S156.

Alfonso Araque,Vladimir Parpura, Rita P. Sanzgiri and Philip G. Haydon
Tripartite synapses: glia the unacknowledged partner.
Trends in Neuroscience, 1999, May 1, Volume 22, Issue 5, P.208-15.

B

Alberto Bacci, Silvia Coco, Elena Pravettoni, Ursula Schenk, Simona Armano, Carolina Frassoni, Claudia Verderio, Pietro De Camilli, and Michela Matteoli.
Chronic Blockade of Glutamate Receptors Enhances Presynaptic Release and Downregulates the Interaction between Synaptophysin-Synaptobrevin–Vesicle-Associated Membrane Protein.
The Journal of Neuroscience, 2001, Sep. 1, 21(17):6588–6596.

Babghart M, Borges K, Isacoff E, Trauner D, Kramer RH.

Light-activated ion channels for remote control of neuronal firing.

Nat Neurosci. 2004, Dec. 7, (12):1381-6.

T.G. Bankel, D. Bowiel, H.K.Lee, R.L. Huganir, A. Schousboe and S.F Traynelis.

Control of GLuR1 AMPA Receptors Function by cAMP – dependent protein kinase.

The Journal of Neuroscience, 2000, Jan. 1, 20(1): 89-102.

Aundrea F. Bartley, Z. Josh Huang, Kimberly M. Huber and Jay R. Gibson
Differential Activity-Dependent, Homeostatic Plasticity of Two Neocortical Inhibitory Circuits.
J Neurophysiol 2008. Oct, 100 (4): 1983-94

M Baumert, P R Maycox, F Navone, P De Camilli, and R Jahn.
Synaptobrevin: an integral membrane protein of 18,000 daltons present in small synaptic vesicles of rat brain.
EMBO J. Feb, 1989, 8(2): 379–384.

Mark F. Bear, Abraham WC
Long term depression in hippocampus.
AMU Rev. Neurosci. 1996, 19:437-62.

Bear MF, Malenka RC.

Synaptic plasticity: LTP and LTD.

Curr Opin Neurobiol. 1994 ,Jun. 4(3):389-99.

Eric C. Beattie, Reed C. Carroll, Xiang Yu, Wade Morishita, Hiroki Yasuda, Mark von Zastrow and Robert C. Malenka.

Regulation of AMPA receptor endocytosis by a signaling mechanism shared with LTD.
nature neuroscience , 2000, Dec. volume 3 no 12, 1291-300

Darwin K. Berg and Zach W. Hall.
Increased extrajunction acetylcholine sensitivity produced by chronic post-synaptic neuromuscular blockade.
J. Physiol. 1975, Jan. 244 (3), 659-676.

André Berndt, Ofer Yizhar, Lisa A Gunaydin, Peter Hegemann & Karl Deisseroth

Bi-stable neural state switches.

Nature Neuroscience, 2009, Feb. 12(2), 229 - 234.

Bhat KM, van Beers EH, Bhat P.
Sloppy paired acts as the Downstream target of Wingless in the Drosophila CNS and interaction between sloppy paired and gooseberry inhibits sloppy paired during neurogenesis.
Development, 2000, Feb. 127(3):655– 665.

Anding Bi, Jinjuan Cui, Yu-Ping Ma, Elena Olshevskaya, Mingliang Pu, Alexander M. Dizhoor, and Zhuo-Hua Pan.
Ectopic Expression of a Microbial-Type Rhodopsin Restores Visual Responses in Mice with Photoreceptor Degeneration.
Neuron, 2006, Apr. 6, 50(1), 23-33.

Guo-qiang Bi & Mu-ming Poo.
Synaptic Modification By Correlated Activity: Hebb's Postulate Revisited
Annual Review Neuroscience, 2001, 24:139-66.

Bi, G. Q. and Poo, M. M.

Synaptic modifications in cultured Hippocampal neurons: dependence on spike timing, synaptic strength, and postsynaptic cell type.
J Neurosci, 1998, Dec. 15, 18(24):10464-72.

Bienenstock, Elie L, Leon Cooper, Paul Munro.
Theory for the development of neural selectivity: orientation specificity and binocular interaction in the visual cortex.
The Journal of Neurosci, 1982, Jan. 2 (1), 32-48.

Bliss TV, Lømo T.
Long-lasting potentiation of synaptic transmission in the dendate areo of the anaesthatized rabbit following stimulatio of the perforant path.
J Physio. 1973, Jul, 232(2), 331-56

Boehm J, Kang MG, Johnson RC, Esteban J, Huganir RL, Malinow R.

Synaptic incorporation of AMPA receptors during LTP is controlled by a PKC phosphorylation site on GluR1.

Neuron, 2006, Jul. 20, 51 (2): 213–25.

Borgdoff AJ, Choquet D.

Regulation of AMPAR receptor lateral movements.

Nature, 2002, Jun. 6, 417 (6889),649-53

Laura N. Borodinsky, Cory M. Root, Julia A. Cronin, Sharon B. Sann, Xiaonan Gu & Nicholas C. Spitzer.

Activity-dependent homeostatic specification of transmitter expression in embryonic neurons.

Nature, 2004, Jun. 3 429, (6991), 523-530.

Boyden ES, Zhang F, Bamberg E, Nagel G, Deisseroth K

Millisecond-timescale genetically targeted optical control of neural activity.

Nat Neurosci, 2005, Sep, 8(9), 1263–1268.

Tiago Branco, Kevin Staras, Kevin J. Darcy, and Yukiko Goda.
Local Dendritic Activity Sets Release Probability at Hippocampal Synapses.
Neuron, 2008, Aug. 14, 59(2), 475-485.

Paul Brookes and Victor M. Darley-Usmar.
Hypothesis: the mitochondrial NO$^{\bullet}$ signaling pathway, and the transduction of nitrosative to oxidative cell signals: an alternative function for cytochrome C oxidase.
Free radical Biology and Medicine, 2002, 15 Feb, V.32, Issue 4, 370-374

Michelle Burbea, Lars Dreier, Jeremy S. Dittman, Maria E. Grunwald, and Joshua M. Kaplan.
Ubiquitin and AP180 Regulate the Abundance of GLR-1 Glutamate Receptors at Postsynaptic Elements in C. Elegans.
Neuron, 2002, July 3, Vol. 35, 107–120,

Marie E Burns and Denis A Baylor.
Activation, deactivation, and adaptation in vertebrate photoreceptor cells.
Annual Review of Neuroscience, 2001, 24: 779-805.

Juan Burrone, Michael O'Byrne & Venkatesh N. Murthy.

Multiple forms of synaptic plasticity triggered by selective suppression of activity in individual neurons.

Nature, 2002, Nov. 28, 420(6914), 414-418,.

György Buzsáki and Andreas Draguhn.

Neuronal Oscillations in Cortical Networks.

Science, 2004, Jun. 25, 304.(5679),1926 – 1929.

C

Cannon, W.B. The Wisdom of the Body, (1932), W.W. Norton

M. A. Carrasco, P. A. Castro, F. J. Sepulveda, M. Cuevas, J. C. Tapia, P. Izaurieta, B. van Zundert and L. G. Aguayo.
Anti-homeostatic synaptic plasticity of glycine receptor function after chronic strychnine in developing cultured mouse spinal neurons.
Journal of Neurochemistry, 2007, Mar, 100(5), 1143–1154.

Carpenter-Hyland, E.P., Woodward, J.J. & Chandler, L.J.
Chronic ethanol induces synaptic but not extrasynaptic targeting of NMDA receptors.
J. Neurosci, 2004, Sep. 8, 24(36), 7859–7868.

Na Chen, Xin Chen and Jin-Hui Wang.

Homeostasis established by coordination of subcellular compartment plasticity improves spike encoding.
Journal of Cell Science, 2008, Sep. 1, 121 (Pt17), 2961-2971.

Christie BR, Abraham WC.
Priming of associative long-term depression in the dentate gyrus by theta frequency synaptic activity.
Neuron. 1992, Jul, 9(1),79-84

Climent E, Pascual M, Renau-Piqueras J, Guerri C.
Ethanol exposure enhances cell death in the developing cerebral cortex: role of brain-derived neurotrophic factor and its signaling pathways.
J Neurosci Res. 2002, Apr. 15, 68(2),213–225.

Mark O. Collins, Holger Husi, Lu Yu, Julia M. Brandon,
Chris N. G. Anderson, Walter P. Blackstock, Jyoti S. Choudhary and
Seth G. N. Grant.
Molecular characterization and comparison of the components and multiprotein complexes in the postsynaptic proteome.
Journal of Neurochemistry, 2006, Apr, 97, 16–23.

D

Richard W. Daniels,Catherine A. Collins,Maria V. Gelfand, Jaime Dant, Elizabeth S. Brooks, David E. Krantz, and Aaron DiAntonio.
Increased Expression of the Drosophila Vesicular Glutamate Transporter Leads to Excess Glutamate Release and a Compensatory Decrease in Quantal Content.
The Journal of Neuroscience, 2004, Nov. 17, 24(46):10466 –10474.

Richard W. Daniels, Catherine A. Collins, Kaiyun Chen, Maria V. Gelfand, David E. Featherstone, and Aaron DiAntonio.
A Single Vesicular Glutamate Transporter Is Sufficient to Fill a Synaptic Vesicle.
Neuron, 2006 Jan. 5, 49(1), 11-16.

N.S. Desai, R.H. Cudmore, S.B. Nelson and G.G. Turrigiano.
Critical periods for experience-dependent synaptic scaling in visual cortex.
Nat. Neurosci, 2002, Aug, 5(8), 783–789.

Ste´phanie De Gois, He´le`ne Varoqui , Martin K.-H. Schafer, Eberhard Weihe, Jeffrey D. Erickson.
Activity-dependent regulation of vesicular glutamate and GABA transporters: A means to scale quantal size.
Neurochemistry International, 2006, May-June, 48, (6-7), 643–649.

Jary Y. Delgado, Marcelo Coba, Christopher N. G. Anderson, Kimberly R. Thompson, Erin E. Gray, Carrie L. Heusner, Kelsey C. Martin, Seth G. N. Grant, and Thomas J. O'Dell.
NMDA Receptor Activation Dephosphorylates AMPA Receptor Glutamate Receptor 1 Subunits at Threonine 840.
Journal of Neuroscience, 2007, Nov, 28:27(48): 13210-13221.

Desai NS, Rutherford LC, Turrigiano GG.
Plasticity in the intrinsic excitability of cortical pyramidal neurons.
Nature Neuroscience 1999, Jun, 2(6), 515-520.

Desai NS, Rutherford LC, Turrigiano GG.
BDNF Regulates the Intrinsic Excitability of Cortical Neurons.
Learn Mem. 1999, May; 6(3): 284–291.

Douglas, R.M.
Long lasting synaptic potentiation in the rat dentate gyrus following brief high frequency stimulation.
Brain Research, 1977, May 6, 126(2), 361-365.

Douglas, R.M. & Goddard, G.
Long-term potentiation of the perforant path - granule cell synapse in the rat hippocampus.
Brain Research, 1975, Mar. 21, 86(2), 205-215.

E

Michael D. Ehlers.
Activity level controls postsynaptic composition and signaling via the ubiquitin-proteasome system.
Nature neuroscience, 2003, Mar, 6(3), 231-42.

Michael D. Ehlers.
Reinsertion or Degradation of AMPA Receptors Determined by Activity-Dependent Endocytic Sorting.
Neuron, 2000, Nov, 28(2), 511–525.

Alaa El-Din El-Husseini, Eric Schnell, Dance M. Chetkovitch, Roger A, Nicoll and David S. Bredt

PSD-95 involvement in maturation of excitatory synapses.

Science, 2000, Nov.17, 290 (5495), 1364-1368.

Julio Echegoyen, Axel Neu, Kevin D. Graber, Ivan Soltesz.
Homeostatic Plasticity Studied Using In Vivo Hippocampal Activity-Blockade: Synaptic Scaling, Intrinsic Plasticity and Age-Dependence.
PLoS ONE. 2007, Aug.8, 2(8), e700.

E. Evergren, F. Benfenati, and O. Shupliakov.
The Synapsin Cycle: A View From the Synaptic Endocytic Zone.
Journal of Neuroscience Research, 2007, Sep, 85(12), 2648–2656.

F

Adriana Ferreira, Hung-The Kao, Jian Feng, Mark Rapoport and Paul Greengard

Synapsin III: Developmental Expression, Subcellular Localization, and Role in Axon Formation.

The Journal of Neuroscience, 2000, May 15, 20(10),3736-3744.

Ferreira A, Rapoport M.

The synapsins: beyonf the regulation of neurotransmitter release.

Cell Mol Life Sci. 2002 Apr, 59(4), 589-95.

J. C. Fiala.
Reconstruct : a free editor for serial section microscopy.
Journal of Microscopy, 2005, Apr, 218 (Pt 1), 52–61.

C. Andrew Frank, Matthew J. Kennedy, Carleton P. Goold, Kurt W. Marek, and Graeme W. Davis.
Mechanisms Underlying the Rapid Induction and Sustained Expression of Synaptic Homeostasis.
Neuron, 2006, Nov. 22, 52(4), 663–677.

C. Andrew Frank, Jan Pielage and Graeme W. Davis.
A Presynaptic Homeostatic Signaling System Composed of the Eph Receptor, Ephexin, Cdc42, and $Ca_V2.1$ Calcium Channels.
Neuron 2009, Feb. 26, 61(4), 556-69.

Naila Ben Fredj & Juan Burrone.

A resting pool of vesicles is responsible for spontaneous vesicle fusion at the synapse.

Nature Neuroscience, 2009, Jun, 12(6), 751 – 758.

G

Melanie A. Gainey, Jennifer R. Hurvitz'Wolff, Mary R. Lambo, and Gina G, Turrigiano.
Synaptic scaling requires the GluR2 subunit of AMPA receptor.
Journal of Neuroscience, 2009, May 20, 29(20):6479-6489.

Micaela Galante, Andrea Nistri and Laura Ballerini.
Opposite changes in synaptic activity of organotypic rat spinal cord cultures after chronic block of AMPA, kainate or glycine and GABAA receptors.
Journal of Physiolog, 2000, Mar, 523(Pt.3) 639-651.

Gerrow K, Romorini S, Nabi SM, Colicos MA, Sala C, El-Husseini A.

A preformed complex of postsynaptic proteins is involved in excitatory synapse development.
Neuron, 2006, Feb, 16, 49(4), 547-62

Bernard F. Godley, Farrukh A. Shamsi, Fong-Qi Liang, Stuart G. Jarrett, Sallyanne Davies, and Mike Boulton.
Blue Light Induces Mitochondrial DNA Damage and Free Radical Production in Epithelial Cells.
The Journal of Biological Chemistry, 2005, Jun. 3, 280(22), 21061–21066.

Bo Gong, Hansen Wang, Steven Gu, Scott P. Heximer and Min Zhuo.
Genetic evidence for the requirement of adenylyl cyclase 1 in synaptic scaling of forebrain cortical neurons.
European Journal of Neuroscience, 2007, Jul, 26(2), 275–288.

Goold CP, Nicoll RA.

Single-cell optogenetic excitation drives homeostatic synaptic depresión

Neuron. 2010 Nov 4,68(3),512-28.

Matthew S. Grubb & Juan Burrone.
Activity-dependent relocation of the axon initial segment fine-tunes neuronal excitability.
Nature, 2010, Jun. 24, 465 (7301), 1070-76.

Maria E. Grunwald, Jerry E. Mellem, Nathalie Strutz, Andres V. Maricq, and Joshua M. Kaplan.
Clathrin-mediated endocytosis is required for compensatory regulation of GLR-1 glutamate receptors after activity blockade.
PNAS, 2004, Mar. 2, 101(9), 3190-5.

Lisa A Gunaydin, Ofer Yizhar1, André Berndt, Vikaas S Sohal, Karl Deisseroth & Peter Hegemann.
Ultrafast optogenetic control.
nature neuroscience, 2010, Mar, 13 (3) , 387-92

H

Bilal Haider, Alvaro Duque, Andrea R. Hasenstaub, and David A. McCormick.

Neocortical Network Activity In Vivo Is Generated through a Dynamic Balance of Excitation and Inhibition.

The Journal of Neuroscience, 2006, Apr. 26, 26(17):4535– 4545.

Edward B. Han and Charles F. Stevens.
Development regulates a switch between post and presynaptic strengthening in response to activity deprivation.
PNAS , 2009, Jun. 30, 106(26), 10817–10822.

Kimberly J. Harms, and Anne Marie Craig.
Synapse composition and organization following chronic activity blockade in cultured hippocampal neurons.
The Journal of Comparative Neurology, 2005, Sep.12, 490(1), 72-84.

Kimberly J. Harms, Kenneth R. Tovar, and Ann Marie Craig.
Synapse-Specific Regulation of AMPA Receptor Subunit Composition by Activity.
The Journal of Neuroscience, 2005, Jul.6, 25(27), 6379–6388.

Kristin Hartmann, Claus Bruehl, Tatyana Golovko, Andreas Draguhn.
Fast Homeostatic Plasticity of Inhibition via Activity-Dependent Vesicular Filling.
PLOS, 2008, Aug.20, 3(8), e2979.

Kenichi N Hartman, Sumon K Pal, Juan Burrone & Venkatesh N Murthy.
Activity-dependent regulation of inhibitory synaptic transmission in hippocampal neurons.
Nature Neuroscience, 2006, May, 9(5), 642-9.

Hawkins RD, Abrams TW, Carew TJ, Kandel ER.
A Cellular mechanism of classical conditioning in Aplysia: activity-dependent amplification of presynaptic facilitation.
Science, 1983, Jan. 28, 219(4584), 400-5.

Hayashi Y, Shi SH, Esteban JA, Piccini A, Poncer JC, Malinow R.
Driving AMPA receptors into synapses by LTP and CaMKII: requirement for GluR1 and PDZ domain interaction.
Science, 2000, Mar. 24, 287(5461), 2262–7.

Hebb, D. O.
The Organization of Behavior: a Neurophysiological Theory.
Wiley, New York, 1949.

Matthias H, Hennig, John Grady, James von Coppenhagen and Evelyne Sernagor
Age-dependent homeostatic plasticity of GABAergic signaling in developing retinal networks.
The Journal of Neuroscience,2011, Aug.24, 31(34), 12159-12164.

Qingming Hou, Dawei Zhang, Larissa Jarzylo, Richard L. Huganir, and Heng-Ye Man.
Homeostatic regulation of AMPA receptor expression at single hippocampal synapses.
PNAS, 2008, Jan.15, 105(2), 775–780.

I

Keiji Ibata, Qian Sun, and Gina G. Turrigiano.
Rapid Synaptic Scaling Induced by Changes in Postsynaptic Firing.
Neuron, 2008, Mar.27, 57(6), 819–826.

Ingrid Ehrlich and Roberto Malinow.
Postsynaptic Density 95 controls AMPA Receptor Incorporation during Long-Term Potentiation and Experience-Driven Synaptic Plasticity.
The Journal of Neuroscience, 2004, Jan. 28, 24(4), 916 –927.

Toru Ishizuka, Masaaki Kakuda, Rikita Araki and Hiromu Yawo.
Kinetic evaluation of photosensitivity in genetically engineered neurons expressing green algae light-gated channels.
Neurosci Res, 2006 Feb, 54(2), 85-94.

J

William Ju,Wade Morishita,Jennifer Tsiu, Guido Gaietta, Thomos Deerinck,Stephen R Adams, Craig C Garner, Roger Y Tsien, Mark H Ellisman & Robert Malenka.

Activity-dependent regulation of dendritic synthesis and trafficking of AMPA receptors.

Nat. Neurosci, 2004, Mar, 7(3), 244–253.

K

Srinivas Kantevari, Masanori Matsuzaki, Yuya Kanemoto, Haruo Kasai & Graham C R Ellis-Davies.

Two-color, two-photon uncaging of glutamate and GABA.

Nature Methods, 2010, Feb, 7(2):123-5.

Shanker Karunanithi, Leo Marin, Kar Wong and Harold L.Atwood.

Quantal Size and Variation Determined by Vesicle Size in Normal and Mutant Drosophila Glutamatergic Synapses.

The Journal of Neuroscience, 2002, Dec.1, 22(23),10267-10276

Uma R. Karmarkar, &Dean V. Buonomano.

Different forms of homeostatic plasticity are engaged with distinct temporal profiles.

European Journal of Neuroscience, Mar, 23(6), 1575-1584.

Katz, B. & Mledi R.
Spontaneous subthreshold activity at denervated amphibian end-plates.
J. Physiol, 1959, 146, 44-45.

Kay L. Humphreys L, Eickholt BJ, Burrone J.

Neuronal activity drives matching of pre-and postsynaptic function fruing synapse maturation.

Nature neuroscience, 2011 Jun, 14(6), 688-90.

Tong-Wey Koh and Hugo J. Bellen.
Synaptotagmin I, a Calcium sensor for neurotransmitter release.
PNAS, 2004, Nov. 23, 101(47), 16648–16652.

Kensuke Futai, Myung Jong Kim, Tsutomu Hashikawa, Peter Scheiffele, Morgan Sheng & Yasunori Hayashi.

Retrograde modulation of presynaptic release probability through signaling mediated by PSD-95–neuroligin.

Nature Neuroscience , 2007, Feb. 15, 10(2), 186–195.

Valerie Kilman, Mark C. W. van Rossum, and Gina G. Turrigiano.

Activity Deprivation Reduces Miniature IPSC Amplitude by Decreasing the Number of Postsynaptic $GABA_A$ Receptors Clustered at Neocortical Synapses.

J. Neurosci, 2002, Feb. 15, 22(4), 1328–1337.

Kim J, Alger BE.

Reduction in endocannabinoid tone is a homeostatic mechanism for specific inhibitory synapses.

Nature Neuroscience 2010, May, 13(5):592-600.

K Kraszewski, O Mundigl, L Daniell, C Verderio, M Matteoli, and P De Camilli.

Synaptic vesicle dynamics in living cultured hippocampal neurons visualized with CY3-conjugated antibodies directed against the lumenal domain of synaptotagmin.

The Journal of Neuroscience, 1995, Jun.1, 15(6),4328-4342.

Sanjay S. Kumar, Alberto Bacci, Viktor Kharazia, and John R. Huguenard.
Developmental Switch of AMPA Receptor Subunits in Neocortical Pyramidal Neurons.
The Journal of Neuroscience, 2002, Apr.15, 22(8):3005–3015.

L

Lee HK, Barbarosie M, Kameyama K, Bear MF, Huganir RL.
Regulation of distinct AMPA receptor phosphorylation sites during bidirectional synaptic plasticity.
Nature, 2000, Jun.22, 405 (6789), 955-959.

Lerma, J.
Roles and rules of kainate receptors in synaptic transmission.
Nature Rev. Neurosci, 2003, Jun, 4(6), 481–495.

Kenneth R. Leslie, Sacha B. Nelson, and Gina G. Turrigiano.

Postsynaptic Depolarization Scales Quantal Amplitude in Cortical Pyramidal Neurons.

The Journal of Neuroscience, 2001, Oct. 1, 21(19), RC170

Levy WB. Steward O.
Synapses as associative memory elements in the hippocampal formation.
Brain. Res, 1979, Oct.19, 175(2), 233-45.

Dimitri V. Lissin, Stephen N. Gomperts, Reed C. Carroll, Chadwick W. Christine, Daniel Kalman, Marina Kitamura, Stephen Hardy, Rogger A. Nicolle, Robert C. Malenka and Mark Von Zastrow.
Activity differentially regulates the surface expression of synaptic AMPA and NMDA glutamate receptors.
PNAS, June 1998, Jun. 9, 95(12), 7097–7102.

Liu G,Choi S, Tsien R.W.

Variability of neurotransmitter concentration and nonsaturation of postsynaptic AMPA receptors at synapses in hippocampal cultures and slices.

Neuron, 1999, Feb, 22(2), 395-409.

Liu ZG.

Molecular mechanism of TNF signaling and beyond.

Cell Research, 2005, Jan, 15(1):24-27.

M. A. Lynch.

Long-Term Potentiation and Memory.
Physiol Rev, 2004, Jan, 84(1): 87–136.

M

Malenka RC, Kauer JA, Perkel DJ, Mauk MD, Kelly PT, Roger A. Nicoll & M. Neal Waxham.
An essential role for postsynaptic calmodulin and protein kinase activity in long-term potentiation.
Nature, 1989, Aug. 17, 340(6234), 554-57.1989.

Robert C. Malenka, and Mark F. Bear.
LTP and LTD: An Embarrassment of Riches.
Neuron, 2004, Sep. 30, 44(1), 5–21.

Malinow, R. & Malenka, R. C.
AMPA receptor trafficking and synaptic plasticity.
Annu. Rev. Neurosci, 2002, 25, 103–126.

Marder, E., and Prinz, A.A.
Modeling stability in neuron and network function: the role of activity in homeostasis.
Bioessays, 2002, Dec, 24(12), 1145–1154.

Bruno Marie, Edward Pym, Sharon Bergquist, and Graeme W. Davis.

Synaptic Homeostasis Is Consolidated by the Cell Fate Gene gooseberry, a Drosophila pax3/7 Homolog.

The Journal of Neuroscience, 2010, Jun. 16, 30(24), 8071-8082.

Henry Markram, Maria Toledo-Rodriguez, Yun Wang, Anirudh Gupta, Gilad Silberberg& Caizhi Wu.

Interneurons of the neocortical inhibitory system.

Nature Reviews Neuroscience, 2004, Oct, 5(10), 793-807.

Giovanni Marsicano & Beat Lutz.

Expression of the cannabinoid receptor CB1 in distinct neuronal subpopulations in the adult mouse forebrain.

European Journal of Neuroscience, 1999, Dec, 11(12), 4213–4225.

Sascha Martens, Michael M. Kozlov, Harvey T. McMahon.
How Synaptotagmin Promotes Membrane Fusion.
Science, 2007, May 25, 316(5828), 1205 – 1208.

L. J. Martin, A. Furuta and C. D. Blackstone.
AMPA Receptor Protein In Developing Rat Brain: Glutamate Receptor-1 Expression And Localization Change At Regional, Cellular, And Subcellular Levels With Maturation
Neuroscience, 1998, Apr, 83(3), 917–928.

Meffert MK, Calakos NC, Scheller RH, Schulman H .
Nitric oxide modulates synaptic vesicle docking fusion reactions.
Neuron, 1996, Jun, 16(6), 1229–1236.

Miesenböck G, De Angelis DA, Rothman JE (1998)
Visualizing secretion and synaptic transmission with pH-sensitive green fluorescent proteins.
Nature, 1989, Jul.9, 394(6689), 192-5.

Kenneth D. Miller.
Synaptic Economics: Competition and Cooperation in Synaptic Plasticity.
Neuron, 1996, Sep, 17(3), 371–374.

Miller, K. D. & MacKay, D. J. C.
The role of constraints in Hebbian learning.
Neural Comput, 1994, 6, 100–124.

Krista L. Moulder, Xiaoping Jiang, Amanda A. Taylor, John W. Olney, and Steven Mennerick.

Physiological Activity Depresses Synaptic Function through an Effect on Vesicle Priming.

The Journal of Neuroscience, 2006, Jun. 14, 26(24), 6618-6626.

Thomas D. Mrsic-Flogel, Sonja B. Hofer, Kenichi Ohki, R. Clay Reid, Tobias Bonhoeffer, and Mark Hubener.
Homeostatic Regulation of Eye-Specific Responses in Visual Cortex during Ocular Dominance Plasticity.
Neuron, 2007, Jun, 21, 54(6), 961–972.

Mulkey RM, Endo S, Shenolikar S, Malenka RC.
Involvement of a calcineurin/inhibitor-1 phosphatase cascade in hippocampal long-term depression.
Nature, 1994, Jun.9, 369(6480), 486-88.

Miceal Muller, Beat H. Gahwiler, Lorry Rietschin, and Scott M. Thompson.
Reversible loss of dendritic spines and altered excitability after
chronic epilepsy in hippocampal slice cultures.
Proc. Nat. Acad. Sci. USA, 1993, Jan, 90(1), 257-261.

Venkatesh N. Murthy, Thomas Schikorski, Charles F. Stevens and Yongling Zhu.
Inactivity Produces Increases in Neurotransmitter Release and Synapse Size.
Neuron, 2001, Nov.20, 32(4), 673–682.

N

Nagel, G., Ollig, D., Fuhrmann, M., Kateriya, S., Musti, A. M., Bamberg, E. & Hegemann, P.
Channelrhodopsin-1: A Light-Gated Proton Channel in Green Algae.
Science, 2002, Jun. 28, 296(5577), 2395–2398.

George Nagel, Tanjef Szellas, Wolfram Huhn, Suneel Kateriya, Nona Adeishvili, Peter Berthold, Doris Ollig, Peter Hegemann, and Ernst Bamberg.
Channelrhodopsin-2, a directly light-gatedcation-selective membrane channel.
PNAS, 2003, Nov.25, 100(24), 13940–13945.

Georg Nagel, Martin Brauner, Jana F. Liewald, Nona Adeishvili, Ernst Bamberg, and Alexander Gottschalk.
Light Activation of Channelrhodopsin-2 in Excitable Cells of Caenorhabditis elegans Triggers Rapid Behavioral Responses.
Current Biology, 2005, Dec.20, 15(24), 2279–2284.

Junichi Nakai, Masamichi Ohjura, and Keiji Imoto.
A high signal-to-noise Ca2+ probe composed of a single green fluorescent protein.
Nature Biotechnology, 2001, Feb, 19(2), 137-141.

Nakamura Y, Okuno S, Sato F, Fujisawa H.

An immunohistochemical study of Ca2+/calmodulin-dependent protein kinase IV in the rat central nervous system:light and electron microscopic observations.

Neuroscience, 1995, Sep, 68(1), 181-94.

Konstantin Nikolic, Nir Grossman, Matthew S. Grubb, Juan Burrone, Chris Toumazou and Patrick Degenaar.
Photocycles of Channelrhodopsin-2.
Photochemistry and Photobiology, 2009, Jan-Feb, 85(1), 400–411.

O

P

Pak DT, Sheng M.

Targeted protein degradation and synapse remodeling by an inducible protein kinase.

Science, 2003 Nov. 21, 302(5649), 1368-73.

Suzanne Paradis, Sean T Sweeney and Graeme W Davis.

Homeostatic Control of Presynaptic Release Is Triggered by Postsynaptic Membrane Depolarization.

Neuron, 2001, May 1, 30(3), 737-749.

Pawlak V, Schupp BJ, Single FN, Seeburg PH, Kohr G.

Impaired synaptic scaling in mouse hippocampal neurones expressing NMDA receptors with reduced calcium permeability.
J. Physiol, 2005, Feb.1, 562(Pt3), 771–83.

Mark Pickering, Derval Cumiskey and John J. O'Connor.
Actions of TNF-α on glutamatergic synaptic transmission in the central nervous system.
Exp Physiol, 2005, Sep, 90(5), 663–670.

R

Ithai Rabinowitch and Idan Segev.
The Interplay Between Homeostatic Synaptic Plasticity and Functional Dendritic Compartments.
J Neurophysiol, 2006, Jul, 96(1), 276–283.

Ithai Rabinowitch and Idan Segev.
Two opposing plasticity mechanisms pulling a single synapse.
Trends Neurosci, 2008, Aug, 31(8), 377-383.

Ranganathan, R., W.A. Harris and C.S. Zuker .
The Molecular Genetics of Invertebrate Phototransduction.
Trends in Neuroscience, 1991, Nov, 14(11) 486-493.

Anuradha Rao and Ann Marie Craig.
Activity Regulates the Synaptic Localization of the NMDA Receptor in Hippocampal Neurons.
Neuron, 1997, Oct, 19(4), 801–812.

Ramakers GJ, Corner MA, Habets AM.

Development in the absence of spontaneous bioelectric activity results in increased stereotyped burst firing in cultures of dissociated cerebral cortex.
Exp Brain Res, 1990, 79(1), 157-66.

John J. Renger, Christophe Egles, and Guosong Liu.
A Developmental Switch in Neurotransmitter Flux Enhances Synaptic Efficacy by Affecting AMPA Receptor Activation.
Neuron, 2001, Feb, 29(2), 469–484.

Mark M. Rich and Peter Wenner.
Sensing and expressing homeostatic synaptic plasticity.
TRENDS in Neurosciences, 2007, Mar, 30(3), 119-25.

Rutherford, L. C., Nelson, S. B. & Turrigiano, G. G.
BDNF has opposite effects on the quantal amplitude of pyramidal neuron and interneuron excitatory synapses.
Neuron, 1998, Sep, 21(3), 521–530.

S

Natalie Sans, Ronald S. Petralia, Ya-Xian Wang, Jaroslav Blahos II, Johannes W. Hell and Robert J. Wenthold.

A developmental change in NMDA receptor-associated proteins at hippocampal synapses.

The Journal of Neuroscience, 2000, Feb. 1, 20(3), 1260-1271.

Jason D. Shepherd, Gavin Rumbaugh, Jing Wu,1 Shoaib Chowdhury,Niels Plath Dietmar Kuhl, Richard L. Huganir.
Arc/Arg3.1 Mediates Homeostatic Synaptic Scaling of AMPA Receptors.
Neuron, 2006, Nov.9, 52(3), 475–484.

Eric Schnell, Max Sizemore, Siavash Karimzadegan, Lu Chen, David S. Bredt, and Roger A. Nicoll.
Direct interactions between PSD-95 and stargazing control synaptic AMPA receptor number.
PNAS, 2002, Oct. 15, 99(21), 13902–13907.

Thomas Schikorski and Charles F. Stevens.
Quantitative Ultrastructural Analysis of Hippocampal Excitatory Synapses.
The Journal of Neuroscience, 1997, Aug. 1, 17(15), 5858–5867.

Christian Schroll, Thomas Riemensperger, Daniel Bucher, Julia Ehmer, Thomas Vo¨ller, Karen Erbguth, Bertram Gerber, Thomas Hendel, Georg Nagel, Erich Buchner, and Andre´ Fiala.
Light-Induced Activation of Distinct Modulatory Neurons Triggers Appetitive or Aversive Learning in Drosophila Larvae.
Current Biology, 2006, Sep. 5 16(17), 1741–1747.

H Schulman.
Nitric oxide: a spatial second messenger.
Molecular Psychiatry, 1997, Jul, 2(4), 296–299.

Daniel P. Seeburg and Morgan Sheng.

Activity-Induced Polo-Like Kinase 2 Is Required for Homeostatic Plasticity of Hippocampal Neurons during Epileptiform Activity.
The Journal of Neuroscience, 2008, Jun.25, 28(26), 6583– 6591.

Seeburg DP, Feliu M, Gaiottino J, Sheng M.
Critical role of CDK5 and Polo-like kinase 2 in homeostatic synaptic plasticity during elevated activity.
Neuron ,2008, May 22, 58(4), 571–583.

Somogyi P, Tamas G, Lujan R, Buhl EH.
Salient features of synaptic organisation in the cerebral cortex.
Brain Res Brain Res Rev, 1998, May, 26(2-3), 113–135.

Stellwagen D, Malenka RC.

Synaptic scaling mediated by glial TNF-alpha.

Nature, 2006, Apr.20, 440(7087), 1054-9.

Stellwagen D, Beattie E.C, Jae Y.S and Malenka R.C

Differential Regulation of AMPA Receptor and GABA Receptor Trafficking by Tumor Necrosis Factor-alpha.

The Journal of Neuroscience, 2005, Mar. 23, 25(12), 3219 –3228.

Michael A. Sutton, Hiroshi T. Ito, Paola Cressy, Christian Kempf, Jessica C. Woo, and Erin M. Schuman.
Miniature Neurotransmission Stabilizes Synaptic Function via Tonic Suppression of Local Dendritic Protein Synthesis.
Cell, 2006, May 19, 125(4), 785–799.

T

Huizhong W. Tao and Mu-ming Poo.
Retrograde signaling at central synapses.
PNAS, 2001, Sep. 25, 98(20), 11009–11015.

Thiagarajan, T.C., Lindskog, M. & Tsien, R.W.
Adaptation to synaptic inactivity in hippocampal neurons.
Neuron, 2005, Sep. 1, 47(5), 725–737.

Thiagarajan, T. C., Piedras-Renteria, E. S. & Tsien, R. W.
α- and β-CaMKII. Inverse regulation by neuronal activity and opposing effects on synaptic strength.
Neuron, 2002, Dec. 19, 36(6), 1103–1114.

Hirofumi Tokuoka and Yukiko Goda.
Activity-dependent coordination of presynaptic release probability and postsynaptic GluR2 abundance at single synapses.
PNAS, 2008, Sep. 23, 105(38), 14656–14661.

Gina Turrigiano.
Homeostatic signaling: the positive side of negative feedback.
Current Opinion in Neurobiology, 2007, Jun, 17(3), 318–324.

Gina G. Turrigiano and Sacha B.Nelson.
Homeostatic plasticity in the developing nervous system.
Nature Reviews, 2004, Feb, 5(2), 97-107.

Gina G. Turrigiano, Kenneth R. Leslie, Niraj S. Desai, Lana C. Rutherford & Sacha B. Nelson.
Activity-dependent scaling of quantal amplitude in neocortical neurons.
Nature, 1998, Feb. 26, 391(6670), 892-6.

Turrigiano G, Abbot LF, Marder E.

Activity-dependent changes in intrinsic properties of cultured neurons.

Science, 1994, May 13, 264(5161), 974-7.

G. G. Turrigiano and E. Marder.

Modulation of identified stomatogastric ganglion neurons in primary cell culture.

Journal of Neurophysiology, 1993, Jun, 69(6), 1993-2002.

V

Valor LM, Charlesworth P, Humphreys L, Anderson CN, Grant SG.

Network activity-independent coordinated gene expression program of the synapse.

Proc Natl Acad Sci U S A. 2007, Mar.13, 104(11), 4658-63.

Tuhin Virmani, Deniz Atasoy, and Ege T. Kavalali.
Synaptic Vesicle Recycling Adapts to Chronic Changes in Activity.
The Journal of Neuroscience, 2006, Feb. 22, 26(8), 2197–2206.

W

Wagenaar DA, Pine J, Potter SM.

An extremely rich repertoire of bursting patterns during the development of cortical cultures

BMC Neuroscience 2006 Feb. 7, 7:11.

Wang H, Peca J, Matsuzaki M, Matsuzaki K, Noguchi J, Qiu L, Wang D, Zhang F, Boyden E, Deisseroth K, Kasai H, Hall WC, Feng G, Augustine GJ.

Hight-speed mapping in synaptic connectivity using photostimulation in Channelrhodopsin-2 transgenic mice.

Proc Natl Acad Sci U S A, 2007, May 8, 104(19), 8143-8.

Xueyong Wang, Kathrin L. Engisch, Yingjie Li, Martin J. Pinter, Timothy C. Cope, and Mark M. Rich.
Decreased Synaptic Activity Shifts the Calcium Dependence of Release at the Mammalian Neuromuscular Junction In Vivo.
The Journal of Neuroscience, 2004, Nov. 24, 24(47), 10687–10692.

Watt AJ, van Rossum MC, MacLeod KM, Nelson SB, Turrigiano GG
Activity coregulates quantal AMPA and NMDA currents at neocortical synapses.
Neuron, 2000, Jun, 26(3), 659-70.

Wenthold RJ, Petralia RS, Blahos J II, Niedzielski AS.
Evidence for multiple AMPA receptor complexes in hippocampal CA1/CA2 neurons.
J. Neuroscience, 1996, Mar. 15, 16(6), 1982-89.

Corette J. Wierenga, Michael F. Walsh, and Gina G. Turrigiano.
Temporal Regulation of the Expression Locus of Homeostatic Plasticity.
J Neurophysiol, 2006, Jun.7, 96(4), 2127–2133.

Jennifer C. Wilhelm and Peter Wenner.
GABAA transmission is a critical step in the process of triggering homeostatic increases in quantal amplitude.
PNAS, 2008, Aug. 12, 105(32), 11412-11417.

Van de Weerdt BC, Madema RH.
Polo-like Kinase: a team in control of the division.

Cell Cycle, 2006 Apr. 5, (8):853-64.

Wickens JR, Abraham WC.
Involvement of L-type calcium channels in heterosynaptic long-term depression in the hippocampus.
Neurosci. Lett. 1991, Sep. 2, 130(1), 128-32.

Wilson NR, Kang J, Hueske EV, Leung T, Varoqui H, Murnick JG, Erickson JD, Liu G.
Presynaptic regulation of quantal size by VGLUT1.
J Neurosci, 2005, Jun.29, 25(26), 6221– 6234.

S. M. Wojcik, J. S. Rhee, E. Herzog, A. Sigler, R. Jahn, S. Takamori, N. Brose, and C. Rosenmund.
An essential role for vesicular glutamate transporter 1 (VGLUT1) in postnatal development and control of quantal size.
PNAS, 2004, May 4, 101(18), 7158–7163.

Xiu Sun and Marina E. Wolf.

Nucleus accumbens neurons exhibit synaptic scaling that is occluded by repeated dopamine pre-exposure.

European Journal of Neuroscience, 2009, Aug, 30(4), 539–550.

Y

Yang SN, Tang YG, Zucker RS.

Selective induction of LTP and LTD by postsynaptic [Ca^{2+}] elavation.

J. Neurophysiology, 1999, Feb, 81(2), 781-87.

Yangling Mu & Mu-ming Poo.

Spike Timing-Dependent LTP/LTD Mediates Visual Experience-Dependent Plasticity in a Developing Retinotectal System.

Neuron, 2006, Apr. 6, 50(1), 115-125.

Yo S, HO IK.

Effects of GABA antagonists, SR96631 and bicuculline, on GABAA receptor-regulated chloride influx in cat cortical synaptoneurosomes.

Neurochem Res, 1990, Sep, 15(9), 905-10.

Z

Boris V. Zemelman, Georgia A. Lee, Minna Ng, and Gero Miesenbock.
Selective Photostimulation of Genetically ChARGed Neurons.
Neuron, 2002, Jan. 3, 33(1), 15–22.

Zhou W, Li X, Liu M, Zhao Y, Zhu G, Luo Q.

Homeostatically regulated synchronized oscillations induced by short-term tetrodotoxin treament in cultured neural network.

Biosystems, 2009 Jan, 95(1), 61-6.

7.Annex

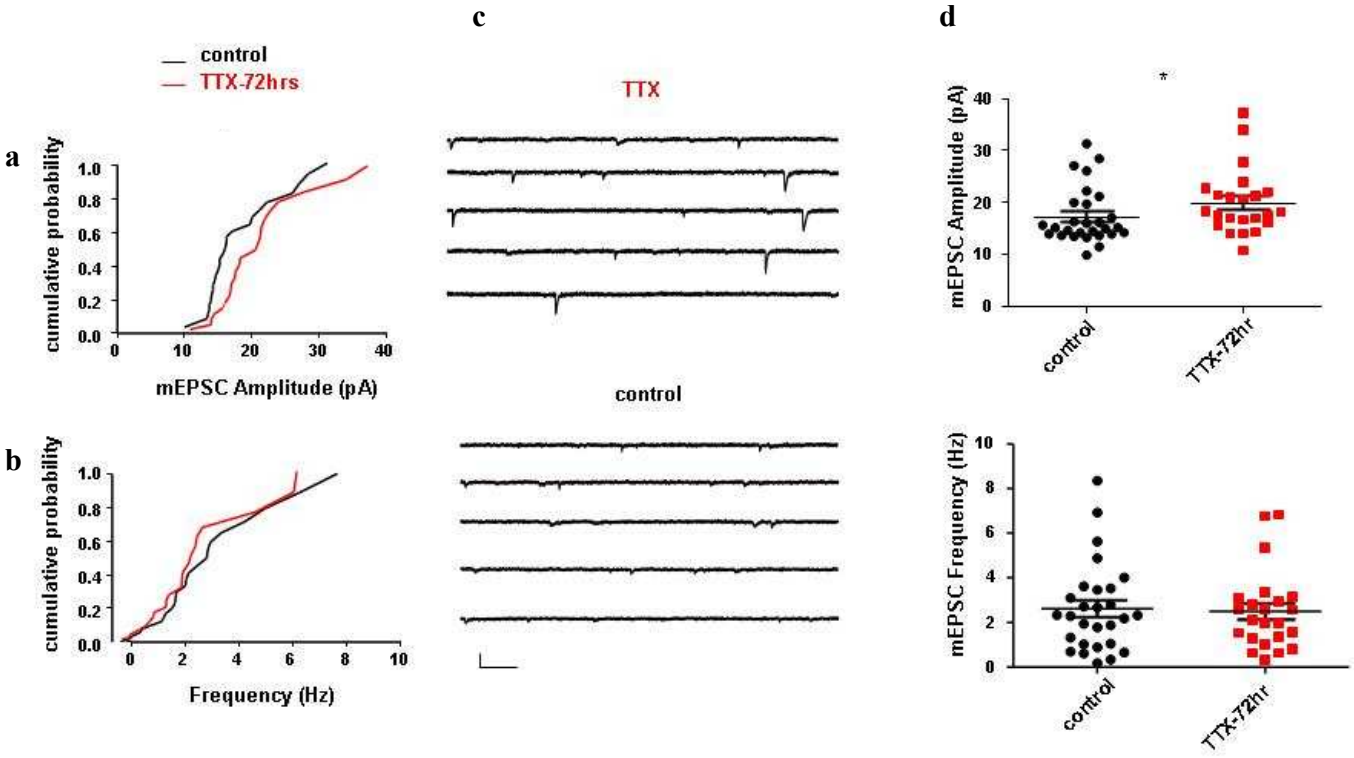

Fig.7.1. Cumulative probability of mEPSCs in cells chronically treated with TTX demonstrates significant differences in amplitude but not frequency when compared to untreated controls.

- **a.** Cumulative probability vs. amplitude for mEPSCs from hippocampal cells treated on DIV10 with TTX (red) for 72hrs compared to controls (black). Mean amplitude: TTX=19.96 pA ± 1.30 n=23 cells; Controls=17.28 pA ± 1.01 n=28 cells, P=0.03, Mann Whitney test. Data taken from 3 separate experiments. Data is expressed as S.E.M. Cumulative distribution is plotted per cell. A power calculation revealed we had a 70% power of being able to detect a change of 4.11 pA.
- **b.** Cumulative probability vs. frequency for mEPSCs from hippocampal cells treated on DIV10 with TTX (black) for 72hrs compared to controls (black). Mean frequency: TTX=2.5 Hz ± 0.37, n=23; Controls=2.62 Hz ± 0.37, n=28, P=0.86, Mann Whitney test. Data taken from 3 separate experiments. Data is expressed as S.E.M. Cumulative distribution is plotted per cell. A power calculation revealed we had an 70% power of being able to detect a change between 1.34 Hz.
- **b.** Example traces each taken from a different cell after a 72hr treatment with TTX on DIV 13 (top) or left untreated as controls (bottom) on DIV 13. Scale =51.2 pA, 106.5 ms
- **c.** Scatter plot of mEPSC amplitudes from hippocampal cells treated on DIV10 with TTX (red) for 72hrs (n=23 cells) compared to controls (black) (n=28 cells). Error bars express S.E.M. Straight line expresses mean value.
- **d.** Scatter plot of mEPSC frequencies from hippocampal cells treated on DIV10 with TTX (red) for 72hrs (n=23 cells) compared to controls (black) (n=28 cells). Error bars express S.E.M. Straight line expresses mean value.

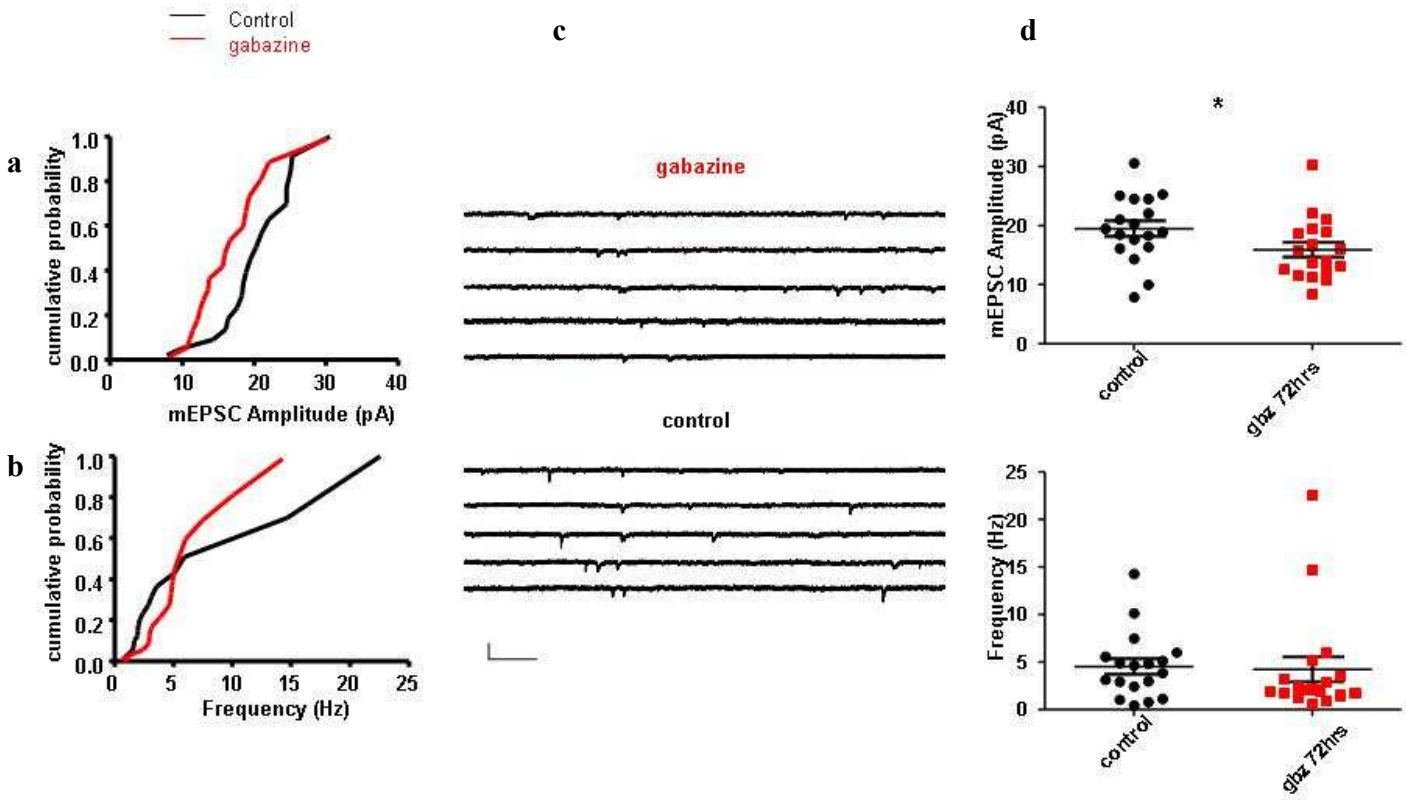

Fig.7.2. Cumulative probability of mEPSCs in cells chronically treated with gabazine demonstrates significant differences in amplitude but not frequency when compared to untreated controls.

- **a.** Cumulative probability vs. amplitude for mEPSCs from hippocampal cells treated on DIV10 with gabazine (red) for 72hrs compared to controls (black). Mean amplitude: gabazine=15.91 pA ± 1.24, n=18 cells; Controls=19.48 pA ± 1.31, n=18 cells, P=0.04, Mann Whitney test. Data taken from 4 separate experiments. Data is expressed as S.E.M. Cumulative distribution is plotted per cell. A power calculation revealed we had a 70% power of being able to detect a change of 3.88 pA.
- **b.** Cumulative probability vs. frequency for mEPSCs from hippocampal cells treated on DIV10 with gabazine (red) for 72hrs compared to controls (black). Mean frequency: gabazine=4.22 ± 1.32, n=18 cells; Controls=4.5 Hz ± 0.82, n=18 cells, P=0.22, Mann Whitney test. Data taken from 4 separate experiments. Data is expressed as S.E.M. Cumulative distribution is plotted per cell. A power calculation revealed we had an 70% power of being able to detect a change of 3.25 Hz.
- **c.** Example traces each taken from a different cell after a 72hr treatment with gabazine on DIV 13 (top) or left untreated as controls (bottom) on DIV 13. Scale =51.2 pA, 106.5 ms.
- **d.** Scatter plot of mEPSC amplitudes from hippocampal cells treated on DIV10 with gabazine (red) for 72hrs (n=23 cells) compared to controls (black) (n=28 cells). Error bars express S.E.M. Straight line expresses mean value.
- **e.** Scatter plot of mEPSC frequencies from hippocampal cells treated on DIV10 with gabazine (red) for 72hrs (n=18 cells) compared to controls (black) (n=18 cells). Error bars express S.E.M. Straight line expresses mean value.

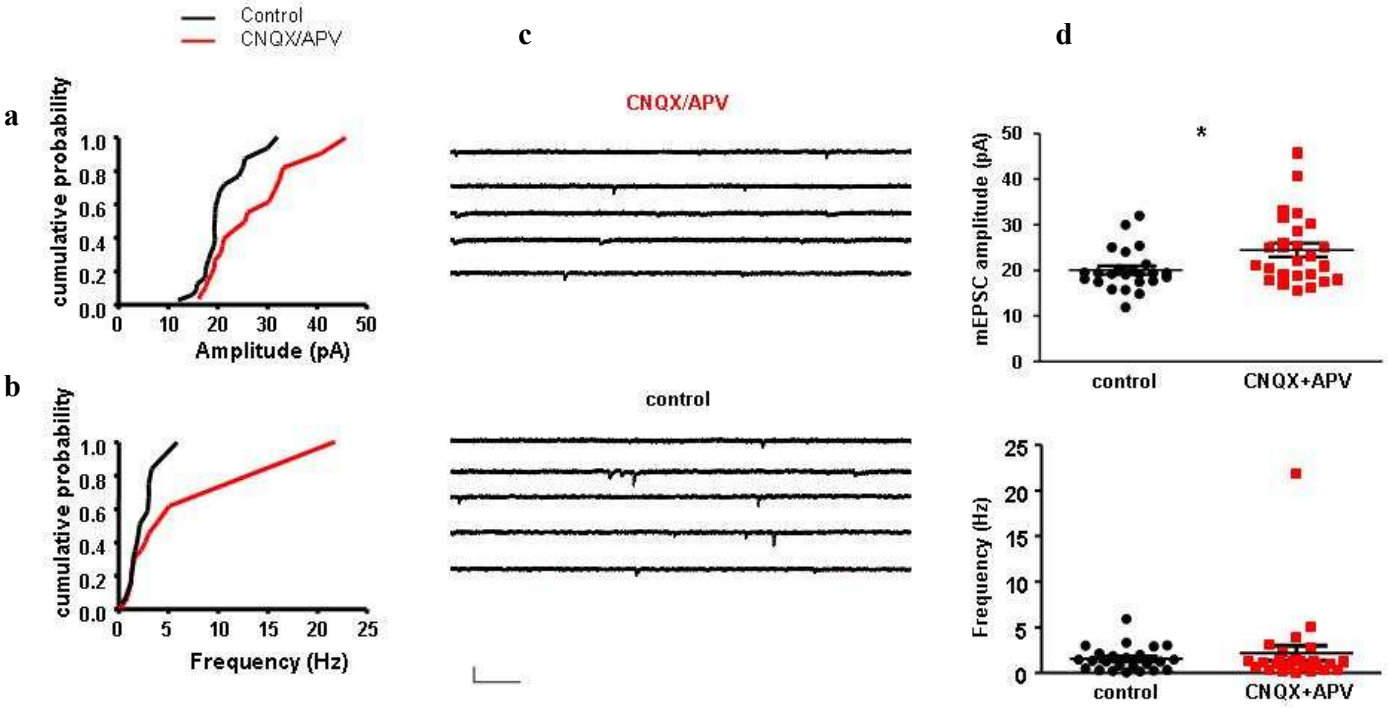

Fig.7.3. Cumulative probability of mEPSCs in cells chronically treated with CNQX/APV demonstrates significant differences in amplitude but not frequency when compared to untreated controls.

- **a.** Cumulative probability vs. amplitude for mEPSCs from hippocampal cells treated on DIV10 with CNQX/APV (red) for 72hrs compared to controls (black). Mean amplitude: CNQX/APV =24.48 pA ± 1.50, n=26 cells; Controls=20.08 pA ± 0.92, n=24 cells, P=0.03, Mann Whitney test. Data taken from 3 separate experiments. Data is expressed as S.E.M. Cumulative distribution is plotted per cell. A power calculation revealed we had a 70% power of being able to detect a change of 4.53 pA.
- **b.** Cumulative probability vs. frequency for mEPSCs from hippocampal cells treated on DIV10 with CNQX/APV (red) for 72hrs compared to controls (black). Mean frequency: CNQX/APV =1.55 Hz ± 0.28 n=26 cells; Controls=2.17 Hz ± 0.82 n=24 cells P=0.82, Mann Whitney test. Data taken from 4 separate experiments. Data is expressed as S.E.M. Cumulative distribution is plotted per cell. A power calculation revealed we had a 70% power of being able to detect a change of 2.27 Hz.
- **c.** Example traces each taken from a different cell after a 72hr treatment with gabazine on DIV 13 (top) or left untreated as controls (bottom) on DIV 13. Scale =51.2 pA, 106.5 ms.
- **d.** Scatter plot of mEPSC amplitudes from hippocampal cells treated on DIV10 with CNQX/APV (red) for 72hrs (n=26 cells) compared to controls (black) (n=24 cells). Error bars express S.E.M. Straight line expresses mean value.
- **e.** Scatter plot of mEPSC frequencies from hippocampal cells treated on DIV10 with CNQX/APV (red) for 72hrs (n=18 cells) compared to controls (black) (n=18 cells). Error bars express S.E.M. Straight line expresses mean value.

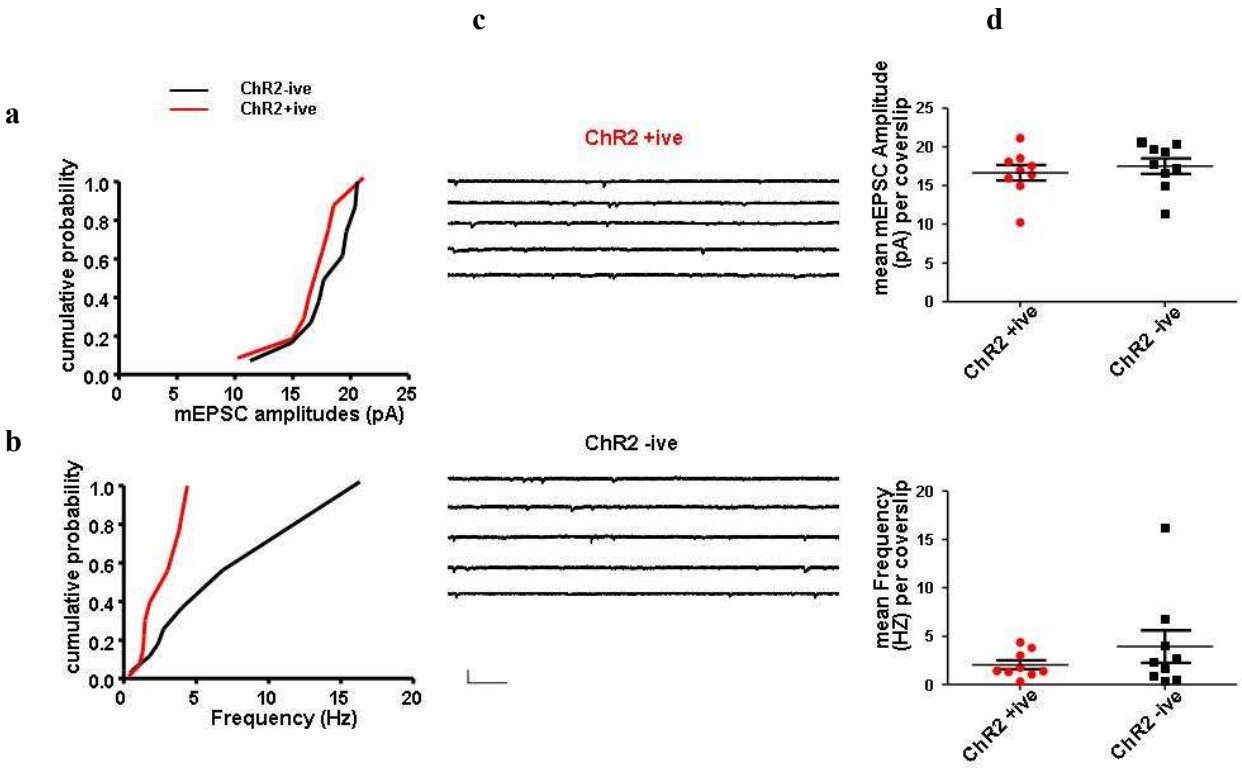

Fig.7.4. Cumulative probability of mEPSCs in cells expressing ChR2 showed no significant differences in amplitude or frequency when compared to ChR2-ive cells from within the same coverslip.

- **a.** Cumulative probability vs. amplitude for mEPSCs from hippocampal cells on DIV13 expressing ChR2 (red) compared to ChR2 –ive cells from within the same coverslip (black). Mean amplitude: ChR2+ive =16.64 ± 1.08 pA n =13 cells, 9 coverslips; ChR2-ive =17.51 ± 1.73 pA n=14 cells, 9 coverslips, unpaired t-test P=0.55. Data taken from 3 separate experiments. Data is expressed as S.E.M. Cumulative distribution is plotted per coverslip. A power calculation revealed we had an70% power of being able to detect a change of 3.74 pA.
- **b.** Cumulative probability vs. frequency for mEPSCs from hippocampal cells on DIV13 expressing ChR2 (red) compared to ChR2 –ive cells from within the same coverslip (black). Mean amplitude: ChR2+ive =2.07 ± 0.45, n=13 cells, 9 coverslips; ChR2-ive =3.94 ± 1.67, n=14 cells, 9 coverslips, Mann Whitney test P= 0.67. Data taken from 3 separate experiments. Data is expressed as S.E.M. Cumulative distribution is plotted per coverslip. A power calculation revealed we had a 70% power of being able to detect a change of 4.59 Hz.
- **c.** Example traces each taken from a different cell expressing ChR2 on DIV 13 (top) or cells which aren't from within the same coverslip as controls (bottom). Scale =51.2 pA, 106.5 ms.
- **d.** Scatter plot of mEPSC amplitudes from hippocampal cells expressing ChR2+ive on DIV10 (red, n=9 coverslips, 13 cells) compared to cells not expressing ChR2 within the same coverslip as controls (black) (n=24 cells, n=9 coverslips, 14 cells). Error bars express S.E.M. Straight line expresses mean value.
- **e.** Scatter plot of mEPSC amplitudes from hippocampal cells expressing ChR2+ive on DIV10 (red, n=9 coverslips, 13 cells) compared to cells not expressing ChR2 within the same coverslip as

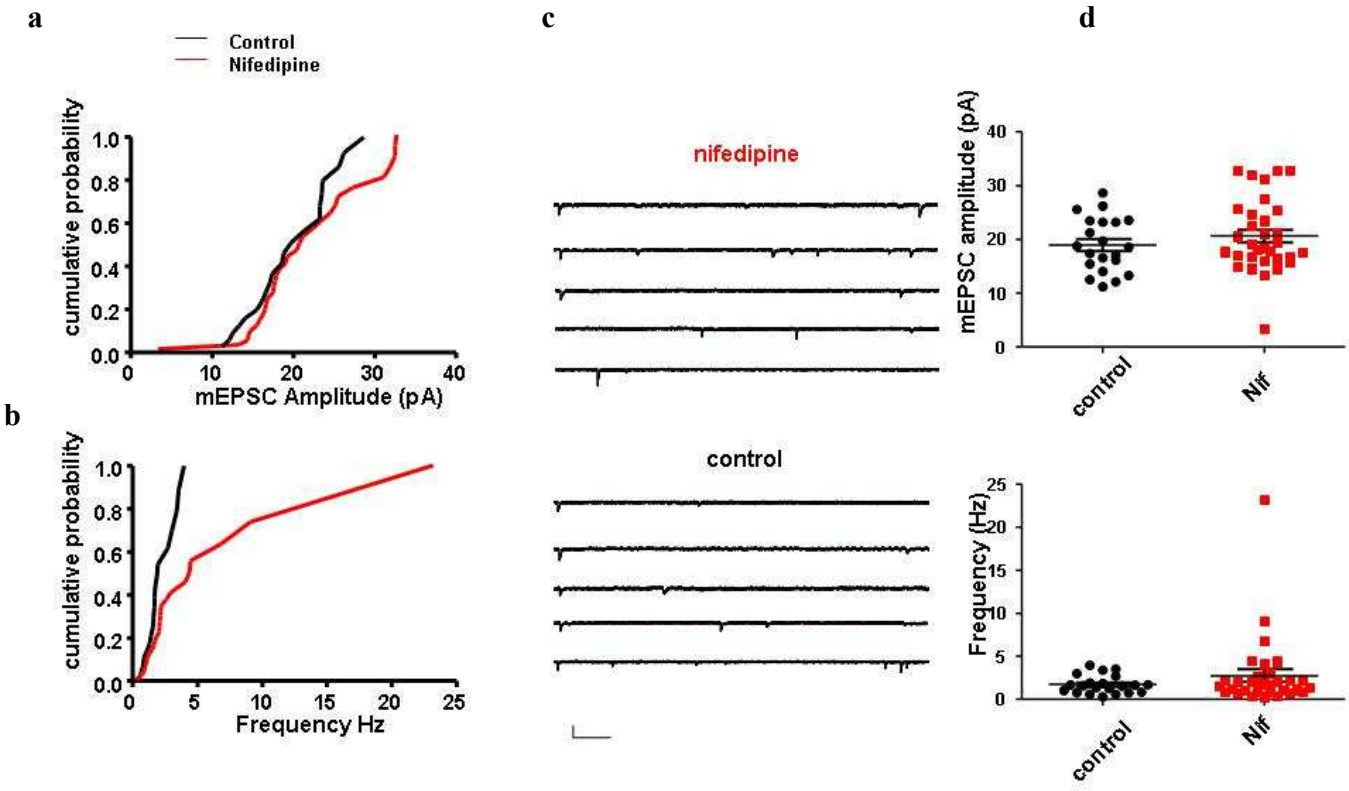

Fig.7.5. Cumulative probability of mEPSCs in cells chronically treated with nifedipine demonstrates no significant differences in amplitude or frequency when compared to untreated controls.

- **a.** Cumulative probability vs. amplitude for mEPSCs from hippocampal cells treated on DIV10 with nifedipine (red) for 72hrs compared to controls (black). Mean amplitude: nifedipine 20.60pA ± 1.2, n=32 cells; Controls=18.96pA ± 1.10, n=21 cells, P= 0.345, Unpaired t-test. Data taken from 3 separate experiments. Data is expressed as S.E.M. A power calculation revealed we had a 70% power of being able to detect a change of 4.38 pA.
- **b.** Cumulative probability vs. frequency for mEPSCs from hippocampal cells treated on DIV10 with CNQX/APV (red) for 72hrs compared to controls (black). Mean frequency: nifedipine =2.76 Hz ± 0.74, n=32 cells; Controls=1.73 Hz ± 0.23, n=21 cells, P=0.60) Mann Whitney Test. Data taken from 3 separate experiments. Data is expressed as S.E.M. A power calculation revealed we had a 70% power of being able to detect a change of 0.89 Hz.
- **c.** Example traces each taken from a different cell after a 72hr treatment with nifedipine on DIV 13 (top) or left untreated as controls (bottom) on DIV 13. Scale =51.2 pA, 106.5 ms.
- **d.** Scatter plot of mEPSC amplitudes from hippocampal cells treated on DIV10 with nifedipine (red) for 72hrs (n=32 cells) compared to controls (black) (n=21 cells). Error bars express S.E.M. Straight line expresses mean value.
- **e.** Scatter plot of mEPSC frequencies from hippocampal cells treated on DIV10 with nifedipine (red) for 72hrs (n=32 cells) compared to controls (black) (n=21 cells). Error bars express S.E.M. Straight line expresses mean value.